이학박사학위논문

파킨슨병 원인유전자 PINK1, Parkin, VDAC1의 분자병리기전 이해

Understanding molecular functions of PINK1, Parkin and VDAC1 in Parkinson's disease

2018 년 2 월

서울대학교 대학원

협동과정 유전공학전공

함 수 진

ABSTRACT

Understanding molecular functions of PINK1, Parkin and VDAC1 in Parkinson's disease

Sujin Ham

Interdisciplinary Graduate Program in Genetic Engineering

Graduate School

Seoul National University

This thesis research was conducted in order to understand the molecular mechanism behind Parkinson's disease by investigating the role of *PINK1*, *Parkin* and *VDAC1* in the cell and animal models for the disease. The activation of Parkin E3 ligase is regulated by interaction between it's UBL and RING1 domains. In healthy cells with normal mitochondrial function, the UBL and the RING1 domain of Parkin bind to each other to inhibit its activity. However, under mitochondrial damage conditions, the upstream regulator PINK1 phosphorylates Parkin at serine 65 in the UBL domain, reducing the binding between the UBL and the RING1 domain.

Phosphorylation of the serine 65 in Parkin induces ubiquitination of Parkin's substrates, such as MFN1, MFN2, and VDAC1, and increases Parkin-mediated mitophagy, suggesting that the phosphorylation plays a critical role in activating the E3 ligase activity of Parkin. In addition, three patient mutations within the UBL domain of Parkin, K27N, R33Q and A46P, sustain the interaction between the UBL and the RING1 domain even after serine 65 phosphorylation by PINK1, which explains how these mutations in Parkin induce Parkinson's disease. These results show that binding between the UBL and the RING1 domain of Parkin plays an important role in the pathogenesis of Parkin-related Parkinson's disease. The two types of VDAC1 ubiquitination by activated Parkin have different impacts on regulation of mitophagy and apoptosis. Mono-ubiquitination of VDAC1 by Parkin on lysine 274 inhibits apoptosis, while poly-ubiquitination of VDAC1 on lysines 12, 20, 53, 109, and 110 promotes mitophagy. Apoptosis, which is regulated by mono-ubiquitination of VDAC1, occurs as a result of increasing mitochondrial calcium uptake. The calcium uptake is regulated by MCU, a calcium channel located in the mitochondrial inner membrane, and mPTP, a mitochondrial pore responsible for apoptosis. The mono- and poly-ubiquitination of VDAC1 occur independently in a PINK1-Parkin pathway-dependent manner. Furthermore, Parkin patient mutation with K211N suppresses the poly-ubiquitination, while Parkin patient

mutation with T415N is defective in the mono-ubiquitination of VDAC1. *Drosophila* model animals containing Parkin K211N mutation consistently show PD-related phenotypes and defective Parkin-mediated mitophagy, while *Drosophila* model animals with T415N mutation shows increased mitochondrial calcium uptake and increased apoptosis. Taken together, this thesis research suggests a detailed mechanism of PD pathogenesis caused by mutations in PINK1 and Parkin, and underlines an etiological importance of PD-associated genes in the regulation of mitochondrial homeostasis. Also, VDAC1 has been proposed as a novel regulator of PD, which extends our current understanding of PD pathogenesis and proposes VDAC1 as a potential candidate for PD medication.

Keywords: Parkinson's disease, PINK1, Parkin, VDAC1, Mitophagy, Apoptosis

Student Number: 2011-20236

TABLE OF CONTENTS

List of Figures

List of Tables

Introduction

Parkinson's disease (PD) is a neurodegenerative disease caused by the loss of dopaminergic neurons in substantial nigra, followed by a variety of symptoms including tremor, rigidity and dyskinesia (Baba et al., 2006). A series of genetic studies has identified a group of genes responsible for the pathogenesis of PD, including SNCA (α-synuclein), PARK2 (Parkin), PARK7 (DJ-1), PARK6 (PINK1), LRRK2 (leucine-rich repeat kinase 2) and PARK5 (UCHL1) whose mutations are known to cause autosomal recessive or dominant parkinsonism (Table 1) (Bonifati, 2001; Hatano et al., 2004; Lesage & Brice, 2009).

One of the PD-associated genes mentioned above is PARK2 which encodes Parkin, an E3 ubiquitin ligase with an ubiquitin-like domain (UBL) on its N-terminus. The catalytic region of Parkin mainly consists of Really Interesting New Gene (RING) finger motifs located at its C-terminus with RING0 domain followed by RING1, In Between RING fingers (IBR) and RING2 domains (Hampe, Ardila-Osorio, Fournier, Brice, & Corti, 2006; N. Matsuda et al., 2006; Trempe et al., 2013). Extensive research on individual Parkin domains has unfolded some of their roles in E3 ligase activity. RING1 is known to be involved in substrate interaction while RING2 is reported to bind to E2 enzymes (Lazarou et al., 2013). The 3D structure of Parkin revealed that the UBL domain forms a compact structure with the

RING motifs at the C-terminus, and inhibits Parkin activation under normal circumstances (Fig. 1). Parkin is activated by phosphorylation at serine 65 located within the UBL domain by PTEN-induced putative kinase 1 (PINK1), which in turn blocks the inhibitory mechanism of the UBL domain and causes Parkin to translocation from the cytoplasm to mitochondria for its full activation (Kondapalli et al., 2012). PINK1, a serine/threonine kinase, is activated under mitochondrial depolarization caused by treatment of carbonyl cyanide m-chlorophenyl hydrazone (CCCP), and accumulates on the surface of damaged mitochondria (Lazarou, Jin, Kane, & Youle, 2012; N. Matsuda et al., 2010; Narendra et al., 2010). PINK1 phosphorylates Parkin and induces its E3 ligase activity. Recently, Noriyuki Matsuda group reported that phosphorylated ubiquitin is essential factor to fully activate Parkin (Koyano et al., 2014). Activated Parkin ubiquitinates its substrates located on the outer mitochondrial membrane, including mitofusin 1 (MFN1), mitofusin 2 (MFN2), translocase of outer membrane 20 (TOM20), miro and voltage-dependent anion-selective channel 1 (VDAC1) (Birsa et al., 2014; Chan et al., 2011; Chen & Dorn, 2013; Geisler et al., 2010; Glauser, Sonnay, Stafa, & Moore, 2011; X. Wang et al., 2011). p62/SQSTM1 adaptor protein containing LC3B and ubiquitin binding motifs are then recruited to the mitochondria, which in turn recruits LC3B that induces autophagosome formation (Fig. 2) (Okatsu et al., 2010). Also

PINK1 recruits two primary autophagy receptors, NDP52 and optineurin, to mitochondria to activate mitophagy, independently of Parkin. Once recruited to mitochondria, NDP52 and optineurin recruit autophagy factors ULK1, DFCP1 and WIPI1 to focal spots proximal to mitochondria. Series of these processes ultimately result in selective degradation of mitochondria in lysosome, which are called mitophagy (Heo, Ordureau, Paulo, Rinehart, & Harper, 2015; Lazarou et al., 2015). Besides mitophagy, the PINK1-Parkin pathway targets various different mitochondrial proteins and plays a critical role in maintaining mitochondrial homeostasis through regulation of mitochondrial dynamics and mitochondria-mediated apoptosis (Carroll, Hollville, & Martin, 2014; W. Yu, Sun, Guo, & Lu, 2011).

VDAC1 is one of the aforementioned Parkin substrates known to be responsible for regulation of mitophagy and apoptosis. VDAC1 localizes at the outer mitochondrial membrane, and forms a pore consisting of 19 beta-strands with beta-barrel structure (Fig. 3) (Hiller et al., 2008). Also, by forming a complex with cyclophilin D from mitochondrial matrix and adenine nucleotide translocase (ANT) from the inner mitochondrial membrane, VDAC1 functions as a critical component of mitochondrial permeability transition pore (mPTP), which transports molecules under 1,500 daltons, such as metabolites, calcium and cytochrome C (Fig. 4)

(Baines, 2009; Bernardi & Di Lisa, 2015; Bonora & Pinton, 2014). VDAC1 is poly-ubiquitinated with K27 ubiquitin linkage by Parkin. Poly-ubiquitinated VDAC1 triggers Parkin-mediated mitophagy through recruitment p62/SQSTM1 and LC3B to mitochondria (Geisler et al., 2010).

Table 1. Genes linked with Parkinson's disease

Locus	Inheritance	Gene	Functions
PARK1/4	AD	***α-Synuclein***	Synaptic vesicle formation ? Inhibits PLD2 ?
PARK2	AR	***Parkin***	E3 ligase
PARK3	AD	***SPR?***	Spiapterine reductase
PARK5	AD?	***UCH-L1***	Ubiquitin C-terminal hydrolase, Deubiquitinase
PARK6	AR	***PINK1***	Ser/Thr protein kinase
PARK7	AR	***DJ-1***	Deglycase ? Peptidase ? Chaperone ?
PARK8	AD	***LRRK2***	Ser/Thr protein kinase
PARK9	AR	***ATP13A2***	Lysosomal ATPase, Transports cations ?
PARK10	AD	***USP24***	Deubiquitinase
PARK11	AD	***GIGYF2***	Grb10-interacting GYF protein
PARK13	AD?	***OMI/HTRA2***	Serine protease
PARK14	AR	***PLA2G6***	Phospholipase
PARK15	AR	***FBXO7***	A component of SCF E3 ligases
PARK17	AD	***VPS35***	A component of the retromer complex
PARK18	AD	***EIF4G1***	A component of mRNA cap-binding eIF4F
PARK19	AR	***DNAJC6***	Hsp40 homolog
PARK20	AR	***SYNJ1***	Synaptojanin1, PI phosphatase
PARK21	AD	***DNAJC13***	Hsp40 homolog
PARK22	AD	***CHCHD2***	Mitochondrial retrograde transcription factor ?
PARK23	AD	***VPS13C***	Vacuolar sorting protein

A

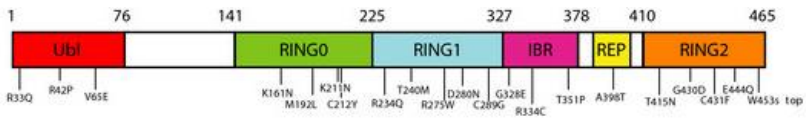

B

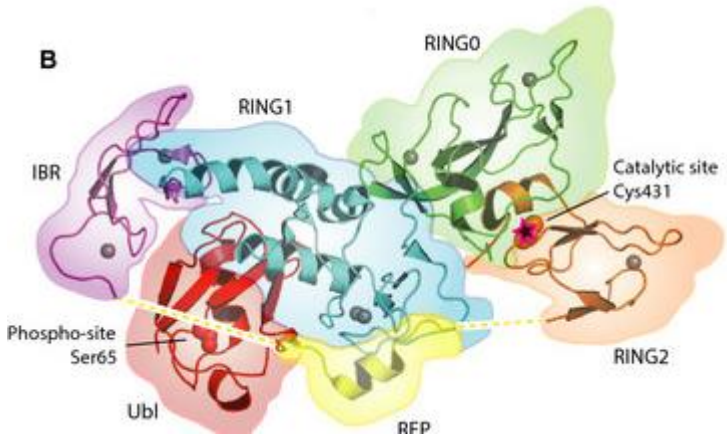

Figure 1. Structure of Parkin

A, Scheme of Parkin domains. Parkin consists of an ubiquitin-like domain (UBL) and really interesting new gene (RING) motifs including RING0, RING1, In-between RING (IBR) and RING2 domains. Indicated mutations are patient mutations in PD. *B,* 3D structure of Parkin. UBL domain has serine 65 phosphorylated by PINK1, and RING2 has catalytic cysteine 431. Referenced by Trempe JF, Sauve V, Grenier K, Seirafi M, Tang MY, Menade M, Al-Abdul-Wahid S, Krett J, Wong K, Kozlov G et al. (2013) Structure of parkin reveals mechanisms for ubiquitin ligase activation. Science 340, 1451–1455.

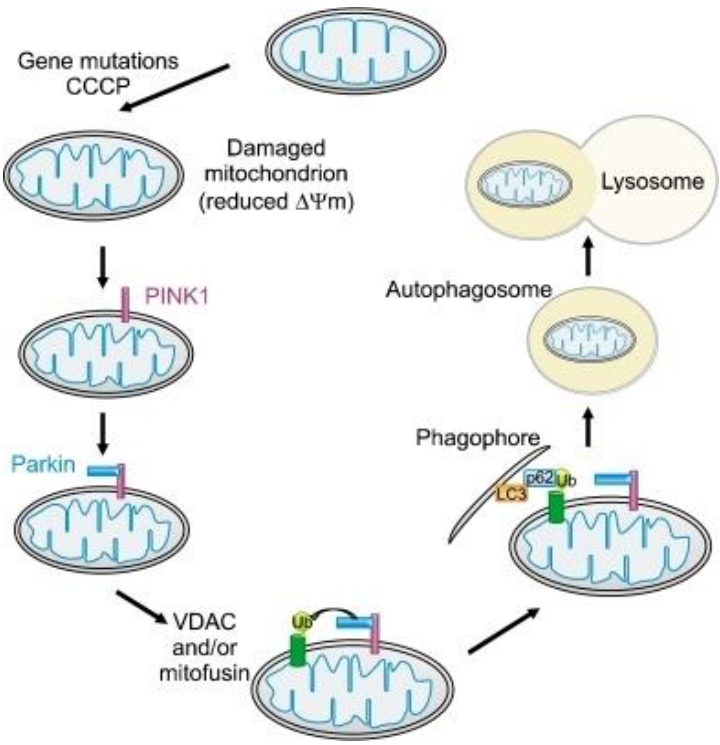

Figure 2. PINK1-Parkin pathway mediates mitophagy

Referenced by Son JH, Shim JH, Kim KH, Ha JY, Han JY (2012) Neuronal autophagy and neurodegenerative diseases. Experimental & Molecular Medicine 44, 89-98.

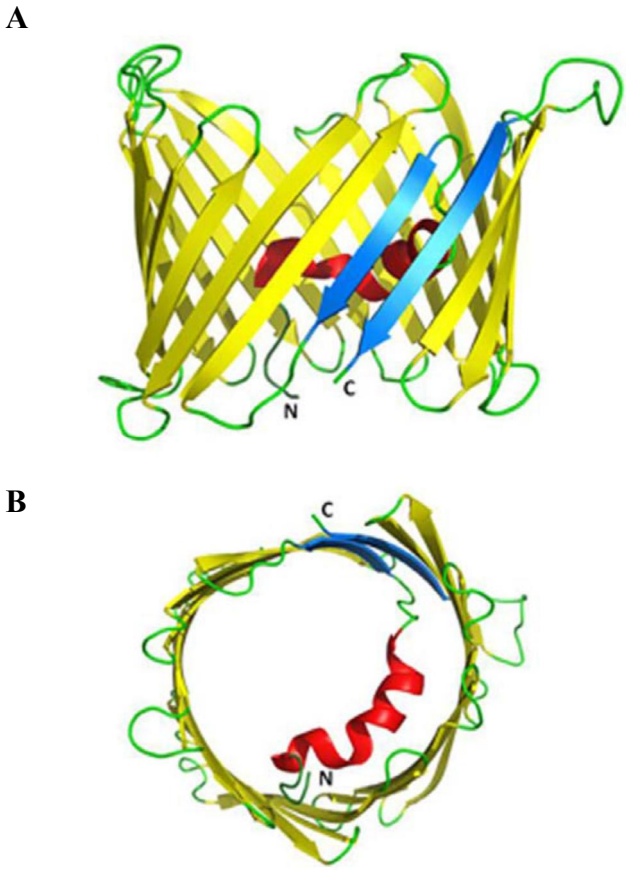

Figure 3. Three-dimensional structure of VDAC1

A, Side-view of the 3D structure of mouse VDAC1 (Ujwal et al., 2008). The β-barrel is consisted by 19 β-strands indicated by yellow colors, and the N-terminal helix is indicated by red color. β-strands 1 and 19 are colored blue. *B*, Top-view of the VDAC1 structure. Referenced by Varda Shoshan-Barmatz and Dario Mizrachi (2012) VDAC1: from structure to cancer therapy. Frontiers in Oncology 2,164.

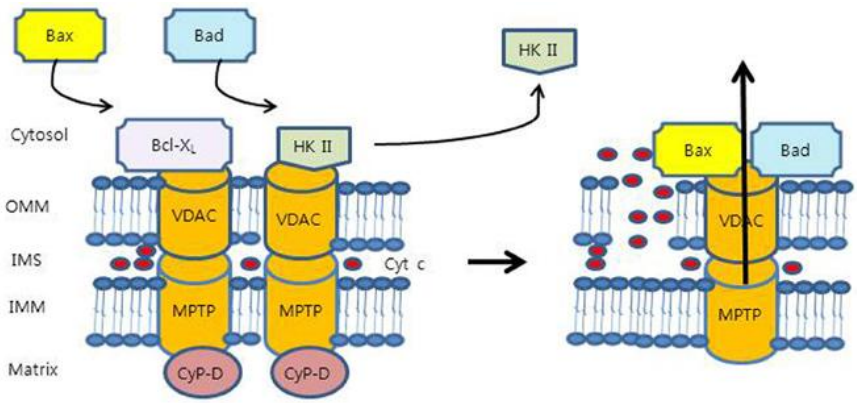

Figure 4. Model describing the regulatory mechanism of apoptosis by VDAC1

VDAC1 is one of the components in the mPTP complex. In normal conditions, VDAC1 pore is closed by interaction with anti-apoptotic protein Bcl-xL and hexokinase 2 (Left panel). Pro-apoptotic proteins such as Bax and Bad can bind to VDAC, which induces cytosolic release of cytochrome C, resulting in apoptosis (Right panel). Referenced by Dong H. Suh, Mi-Kyung Kim, Hee S. Kim, Hyun H. Chung and Yong S. Song (2013) Mitochondrial permeability transition pore as a selective target for anti-cancer therapy. Frontiers in Oncology 3, 41.

VDAC1 is also reported to regulate apoptosis through opening and closing its pore. According to the recent studies, anti-apoptotic proteins such as B-cell lymphoma 2 (Bcl-2) and B-cell lymphoma-extra large (Bcl-xL) (Lan et al., 2010; Shi et al., 2003; Tsujimoto & Shimizu, 2000) or Hexokinase 1 and 2 (HK1 and 2) (Abu-Hamad, Zaid, Israelson, Nahon, & Shoshan-Barmatz, 2008; Arzoine, Zilberberg, Ben-Romano, & Shoshan-Barmatz, 2009; Azoulay-Zohar, Israelson, Abu-Hamad, & Shoshan-Barmatz, 2004; Shoshan-Barmatz, Zakar, Rosenthal, & Abu-Hamad, 2009) inhibit apoptosis by binding to VDAC1, which closes its pore in order to block the cytosolic transport of apoptosis signaling molecules including cytochrome C (Shimizu, Matsuoka, Shinohara, Yoneda, & Tsujimoto, 2001; Shoshan-Barmatz, Krelin, & Chen, 2017). However, pro-apoptotic proteins, such as Bcl-2-associated X protein (Bax) and Bax-like BH3 protein (BID), bind to VDAC1, and open its pore to allow mitochondrial ROS formation, which leads to the release of cytochrome C into the cytosol (Fig. 4). In addition, self-oligomerization of VDAC1 is also reported to regulate apoptosis (Keinan, Pahima, Ben-Hail, & Shoshan-Barmatz, 2013; Nurit Keinan, 2010; Shoshan-Barmatz, Mizrachi, & Keinan, 2013). Apoptotic stimulus such as intracellular H_2O_2 is known to increase oligomerization of VDAC1, and recent results using cryo-electron microscopy showed that VDAC1 indeed forms a dimer and/or a hexamer structure (Goncalves,

Buzhynskyy, Prima, Sturgis, & Scheuring, 2007; Ujwal, Cascio, Chaptal, Ping, & Abramson, 2009). An increase in VDAC1 oligomerization leads to release of apoptotic signaling molecules, including cytochrome C, to the cytosol, which in turn induces apoptosis.

VDAC1-mediated mitochondrial calcium influx is an important mechanism in regulation of apoptosis. VDAC1 mediates mitochondrial calcium influx by binding to ER-localized IP_3 receptor (IP_3R) and grp75, which tethers mitochondria and ER, forming mitochondria-associated ER membranes (MAM) (Patergnani et al., 2011; Szabadkai et al., 2006). This suggests a mechanism in which an increase in calcium level in ER or in the cytosol induces VDAC1-mediated calcium transport into mitochondria. The mitochondrial calcium uniporter (MCU) in the inner mitochondrial membrane plays a crucial role in mediating calcium flux all the way into the matrix (Fig. 5). A recent study reported that VDAC1 directly interacts with MCU, which enables calcium influx into the matrix (Liao et al., 2015). An increase in calcium influx causes mitochondrial swelling, which leads to rupture of the outer mitochondrial membrane and subsequent release of cytochrome C to the cytosol resulting in apoptosis (Shoshan-Barmatz, De, & Meir, 2017).

This thesis study is divided into two parts. Firstly, the mechanism of PARK2 (Parkin) activation by the UBL domain has been studied. Secondly, the regulatory mechanism of mitophagy and apoptosis by mono- and poly-ubiquitination of VDAC1 has been investigated. As a conclusion, I suggest that VDAC1 is critical for the regulation of mitochondrial homeostasis in the PINK1-Parkin pathway and is a potential medication target for PD.

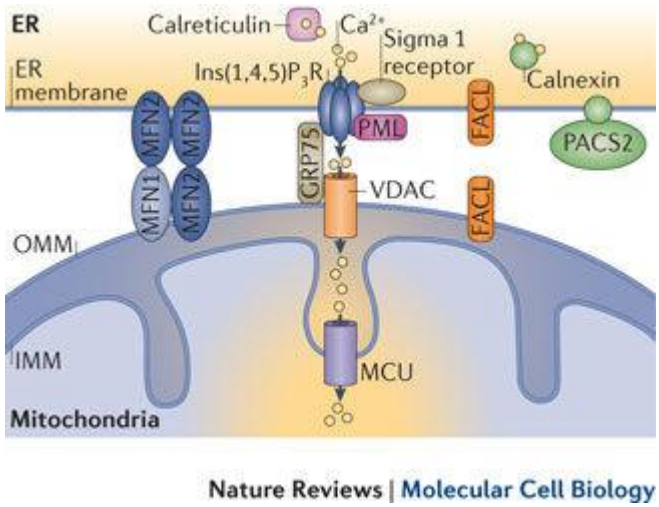

Figure 5. Mitochondrial calcium uptake in ER-mitochondrial contact via interaction between VDAC1 and IP_3R

Close interactions between the endoplasmic reticulum (ER) and mitochondria are essential for rapid and sustained Ca^{2+} uptake by mitochondria, which are responsible for high Ca^{2+} microdomains in VDACs at the outer mitochondrial membrane (OMM). Transportation of Ca^{2+} into the mitochondrial matrix occurs via the mitochondrial Ca^{2+} uniporter (MCU), which rapidly accumulates Ca^{2+} across the steep electrochemical gradient. Referenced by Rosario Rizzuto (2012) Mitochondria as sensors and regulators of calcium signalling. Nature Reviews Molecular Cell Bology 13, 566-578.

Materials and Methods

PART 1. Regulation of Parkin E3 ligase by its own UBL domain

Antibodies and reagents

Rabbit anti-HA (Cell Signaling Technology), mouse anti-GST (Upstate Biotechnology), rabbit anti-GFP (Santa Cruz), mouse or rabbit anti-Myc (Cell Signaling Technology), rabbit anti-ubiquitin (Cell Signaling Technology), mouse anti-Flag (Medical and Biological Laboratories), mouse anti-MFN2 (Millipore), mouse anti-MFN1 (Abcam), mouse anti-VDAC1 (Santa Cruz), mouse anti-NDUFS3 (Abcam), rabbit anti-COIV4 (Abcam), mouse anti-TIM23 (BD Biosciences), and mouse anti-beta-tubulin (Developmental Studies Hybridoma Bank) antibody were used for immunoblot analyses. Rabbit anti-TOM20 (Santa Cruz) mouse anti-GST (Upstate) antibody, rabbit anti-SQSTM1/p62 (Cell Signaling), and rabbit anti-LC3B antibody (Cell Signaling) were used for immunocytochemistry. CCCP was purchased from Calbiochem. Glutathione-Sepharose 4B beads (GE Healthcare) were used for GST pull down assays.

Plasmids

The N-terminal GST-tagged pEBG vector was used to generate truncated Parkin constructs. The N-terminal GFP-tagged pGFPC1 vector was used to generate the Parkin UBL WT domain and its point mutant constructs (S65A and S65D). For site-directed mutagenesis,

QuickChangeTM kit (Stratagene) was used. Human PINK1 WT 3×Myc, kinase-dead human PINK1 3KD (K219A, D362A and D384A) 3×Myc, N-terminus HA-tagged human VDAC1, and N-terminus Flag-tagged human Parkin were generated using the pcDNA3.1 zeo (+) vector. The pRK5 vector was used to express N-terminus HA-tagged human ubiquitin. The pSuper neo/GFP plasmid was used to express VDAC1 shRNA to knockdown endogenous VDAC1 expression in cells.

Cell culture and transfection

HEK293T and HeLa cells were cultured in DMEM (Invitrogen) supplemented with 10% fetal bovine serum (Invitrogen) at 37°C in a humidified atmosphere of 5% CO_2. HeLa cells stably expressing GFP-Parkin were cultured in advanced DMEM (Invitrogen) with 10% fetal bovine serum (Invitrogen), 5 μg/ml puromycin (Invitrogen), 200 mM L-glutamine (Invitrogen) at 37°C in a humidified atmosphere of 5% CO_2. Expression plasmids were transfected using Lipofectamine Plus Reagent (Invitrogen) or PEI (Polyethylenimine; Sigma) according to the manufacturer's instructions.

Cell lysis and immunoblotting

Cells were prepared in Lysis buffer A (25 mM Tris pH 7.5, 150 mM NaCl, 1 mM EDTA, 50 mM NaF, 1 mM sodium vanadate, 2 mM DTT, 1

mM PMSF, 10 g/ml leupeptin, 1 g/ml pepstatin A, and 0.1% NP-40) for GST pull-down assays. Mitochondrial protein immunoblot analyses were performed using RIPA buffer (50 mM Tris pH 8.0, 150 mM NaCl, 0.5% sodium deoxycholate, 1% NP-40, 0.1% SDS, 2 mM DTT, 1 mM PMSF, 10 g/ml leupeptin, and 1 g/ml pepstatin A). Total protein was quantified using the BCA protein assay kit (Pierce). Lysates were subjected to SDS-PAGE analysis followed by immunoblotting according to standard procedures. The blots were developed and visualized using LAS-4000 (Fujifilm).

Ubiquitination assay

Cells were lysed with Lysis buffer B (2% SDS, 150 mM NaCl, and 10 mM Tris, pH 8.0) with the protease inhibitor cocktail (Tajeddine et al.). Transfected cells were harvested and boiled for 10 min at 95^{o}C. Lysis buffer A and Lysis buffer B were mixed at a 10:1 ratio. Samples were incubated at 4^{o}C for 1 hr and centrifuged at 16,000×g for 20 min. Glutathione-Sepharose 4B beads were added to the supernatant of cell lysates and were incubated with rotation at 4^{o}C for 60 min. Beads were washed four times with Lysis buffer A without NP-40. Laemmli 2× sample buffer was added and samples were boiled for 10 min at 95^{o}C and subjected to SDS-PAGE analysis.

Immunofluorescence

HeLa cells were sub-cultured on coverslips in a 12-well tissue culture plate. Cells were treated with 20 μM CCCP or DMSO for 4 hr, washed once with PBS, fixed in 4% paraformaldehyde for 15 min, and permeabilized with 0.5% Triton X-100 in PBS for 5 min. For SQSTM1/p62 and LC3B staining, cells were permeabilized with ice-cold 100% methanol for 20 min. Then, the cells were washed with 0.1% Triton X-100 in PBS (PBS-T) and incubated in blocking solution (4% BSA and 1% normal goat serum in PBS-T) for 1 hr. Primary antibodies were added to the blocking solution and the cells were incubated overnight at 4°C. After washing with PBS-T four times, cells were incubated with appropriate secondary antibodies in blocking solution for 1 hr at room temperature. The antibody-labeled cells were washed with PBS-T for six times and were mounted with mounting solution [100 mg/ml 1,4-diazabicyclo[2.2.2] octane (DABCO) in 90% glycerol]. The slides were observed with a LSM710 laser scanning confocal microscope (Carl Zeiss). All of the immunostaining experiments with HeLa cells were conducted at least three times.

Statistical analysis

The statistical analyses were performed using ANOVA Tukey's test or unpaired *t*-test. The *p* values were calculated from three independent experiments.

PART2: PINK1-Parkin pathway regulates mitophagy and apoptosis through VDAC1 mono- and poly-ubiquitination

Constructs and reagents

Wild-type VDAC1 plasmid was constructed into pcDNA3.1 zeo (+) N-terminal HA-tagged vector and VDAC1 mutants (K12R, K20R, K53R, K109R, K110R and K274R) were generated using a site-directed point mutagenesis method. Flag-tagged (N-terminus) human ubiquitin was cloned in pcDNA3.1 vector and used in construction of ubiquitin lysine mutants (K6R, K11R, K27R, K29R, K33R, K48R and K63R). N-terminus GST-tagged pEBG vector, N-terminus YFP-tagged CMV vector, and N-terminus Myc-tagged pcDNA3.1 zeo (+) vector were used to design Parkin construct used in this study. Parkin C431S, an activity-dead mutation of Parkin, and other Parkin PD patient mutations were constructed by site-directed mutagenesis in either pEBG vector or Myc-tagged pcDNA3.1 zeo (+) vector. In addition, human PINK1 WT 3×Myc and human PINK1 kinase-dead 3KD (K219A, D362A, and D384A) 3×Myc were cloned into pcDNA3.1 zeo (+) vector. Flag-tagged mouse BAX was also cloned into pCDNA3.1 zeo (+) vector.

siRNAs for E2 enzymes used in this study were CDC34

(1028589V), UBE2S (1173805), UBE2D2 (1159045), UBE2D4 (1159057), UBE2A (1159007), UBE2D1 (1159034), UBE2C (1159027), UBE2D3 (1159053), UBE2T (1159238), UBE2N (1159184) and UBE2L3 (1159156). All siRNAs were purchased from Bioneer. Also, cells were treated with carbonyl cyanide m-chlorophenyl hydrazone (CCCP, Calbiochem), Ru 360 (Calbiochem) or cyclosporin A (CsA, Sigma).

Cell culture and transfection

HEK293T, HeLa cells, and mouse embryonic fibroblast (MEF) VDAC1 or Parkin wild type or knockout cell lines were cultured in DMEM (Welgene) supplemented with 10% fetal bovine serum (Invitrogen) at 37°C in a humidified atmosphere of 5% CO_2. HeLa cells stably expressing GFP-tagged Parkin were cultured in advanced DMEM (Invitrogen) with 10% fetal bovine serum (Invitrogen), 5 μg/ml puromycin (Invitrogen), and 200 mM L-glutamine (Welgene) at 37°C in a humidified atmosphere of 5% CO_2.

24 hr prior to transfection, cells were seeded up to 70% in confluency. HEK293T cells were transfected using polyethylenimine (PEI) reagent (Sigma), in which DNA and PEI were mixed together at 1:3 ratio and incubated for 15 min. HeLa and GFP-Parkin-expressing HeLa cells were transfected using lipofectamine LTX (Invitrogen), and MEF cells were transfected using lipofectamine 3000 (Invitrogen) according to the

manufacturer's instruction.

RNA interference

Silencing E2 enzymes was performed with validated siRNA (Bioneer). HEK293 cells were transfected with 20 nM siRNA and DNA constructs for 48 hr using lipofectamine 2000 (Invitrogen) according to the manufacturer's instruction.

Antibodies

Antibodies used for western blot (WB) and immunofluorescence (IF) were rabbit anti-HA (WB, 1:1,000; IF, 1:200; Cell Signaling), mouse anti-Flag (WB, 1:1,000; IF, 1:200; MBL), rabbit anti-ubiquitin (WB, 1:1,000, Cell signaling), mouse anti-GST (WB, 1:1,000, Upstate), mouse anti-Myc (WB, 1:1000, MBL), rabbit anti-p62/SQSTM1 (IF, 1:200; Cell Signaling), rabbit anti-LC3B (IF, 1:200; Cell Signaling), rabbit anti-MFN1 (WB, 1:1,000, Abcam), mouse anti-MFN2 (WB, 1:1,000, Abcam), rabbit anti-COXIV (WB, 1:1,000, Abcam), mouse anti-ATP5A (WB, 1:1,000, Abcam), mouse anti-tubulin (WB, 1:1,000, E7 clone, DSHB), mouse anti-cytochrome C (IF, 1:200, Abcam), rabbit anti-cleaved PARP (WB, 1:1,000, Cell Signaling), and rabbit anti-cleaved caspase3 antibody (WB, 1:1,000, Cell Signaling). Peroxidase-conjugated secondary antibodies, mouse anti-TRIT antibody and rabbit anti-Alexa Flour-647 antibodies were purchased from Jackson Laboratory.

Immunofluorescence

HeLa cells, HeLa cells stably expressing GFP-Parkin, and MEF cell lines were sub-cultured on coverslips in a 12-well tissue culture plate. Cells were treated with 20 μM CCCP or DMSO as indicated and fixed in 4% paraformaldehyde for 15 min, and permeabilized with 0.5% Triton X-100 in PBS for 5 min. For staining of p62/SQSTM1, LC3B and cytochrome C, cells were permeabilized with ice-cold 100% methanol for 20 min, and then the cells were incubated in blocking solution (4% BSA and 1% normal goat serum in PBS-T) for 1 hr at room temperature. Primary antibodies were added to blocking solution and the cells were incubated overnight at 4^{o}C. After washing with PBS-T for four times, cells were incubated with appropriate secondary antibodies in blocking solution for 1 hr at room temperature. The antibody-labeled cells were washed with PBS-T for six times and were mounted with mounting solution [100 mg/ml 1,4-diazabicyclo[2.2.2] octane (DABCO) in 90% glycerol]. The slides were observed with a LSM710 laser scanning confocal microscope (Carl Zeiss). All of the immunostaining experiments with HeLa cells were conducted at least three times (n=200). For the Delta vision^{TM} OMX SR microscopy, protocols for detecting immnunofluorescence were identical. VECTASHIELD (VECTA) was used for mounting solution.

Immunoprecipitation and immunoblotting

For immunoprecipitation, cells were lysed using lysis buffer A (20 mM Tris pH 7.5, 100 mM NaCl, 1 mM EDTA, 2 mM EGTA, 50 mM β-glycerophosphate, 50 mM NaF, 1 mM sodium vanadate, 2 mM DTT, 1 mM PMSF, 10 g/ml leupeptin, 1 g/ml pepstatin A, and 1 % Triton X-100) and subjected to immunoprecipitation and immunoblots according to standard procedures. Cell lysates were centrifuged at 3,000*g* and 4°C for 15 min, and then incubated overnight after primary antibodies were added. Lysates were then incubated with protein A/G agarose beads for 2 hr at 4°C, washed 3 times in detergent-free lysis buffer A, and eluted with 2× Laemmli buffer at 95°C. Immunoblot analyses for mitochondrial proteins were performed using RIPA buffer (50 mM Tris pH 8.0, 150 mM NaCl, 0.5% sodium deoxycholate, 1% NP-40, 0.1% SDS, 2 mM DTT, 1 mM PMSF, 10 g/ml leupeptin, and 1 g/ml pepstatin A). Total protein was quantified using the BCA protein assay kit (Pierce). Lysates were subjected to SDS-PAGE analysis followed by immunoblotting according to standard procedures. The blots were developed and visualized using LAS-4000 (Fujifilm).

Statistical analysis

The statistical analyses were performed using ANOVA Tukey's test or unpaired *t*-test. The *p* values were calculated from three independent experiments

Fly stocks

UAS-Porin^{WT}-Flag transgenic flies were previously generated (Park et al., 2010). pUAST-Porin^{K273R}-Flag and pUAST-Porin^{PolyKR}-Flag were generated by mutating pUAST-Flag-Porin^{WT} and microinjected into w^{1118} embryos. All flies were grown on standard cornmeal-yeast-agar medium at 25^{o}C.

Quantification of the wing phenotypes of flies

For quantification, wing phenotypes were measured from female flies at 3 days (n > 100).

Behavioral assays

For the assay of climbing speed, groups of ten 3-day-old females were transferred into 18-cm-long vials and incubated for 5 min at room temperature for environmental acclimatization. After tapping the flies completely down to the bottom, their climbing time for the 15 cm finish line was measured. Five trials were performed for each group and repeated with four different groups. The average climbing time (^s.d.) was calculated for each genotype.

Muscle section and mitochondrial staining

For streptavidin staining or mitoGFP imaging, the head of flies was

removed surgically and the rest of body was fixed in 4% formaldehyde phosphate-buffered saline (PBS) solution for 1 hr at room temperature. After fixation, thoraces were cut in half by dissecting vertically along the bristles in the middle of the thorax and washed by PBS-0.1% Triton X-100 (PBST). The samples were blocked for 30 min at room temperature with PBST containing 3% bovine serum albumin (BSA). Samples were incubated with Alexa 488-conjugated streptavidin (Invitrogen) and TRITC-phalloidine (Sigma) for mitochondria and muscle fiber staining, respectively, at 4°C for 16 hr. The samples were washed with PBST and mounted in 80% glycerol-PBS solution, and then observed with LSM 710 confocal microscope.

TH immunostaining and quantification of DA neurons

30-day-old adult fly brains were fixed with 4% paraformaldehyde and stained with anti-TH antibody as described previously (Park et al., 2006). The samples were observed and imaged by LSM 710 confocal microscope (Carl Zeiss). For quantification of DA neurons, dorsolateral region 1 (DL1) from 10 brains of each genotype were observed in a blind fashion to eliminate bias.

TUNEL assay

Dissected 3-day-old adult thoraces were fixed in 4% paraformaldehyde (PFA) and washed with PBS. Samples were incubated in

0.1 M sodium citrate at 65°C, and cell death was detected using an in situ cell death detection kit (Tajeddine et al.). After TUNEL reaction, the samples were stained by Hoechst (Invitrogen) to detect the nuclei.

Results and Discussion

PART 1

Regulation of Parkin E3 ligase

by its own UBL domain

Background

Autosomal recessive early onset parkinsonism is linked to several loci, including *PARK2* and *PARK6* (Kitada et al., 1998). The *PARK2* gene encodes Parkin, an E3 ubiquitin ligase that consists of 465 amino acid residues. Parkin is composed of an ubiquitin-like (UBL) domain at the N-terminus and a R1-IBR-R2 motif at the C-terminus (Hampe et al., 2006; N. Matsuda et al., 2006; Trempe et al., 2013). Structurally, Parkin resembles a RING-type E3 ligase, but it functions as a RING/HECT hybrid E3 ligase (Beasley, Hristova, & Shaw, 2007; Berndsen & Wolberger, 2014; Fiesel, Moussaud-Lamodiere, Ando, & Springer, 2014; Riley et al., 2013). Parkin functions like a RING-type E3 ligase by interacting with E2 enzymes, UbcH7 and UbcH8, via the IBR domain while the RING1 domain binds to substrates, allowing direct ubiquitination of substrates. Parkin can also function like a HECT-type E3 ligase by catalyzing the transfer of ubiquitin from an E2 ubiquitin-conjugating enzyme to substrates via the active-site residues, C431 and H433. E2 enzymes that support Parkin function as a HECT-type E3 ligase are UbcH7, UbcH8, and Ubc13/Uev1a heterodimer (Lazarou et al., 2013; Wenzel, Lissounov, Brzovic, & Klevit, 2011).

Previous studies have reported that the UBL domain regulates the activity of the proteins that harbor the domain (Aguileta et al., 2015; Elliott et al., 2011; Faesen, Luna-Vargas, & Sixma, 2012; Harper, Besong, Emsley,

Scott, & Dreveny, 2011; Wauer & Komander, 2013). Ubiquitin-specific protease 14 (USP14), a deubiquitinase, associates with the 26S proteasome via its UBL domain and enhances the catalytic function of the proteasome (Hu et al., 2005). The UBL domain also competes with ubiquitin for binding to the catalytic domain of USP4, suppressing the deubiquitinase mechanism of USP4 (Clerici, Luna-Vargas, Faesen, & Sixma, 2014). Haem-oxidized IRP2 ubiquitin ligase-1 (HOIL-1) is an E3 ligase that contains a UBL domain. The UBL domain of HOIL-1 interacts with the 26S proteasome to promote degradation of its substrates by the ubiquitin-proteasome system (Beasley, Safadi, Barber, & Shaw, 2012). The deletion of the UBL domain in Parkin also enhances Parkin auto-ubiquitination activity (Chaugule et al., 2011). Furthermore, an X-ray crystal structure of Parkin revealed that the UBL domain of Parkin binds to its C-terminal catalytic region to block association with E2 (Trempe et al., 2013). These findings raised the possibility that the UBL domain is critical for the regulation of Parkin activation.

Here, I investigate the molecular mechanism that underlies the function of the R1 and the UBL domain of Parkin. I found that the UBL domain of Parkin suppresses Parkin auto-ubiquitination, substrate ubiquitination, mitochondria translocation, and mitophagy via interaction with the R1 domain of the E3 ligase. I also showed that the interaction

between the R1 domain and the UBL domain is diminished when the UBL domain was phosphorylated at S65 by PINK1. Furthermore, I showed that the UBL domain competes with the substrates of Parkin such as VDAC1 for interaction with R1 domain, which regulates Parkin activity. Consistent with these *in vitro* data, Parkin mutations in the UBL domain of PD patients affected the interaction between the R1 domain and the UBL domain. Together, these results suggest that such interaction is critical for proper regulation of Parkin functions both *in vitro* and *in vivo*.

Parkin UBL domain interacts with the R1 domain

Recently, the UBL domain of Parkin has been linked to the auto-inhibitory function of Parkin (Chaugule et al., 2011). However, the mechanism of how the UBL domain and other domains regulate Parkin activation is not known. To identify the regions of Parkin that contribute to the auto-regulatory activity of Parkin, I generated GST-tagged truncation mutants of Parkin (Fig. 6), overexpressed the constructs in HEK293T cells expressing HA-tagged human ubiquitin, and tested their function *in vitro* using an auto-ubiquitination assay. Compared to full-length (FL) Parkin, auto-ubiquitination activity was increased by Parkin mutants that lack the UBL domain, namely by the UBL domain-deletion mutant (ΔUBL) or by the C-terminal RING motifs, R1-IBR-R2 (C) (Fig. 7*A*). To determine whether the UBL domain can suppress the function of Parkin, I tested whether overexpression of the UBL domain with the truncation mutants could suppress their auto-ubiquitination activity. Strikingly, the auto-ubiquitination activity of ΔUBL or C was noticeably lower with overexpression of the UBL domain (Fig. 7*B*), indicating that Parkin auto-ubiquitination is negatively regulated by the UBL domain, in agreement with the previous report (Chaugule et al., 2011).

I hypothesized that the auto-ubiquitination activity of Parkin could be suppressed by direct interaction of the UBL domain with the domains in

the C-terminus of Parkin. To test this hypothesis, I performed co-immunoprecipitation (co-IP) of the GFP-tagged UBL domain with the GST-fused C-terminal regions of Parkin. I confirmed a direct interaction between the UBL domain and C (Fig. 8*A*), and, moreover, found that the R1 domain is sufficient for this interaction (Fig. 8*B*). From these data, I concluded that the UBL domain binds to the R1 domain, through which E2 enzymes interact with Parkin substrates, to negatively regulate Parkin activity. Conserved cysteine residues in the R1 domain, including C238, are important for maintaining the structure of the RING-finger motif of the R1 domain. Mutation of cysteine 238 to serine (C238S) prevented binding of the UBL domain to the R1 domain (Fig. 9) (Ozawa et al., 2013; Trempe et al., 2013). This result indicates that the proper folding of the R1 domain is critical for the interaction between the R1 domain and the UBL domain.

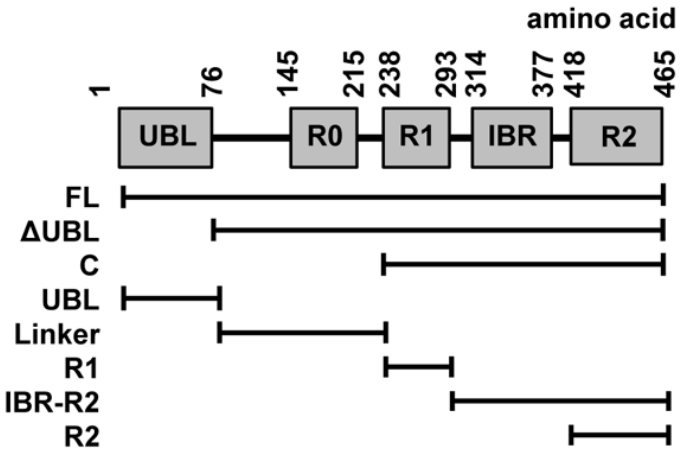

Figure 6. Schematic representation of the domains in human Parkin protein

Full-length (FL) Parkin and truncated Parkin constructs used for this study were shown, including ΔUBL (deletion of the UBL domain), C (R1-IBR-R2), UBL, Linker, R1, IBR-R2, and R2.

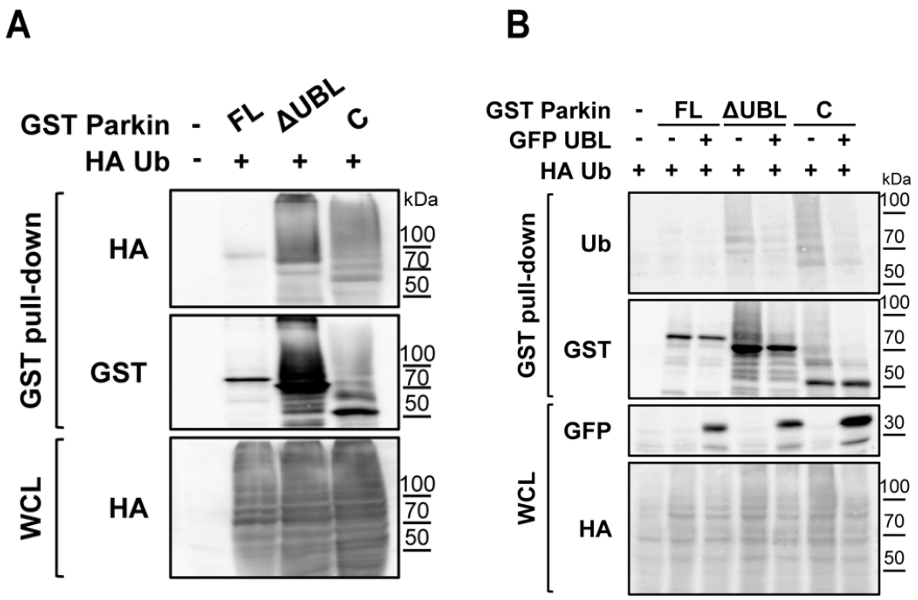

Figure 7. Auto-ubiquitination assays of Parkin in HEK293T cells

Samples were subjected to GST pull-down and analyzed by immunoblot with indicated antibodies.

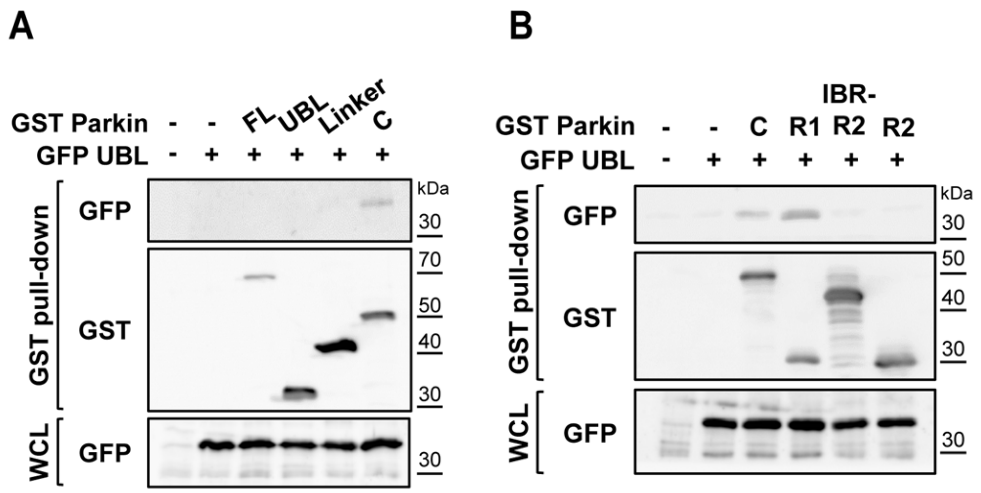

Figure 8. Interaction between the UBL domain and various Parkin deletion mutants

GST-tagged Parkin constructs and GFP-tagged UBL construct were co-expressed in HEK293T cells. Samples were analyzed by immunoblot with indicated antibodies.

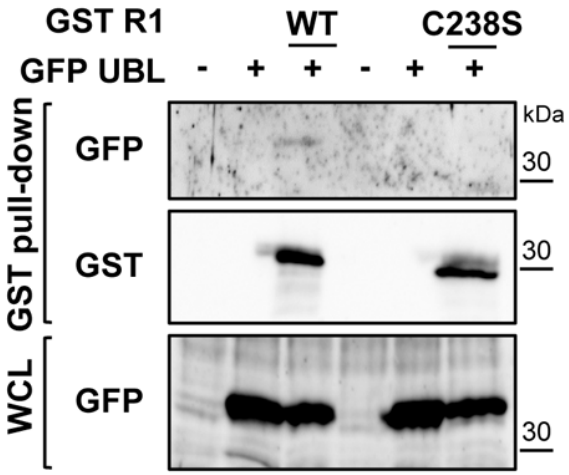

Figure 9. **Interaction between the UBL domain and the R1 domain with mutations**

GST-tagged WT or C238S mutant R1 domain and GFP-tagged UBL domain were expressed in HEK 293T cells. GST pull-down samples were analyzed by immunoblot with anti-GFP antibody (top panel) or anti-GST antibody (middle panel) as indicated. WCL were used to detect the expression levels of GFP-tagged UBL domain (bottom panel).

PINK1 negatively regulates the interaction between the UBL and the R1 domain

PINK1 is an upstream kinase of Parkin that enhances Parkin activity by phosphorylation of the UBL domain (Kazlauskaite, Kelly, et al., 2014; Kondapalli et al., 2012; Shiba-Fukushima et al., 2012). I wanted to determine whether PINK1 regulates the binding between the UBL domain and the R1 domain of Parkin. GST pull-down assays were performed in HEK293T cells overexpressing the GST-tagged Parkin R1 domain and C with the GFP-tagged UBL domain. In CCCP-treated cells (20 μM), the interaction between the UBL domain and C and between the UBL domain and the R1 domain were reduced (Fig. 10*A* and *B*, respectively). To test whether the effect of CCCP treatment is PINK1-dependent, I performed co-IP of the R1 domain and the UBL domain in HEK293T cells overexpressing WT PINK1 or a kinase-dead PINK1 mutant (3KD; K219A/D362A/D384A). Under CCCP treatment, the UBL domain showed a strong interaction with the R1 domain in cells expressing PINK1 3KD, at a level comparable to that in cells with no exogenous PINK1 control, whereas the interaction was weak in WT PINK1-expressing cells (Fig. 11). Together, these results suggest that PINK1 interferes with the interaction between the UBL domain and the R1 domain of Parkin.

Since PINK1 activates Parkin by phosphorylation at S65 of the UBL

domain, I tested whether the phosphorylation contributes to the binding between the UBL domain and the R1 domain. To do this, I performed co-IP of the R1 domain with the WT UBL domain or derivatives of the UBL domain, in which S65 was mutated to alanine or glutamate.

The interaction between the UBL phosphomimetic S65D mutant and the R1 domain was very weak, whereas the interaction between the nonphosphorylatable S65A mutant and the R1 domain was at a level comparable to WT (Fig. 12*A*). Furthermore, the interaction between the R1 domain and the UBL S65A mutant did not show significant difference upon treatment with CCCP (Fig. 12*B*). Thus, I concluded that the interaction between the R1 domain and the UBL domain is regulated by phosphorylation of the UBL domain at S65.

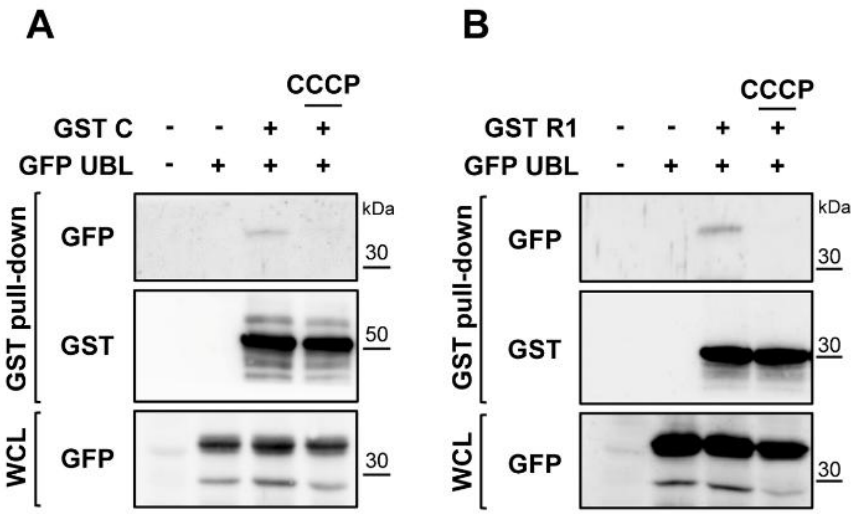

Figure 10. Interaction between the R1 domain and the UBL domain upon CCCP treatment

Cells were treated with 20 μM CCCP for 4 hr. Cell lysates were subjected to GST pull-down and immunoblotted with indicated antibodies.

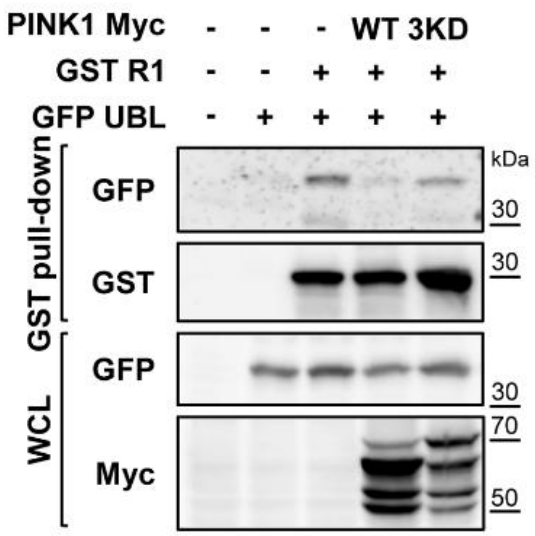

Figure 11. Interaction between the R1 domain and the UBL domain is dependent on PINK1 kinase activity

The C-terminus 3×Myc-tagged PINK1 wild-type (WT) or kinase dead mutant (3KD; K219A, D362A, and D384A) was co-expressed with GST-tagged R1 and GFP-tagged UBL domain in HEK293T as indicated. GST pull-down samples and whole cell lysates were immunoblotted with indicated antibodies.

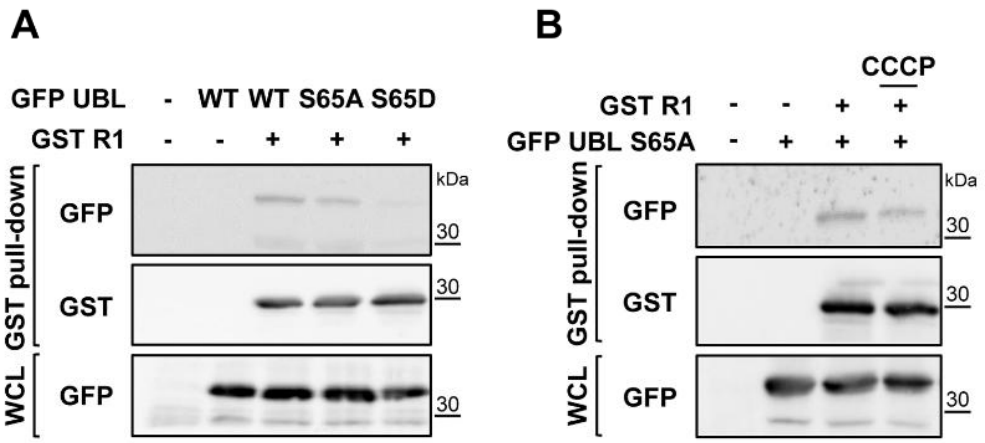

Figure 12. Interaction between the R1 domain and the UBL domain with mutations in serine 65

A, The GFP-tagged UBL WT, S65A, or S65D domain was co-expressed with the GST-tagged R1 domain. GST pull-down samples and whole cell lysates were immunoblotted with indicated antibodies. *B*, The GFP-tagged S65A mutant UBL domain was co-expressed with the GST-tagged R1 domain. Where indicated, cells were treated with 20 μM CCCP for 4 hr.

The UBL domain negatively regulates Parkin activity

To determine whether the weakened interaction between the UBL domain and the R1 domain by phosphorylation at S65 has an effect on Parkin activation, I performed an auto-ubiquitination assay using FL WT Parkin or FL Parkin with S65A or S65D mutation. FL Parkin with S65D mutation showed stronger auto-ubiquitination activity compared to FL WT Parkin or FL Parkin with S65A mutation (Fig. 13*A*), indicating that phosphorylation of Parkin at S65 promotes its E3 ligase activity, in agreement with previous studies (Kondapalli et al., 2012; Shiba-Fukushima et al., 2012). Furthermore, overexpression of the UBL domain strongly suppressed auto-ubiquitination of FL WT Parkin or FL Parkin with S65A or S65D mutation (Fig. 13*A*). These data suggest that exogenous UBL domain blocks Parkin auto-ubiquitination activity by an intermolecular interaction.

I also co-expressed FL WT Parkin with the WT UBL domain or the UBL domain with S65A or S65D mutation in HeLa cells, which have little or no endogenous Parkin expression, and treated the cells with 10 μM CCCP to induce Parkin auto-ubiquitination. As expected, the poly-ubiquitination level in cells expressing FL Parkin alone was comparable to control and, with CCCP treatment, the poly-ubiquitination levels were significantly increased (Fig. 13*B*). The CCCP-induced increase in poly-ubiquitination was noticeably reduced with co-expression of the WT UBL

domain or the UBL domain with S65A mutation, but less with co-expression of the S65D mutant (Fig. 13*B*).

I next sought to determine whether the UBL domain affects Parkin E3 ligase activity by checking the ubiquitination levels of Parkin substrates, VDAC1, Mfn1 and Mfn2. I used a HeLa cell line stably expressing GFP-tagged Parkin, and transfected with the GFP-tagged UBL domain with WT, S65A or S65D mutation. I treated the cells with 10 μM CCCP to measure poly-ubiquitination levels of endogenous substrate proteins. As in the case of Parkin auto-ubiquitination, expression of the UBL domain inhibited the CCCP-induced poly-ubiquitination of Parkin substrates, such as VDAC1, Mfn1, and Mfn2 (Fig. 14). I also observed that the poly-ubiquitination of substrates was reduced with expression of the UBL domain with WT Parkin or Parkin with S65A mutation; however, expression of Parkin with S65D mutation did not affect the poly-ubiquitination level of Parkin substrates (Fig. 14).

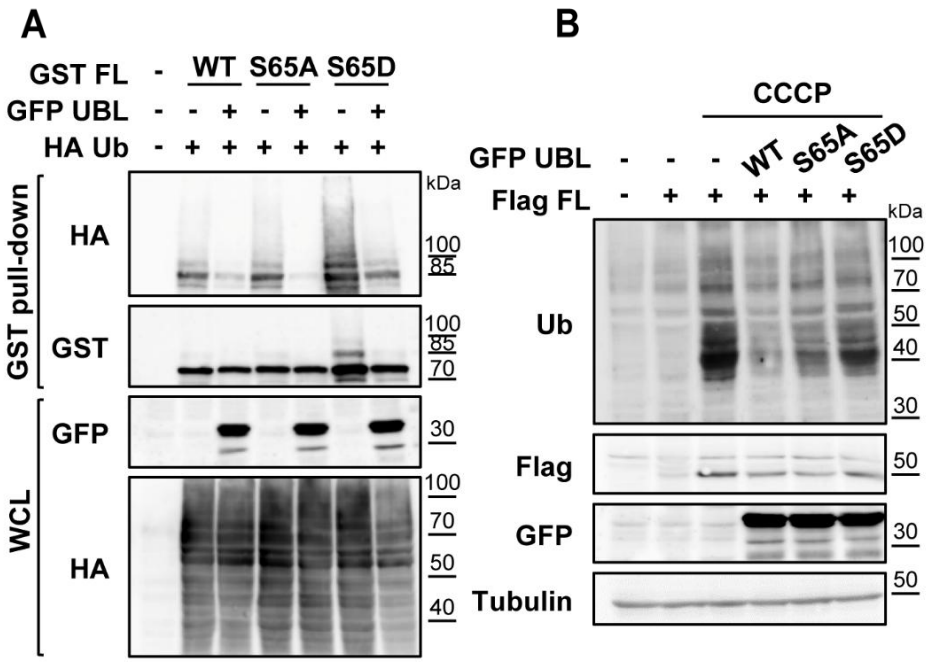

Figure 13. Auto-ubiquitination assays for Parkin with mutations in serine 65

A, The GST-tagged FL WT, S65A, or S65D Parkin was co-expressed with the GFP-tagged UBL WT, S65A, or S65D domain and HA-tagged human Ub in HEK293T cells. GST pull-down samples were analyzed with indicated antibodies. *B*, Flag-tagged FL Parkin and the GFP-tagged WT, S65A, or S65D UBL domain constructs were co-expressed in HeLa cells as indicated. Transfected cells were treated with 20 μM CCCP for 4 hr. WCL were prepared and analyzed for immunoblot with indicated antibodies.

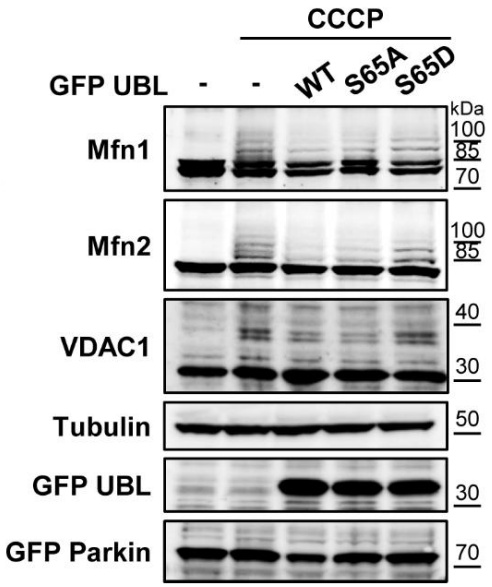

Figure 14. Ubiquitination assays for various Parkin substrates

HeLa cells stably expressing GFP-tagged Parkin were transfected with HA-tagged ubiquitin and the GFP-tagged UBL WT, S65A, or S65D domain and were treated with 10 μM CCCP for 4 hr. WCL were quantified and immunoblotted for endogenous mitochondrial proteins as indicated. Anti-GFP antibody was used to detect the UBL domain and Parkin proteins.

The UBL domain negatively regulates Parkin-mediated mitophagy

I further investigated whether expression of the UBL domain may inhibit this process. The WT UBL domain, the UBL domain with S65A mutation, or the UBL domain with S65D mutation was overexpressed in a HeLa cell line stably expressing GFP-Parkin, and the levels of endogenous mitochondrial proteins were analyzed after treatment with or without 10 μM CCCP for 12 hr. With CCCP treatment, the protein levels of Mfn1, Mfn2, VDAC1, COXIV, TIM23, and NDUFS3 were reduced compared to controls that were not treated with CCCP. Overexpression of the WT UBL domain or the UBL domain with S65A mutation partially prevented the reduction of the protein levels. However, overexpression of the UBL domain with S65D mutation was unable to prevent the CCCP-induced reduction of mitochondrial protein levels (Fig. 15). Next, I observed mitochondria undergoing CCCP-induced mitophagy by using the mitochondrial marker TOM20 (Bingol et al., 2014; Geisler et al., 2010). Levels of TOM20 staining were markedly decreased in HeLa cells expressing GST-tagged FL Parkin with CCCP treatment for 12 hr (Fig. 16). In cells co-expressing FL Parkin and the GFP-tagged wild-type (WT) or S65A UBL domain, TOM20 staining was not decreased with treatment of CCCP compared to control cells expressing FL Parkin alone; however, in cells co-expressing FL Parkin and the S65D UBL domain, TOM20 staining levels were significantly

weaker with CCCP treatment compared to control (Fig. 16). Previous studies have shown that, following CCCP treatment, Parkin translocates to the mitochondria and ubiquitinates various substrates in the mitochondria, and that an adaptor protein containing the LC3B-interaction region (LIR), such as p62/SQSTM1, is recruited to the mitochondria, followed by recruitment of LC3B. This sequence of mitophagy events can be visualized by immunostaining of p62/SQSTM1 and LC3B (Geisler et al., 2010; C. Huang et al., 2011; Okatsu et al., 2010). I further characterized the role of the WT, S65A, or S65D UBL domain in the steps leading to Parkin-mediated mitophagy. In HeLa cells overexpressing FL Parkin, I observed co-localization of Parkin and p62/SQSTM1 in mitochondria, with CCCP treatment for 12 hr (Fig. 17*A*). However, when FL Parkin and the WT or S65A UBL domain were co-expressed, p62/SQSTM1 was not recruited to mitochondria (Fig. 17*A*). In contrast, I observed co-localization of Parkin and p62/SQSTM1 in cells co-expressing the UBL domain with S65D mutation and FL Parkin (Fig. 17*A*). Similar results were observed when CCCP-treated cells were stained with antibody against LC3B; lower levels of LC3B were detected in the mitochondria with the expression of the WT UBL domain or the UBL domain with S65A mutation, whereas LC3B were detected in mitochondria in cells co-expressing the S65D UBL domain at similar levels compared to cells expressing FL Parkin alone (Fig. 17*B*).

These results indicate that the UBL domain can inhibit activation of Parkin E3 ligase activity and Parkin-induced mitophagy, and that this inhibitory function of the UBL domain is negatively regulated by PINK1-dependent phosphorylation at S65.

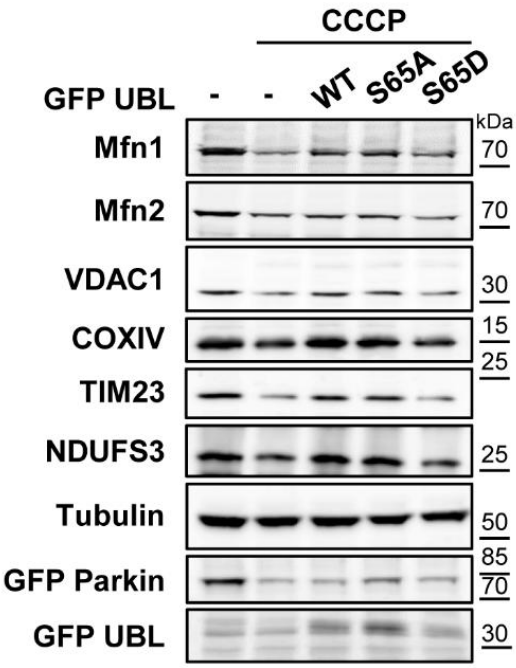

Figure 15. Removal of damaged mitochondria by Parkin-mediated mitophagy

HeLa cells stably expressing GFP-tagged Parkin were transfected with the GFP-tagged UBL WT, S65A or S65D domain and were treated with 10 μM CCCP for 12 hr as indicated. Cell lysates were subjected to immunoblot analyses for endogenous mitochondrial proteins with indicated antibodies.

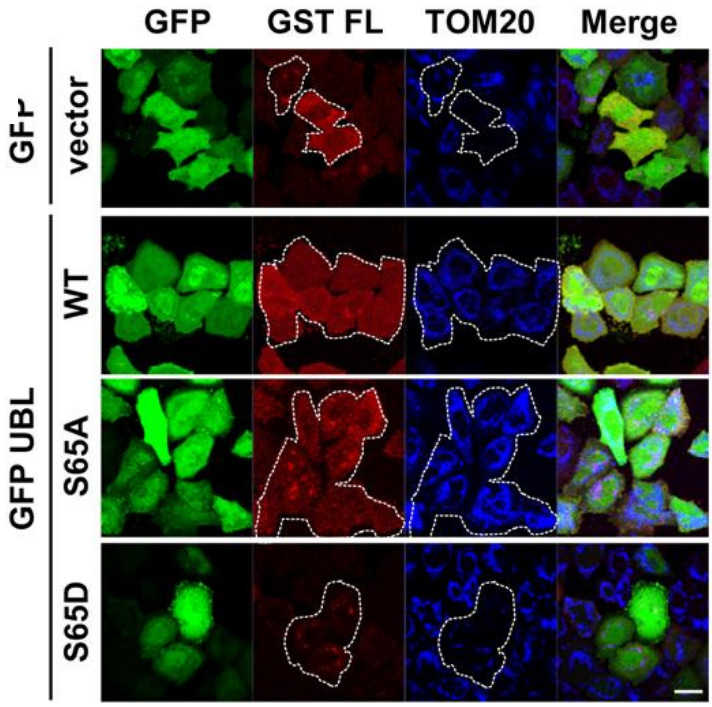

Figure 16. Inhibition of mitophagy by the UBL domain of Parkin

Confocal images of HeLa cells transfected as indicated and treated with 20 μM CCCP for 12 hr. Cells expressing both GST-tagged FL Parkin and the GFP-tagged UBL were marked by dotted circles. GST-tagged FL Parkin proteins were immunolabeled with anti-GST antibody (red) and mitochondria were labeled with anti-TOM20 antibody (Grant et al.). The WT, S65A and S65D UBL domain were GFP tagged (green). Bars, 20 μm. The WT, S65A and S65D UBL domain were GFP tagged (green). Bars, 20 μm.

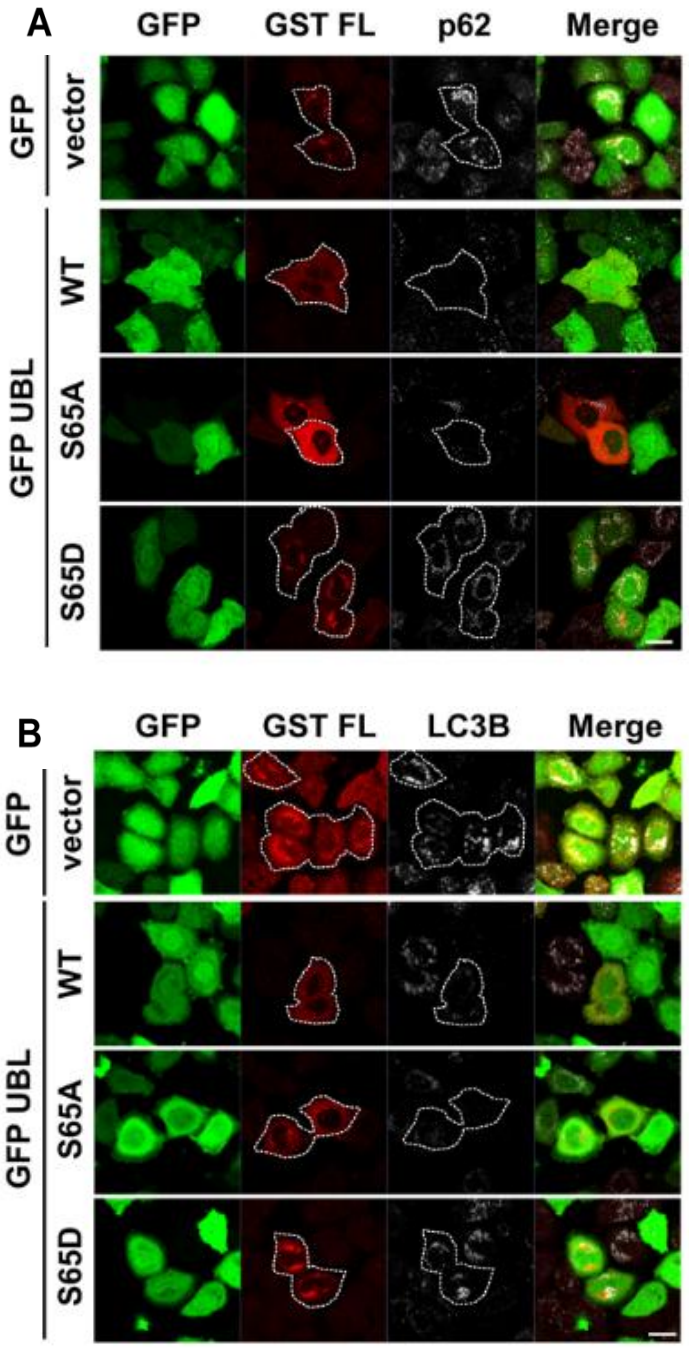
A
GFP
GST FL
p62
Merge
GFP
vector
GFP UBL
WT
S65A
S65D
B
GFP
GST FL
LC3B
Merge
GFP
vector
GFP UBL
WT
S65A
S65D

Figure 17. Impaired recruitment of p62/SQSTM1 and LC3B to damaged mitochondria by the UBL domain of Parkin

Confocal images of HeLa cells transfected as indicated and treated with 20 μM CCCP for 12 hr. GST-tagged FL Parkin protein was immunolabeled with anti-GST antibody (red). To detect mitophagy, cells were stained with anti-p62/SQSTM1 (p62) antibody (gray, *A*) or anti-LC3B antibody (gray, *B*). The WT, S65A and S65D UBL domain were GFP tagged (green). Bars, 20 μm.

The UBL domain regulates Parkin translocation to the mitochondria

Parkin is cytoplasmic but translocates to mitochondria upon activation by PINK1. I sought to determine whether the UBL domain regulates mitochondrial translocation of Parkin. I expressed FL Parkin in HeLa cells, treated the cells with 20 μM CCCP, and observed Parkin translocation to mitochondria using confocal microscopy. FL Parkin was localized in the cytoplasm but translocated to mitochondria with CCCP treatment, as expected (Fig. 18*A*). Surprisingly, when the WT UBL domain was co-expressed with FL Parkin, Parkin showed less localization to mitochondria. However, when the UBL S65D mutant was expressed with FL Parkin, Parkin highly localized to mitochondria (Fig. 18*B*). Quantitative analyses revealed that out of 200 cells that were counted, about 20% of cells showed reduced translocation of FL Parkin to mitochondria when the WT UBL domain was co-expressed; however, co-expression of the UBL domain with S65D mutation showed no difference in the mitochondrial translocation of Parkin compared to control cells that did not express exogenous UBL domain (Fig. 18*C*). Therefore, I concluded that the UBL domain of Parkin negatively regulates CCCP-induced mitochondrial translocation of Parkin.

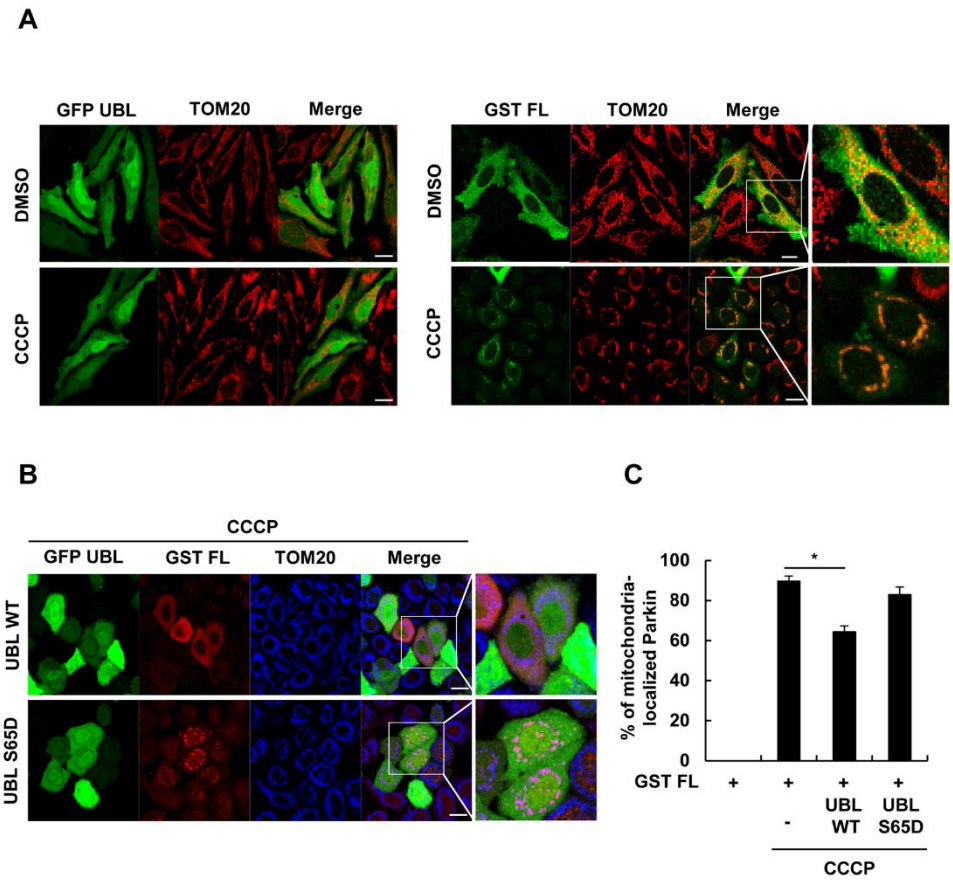
A
GFP UBL
TOM20
Merge
GST FL
TOM20
Merge
DMSO
CCCP
DMSO
CCCP
B
CCCP
GFP UBL
GST FL
TOM20
Merge
UBL WT
UBL S65D
C
% of mitochondria-localized Parkin
100
80
60
40
20
0
*
GST FL
+
+
-
+
UBL WT
+
UBL S65D
CCCP

Figure 18. Delayed Parkin translocation to the mitochondria by the UBL domain

A, Confocal images of Parkin translocation to the mitochondria in HeLa cells. HeLa cells transfected with GST-tagged FL Parkin or the GFP-tagged UBL domain constructs (green) were treated with DMSO (top panel) or 20 μM CCCP (bottom panel) for 4 hr. GST-tagged Parkin protein was immunolabeled with anti-GST antibody (green) and the mitochondria were labeled with anti-TOM20 antibody (red). Bars, 20 μm. *B*, HeLa cells were transfected with plasmids expressing GST-tagged FL Parkin and the GFP-tagged UBL domain with WT or S65D mutation. The cells were treated with 10 μM CCCP for 4 hr and were measured for the subcellular localization of the GFP-tagged UBL WT or S65D (green). The same cells were also immunostained for GST-tagged FL Parkin with anti-GST antibody (red) and for mitochondria with anti-TOM20 antibody (Grant et al.). Bars, 20 μm. C, Quantification of the percentage of Parkin localized to the mitochondria. n = 200. Error bars: S.D. *, $p < 0.05$ by ANOVA Tukey's test.

The UBL domain regulates interaction between Parkin and its substrate VDAC1

The Parkin R1 domain is necessary for Parkin binding to E2 enzymes or its substrates (Y. Zhang et al., 2000). I found above that poly-ubiquitination or mitophagy of Parkin substrates, Mfn1, Mfn2, and VDAC are regulated by the direct interaction of the Parkin UBL domain and the R1 domain (Fig. 14 and 15). This suggests that the interaction may affect Parkin binding to its substrates. Prior to testing this possibility, I first sought to identify Parkin substrates that directly bind to Parkin among previously reported substrates that showed direct binding, namely Mfn1, Mfn2, VDAC1 and Drp1, by co-IP with FL Parkin (Chen & Dorn, 2013; Sun, Vashisht, Tchieu, Wohlschlegel, & Dreier, 2012; Tanaka et al., 2010; H. Wang et al., 2011). I observed that only VDAC1 directly interacts with Parkin (Fig. 19). Next, to identify which region of Parkin interacts with VDAC1, I examined the ability of Parkin deletion mutants to bind to VDAC1. I found that C (Fig. 20*A*) and, more specifically, the R1 domain of Parkin are sufficient for Parkin interaction with VDAC1 (Fig. 20*B*).

To determine whether this inhibition occurs by interfering with the interaction between the R1 domain and VDAC1, I performed co-IP to measure the interaction between the R1 domain and VDAC1 when the WT UBL domain or the UBL S65A or S65D mutant was co-expressed. With co-

expression of the WT UBL domain or the UBL domain with S65A mutation, the interaction between the R1 domain and VDAC1 was noticeably reduced, but co-expression of the UBL domain with S65D mutation showed little or no difference in the ability to interact (Fig. 21). Thus, I concluded that the UBL domain and VDAC1 competitively binds to the R1 domain of Parkin. Furthermore, these results suggest that the UBL domain of Parkin simultaneously regulates the activation of Parkin E3 ligase activity and the interaction between Parkin and its substrates.

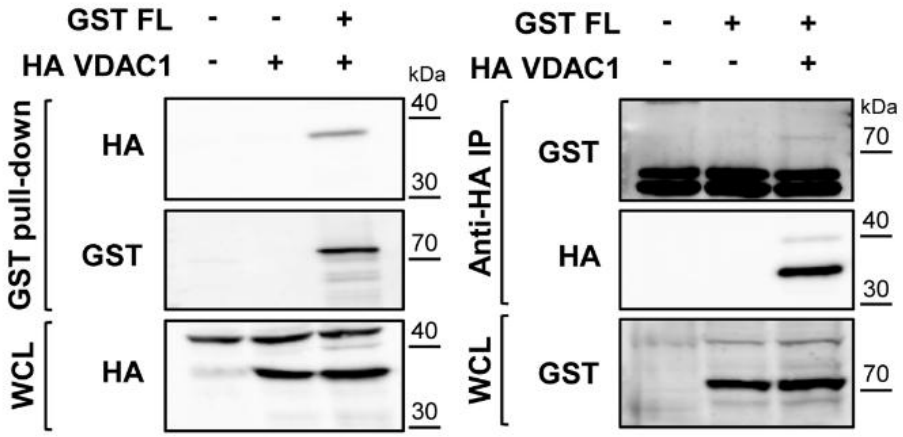

Figure 19. Parkin directly binds to VDAC1

GST-tagged FL Parkin construct was co-expressed with HA-tagged VDAC1 in HEK293T cells as indicated. WCL were subjected to GST pull-down or immunoprecipitation with anti-HA antibody, followed by SDS-PAGE and immunoblot analyses with the indicated antibodies.

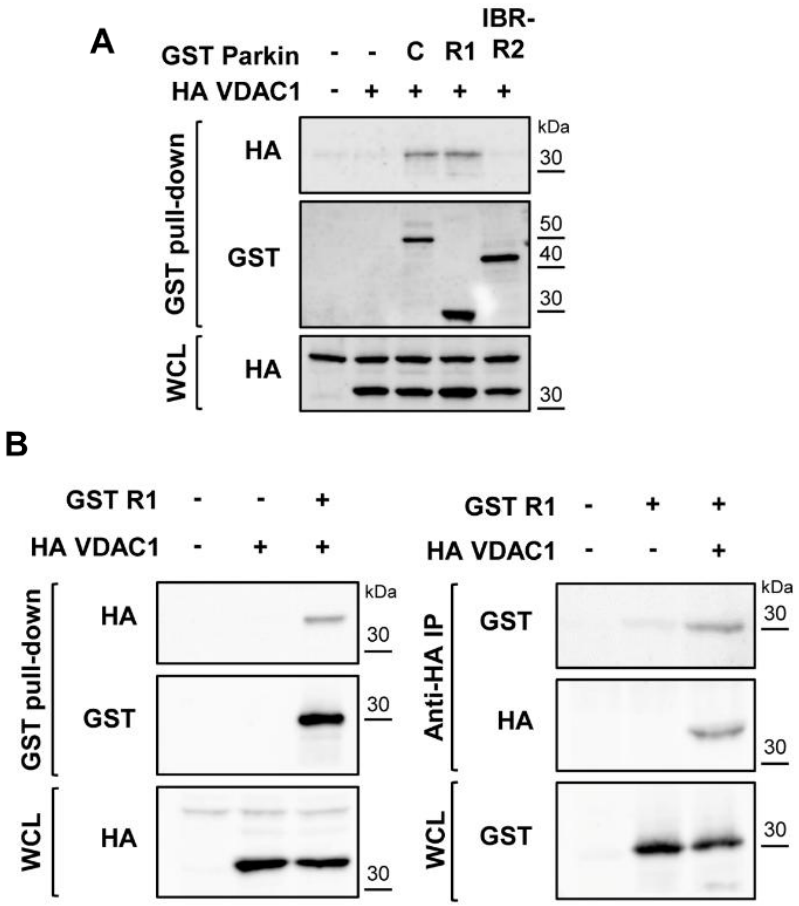

Figure 20. The R1 domain of Parkin interacts with VDAC1

A-B, The GST-tagged C, R1 or IBR-R2 Parkin constructs was co-expressed with HA-tagged VDAC1 in HEK293T cells as indicated. WCL were subjected to GST pull-down or immunoprecipitation with anti-HA antibody, followed by SDS-PAGE and immunoblot analyses with the indicated antibodies.

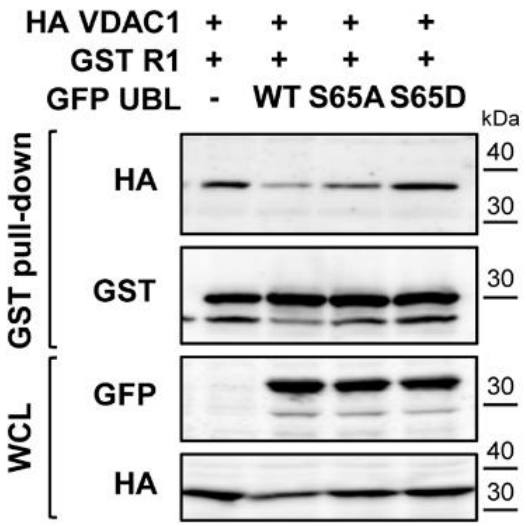

Figure 21. Interaction between VDAC1 and the R1 domain of Parkin is regulated by serine 65 phosphorylation in Parkin

The GST-tagged R1 Parkin construct was co-expressed with HA-tagged VDAC1 and the GFP-tagged UBL WT, S65A, and S65D in HEK293T cells as indicated. WCL were subjected to GST pull-down or immunoprecipitation with anti-HA antibody, followed by SDS-PAGE and immunoblot analyses with the indicated antibodies.

Mutations of the UBL domain identified in PD patients affect Parkin activity

To determine whether the UBL domain plays a role in the pathogenesis of Parkinson's disease, I utilized five mutants of the UBL domain (K27N, R33Q, R42P, A46P and K48A) in Parkin that were previously reported in PD patients (Dev, van der Putten, Sommer, & Rovelli, 2003; Henn, Gostner, Lackner, Tatzelt, & Winklhofer, 2005; Oliveira et al., 2003; E. K. Tan & Skipper, 2007; Terreni, Calabrese, Calella, Forloni, & Mariani, 2001).

I observed the intracellular localization of Parkin in HeLa cells expressing FL WT Parkin or FL Parkin with the pathogenic mutations in the UBL domain. As a negative control, I utilized Parkin with T240R mutation in the R1 domain or C431S mutation in the R2 domain, which are known to hinder interaction with the E2 enzyme or prevent activation of Parkin, respectively (Riley et al., 2013; Shimura et al., 2000). When treated with CCCP, WT, R42P and K48A FL Parkin localized to the mitochondria, but K27N, R33Q and A46P FL Parkin mutants distributed throughout the cytosol (Fig. 22*A*). Also, in agreement with previous reports (Geisler et al., 2010; Geisler, Vollmer, Golombek, & Kahle, 2014; Lazarou et al., 2013; C. Zhang et al., 2014), the T240R or C431S FL Parkin mutant did not translocate to mitochondria (Fig. 22*A*). Quantitative analysis revealed that

about 84% of cells showed translocation of WT FL Parkin to mitochondria with CCCP treatment; however, in cells expressing K27N, R33Q, or A46P mutant, Parkin localization to mitochondria was rare or not detected (Fig. 22*B*). In cells expressing FL Parkin with R42P or K48A mutation, Parkin was localized to mitochondria in 67% or 78% of the cells, respectively (Fig. 22*B*).

To test whether the defect in mitochondrial localization of the pathogenic Parkin mutants is a result of altered interaction between the UBL domain and the R1 domain, I performed an auto-ubiquitination assay to test the inhibitory function of the UBL domain. The auto-ubiquitination activity of FL Parkin with R42P or K48A mutation was higher than that of FL WT Parkin without CCCP treatment indicating that the UBL domain with R42P or K48A mutation loses the ability to tightly regulate Parkin activation (Fig. 7*A*). I also observed that auto-ubiquitination activity of FL WT Parkin and FL Parkin with R42P or K48A mutation was induced by CCCP treatment, compared to that in untreated controls (Fig. 23*A*). However, auto-ubiquitination activity of FL Parkin with K27N, R33 or A46P mutation was low or barely detectable even with CCCP treatment (Fig. 23*A*). These results indicate that K27N, R33Q, or A46P mutation in the UBL domain blocks Parkin activation upon CCCP treatment.

I tested whether auto-ubiquitination levels differ between cells

expressing Parkin mutants that do not lead to an increased auto-ubiquitination, K27N, R33Q or A46P, and Parkin T240R or C431S mutants with CCCP treatment. I found that auto-ubiquitination levels were comparable in cells expressing K27N, R33Q or A46P Parkin mutant and the T240R or C431S mutant controls, even with CCCP treatment (Fig. 23*B*).

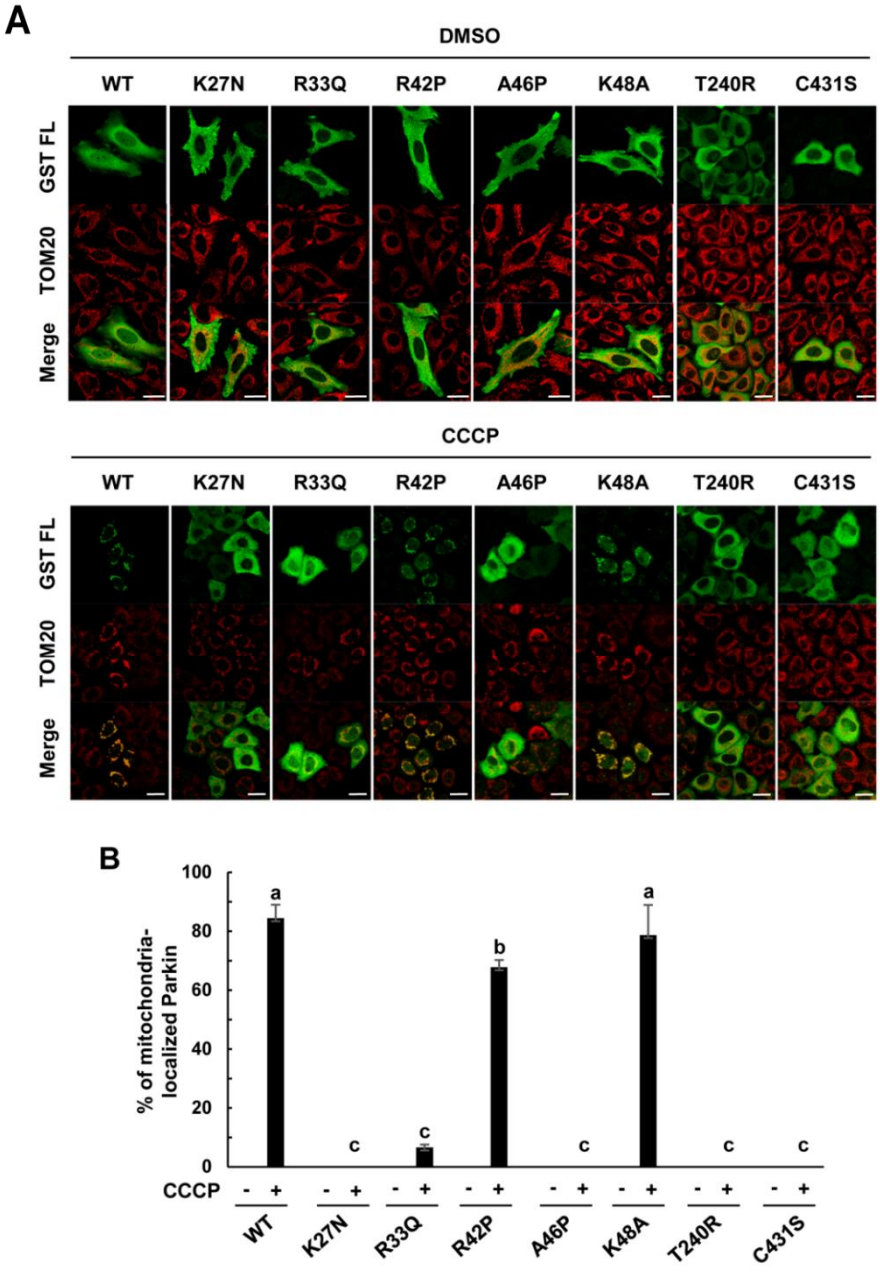
A
DMSO
WT
K27N
R33Q
R42P
A46P
K48A
T240R
C431S
GST FL
TOM20
Merge
CCCP
B
% of mitochondria-localized Parkin
100
80
60
40
20
0
a
b
c
CCCP
- +

Figure 22. Mitochondrial translocation of Parkin with PD pathogenic mutations in the UBL domain

A, Confocal microscopy images of WT Parkin and mutant Parkin with pathogenic mutations in the UBL domain and catalytic sites, such as K27N, R33Q, R42P, A46P, K48A, T240R and C431S. HeLa cells transfected with GST-tagged FL Parkin were treated with DMSO or 20 μM CCCP for 2 hr. Cells were immunostained for GST-tagged FL Parkin constructs with anti-GST antibody (green) and for mitochondria with anti-TOM20 antibody (red). Bars, 20 μm. *B,* Quantification of the percentage of Parkin localized to the mitochondria. n = 200. Error bars: S.D. Different letters indicate the statistical significance by ANOVA Tukey's test. Statistical significance is $p < 0.05$.

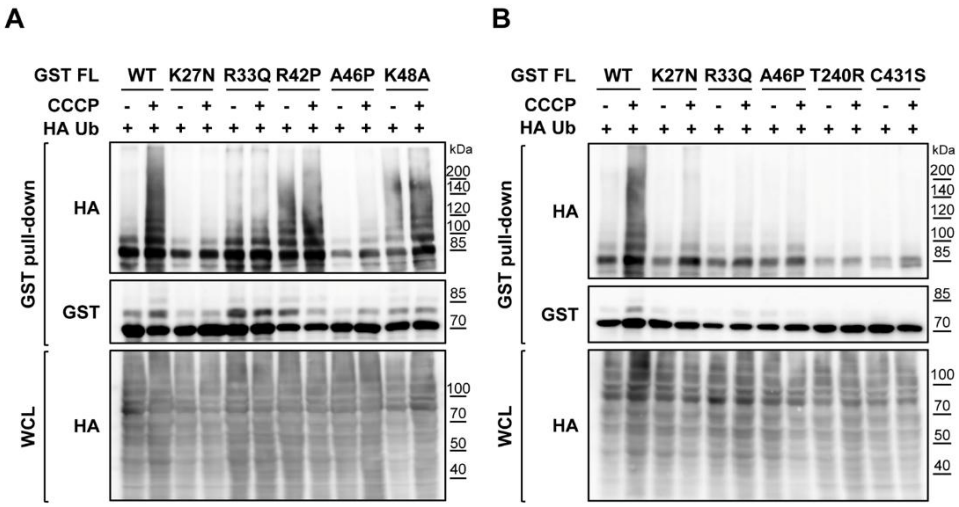

Figure 23. PD pathogenic mutations in the UBL domain disrupt Parkin auto-ubiquitination

A, Auto-ubiquitination assays for Parkin pathogenic mutants in the UBL domain (K27N, R33Q, R42P, A46P and K48A). HEK293T cells were transfected with GST-tagged FL Parkin mutants in the UBL domain and HA-tagged Ub as indicated. Samples were subjected to GST pull-down and immunoblotted with indicated antibodies. HEK293T cells were non-treated or treated with 20 μM CCCP for 2 hr. *B,* Auto-ubiquitination assays for negative controls (T240R and C431S) and Parkin pathogenic mutants in the UBL domain (K27N, R33Q and A46P). HEK293T cells were transfected with GST-tagged FL Parkin mutants and HA-tagged Ub as indicated. HEK293T cells were non-treated or treated with 20 μM CCCP for 2 hr.

To investigate whether the changes in the auto-ubiquitination level of the mutant Parkin proteins are due to changed interactions between the R1 domain and the UBL domain, I examined whether the ability of the UBL domain with K27N, R33Q, R42P, A46P or K48A mutation to bind to the R1 domain is altered compared to the WT UBL domain. Interaction between the R1 domain and the UBL domain with R42P or K48A mutation was decreased compared to the WT UBL domain, as determined by co-IP (Fig. 24*A*). Strikingly, although the interaction between the R1 domain and the WT UBL domain or between the R1 domain and the UBL domain with R42P or K48A mutation was dramatically decreased upon CCCP treatment, the interaction between the R1 domain and the UBL domain with K27N, R33Q, or A46P mutation was not affected by CCCP treatment (Fig. 24*B*). Interestingly, this unaffected interaction between the R1 domain and the UBL domain by CCCP treatment correlated well with the decreased auto-ubiquitination and mitochondria localization levels of FL Parkin with K27N, R33Q, or A46P mutation (Fig. 22 and Fig. 23).

Together, these results strongly suggest that the mechanism of regulating Parkin activation by the interaction between the UBL domain and the R1 domain is linked to PD pathogenesis, and that the interaction can be a key target in developing effective treatments against Parkin-mediated pathogenesis.

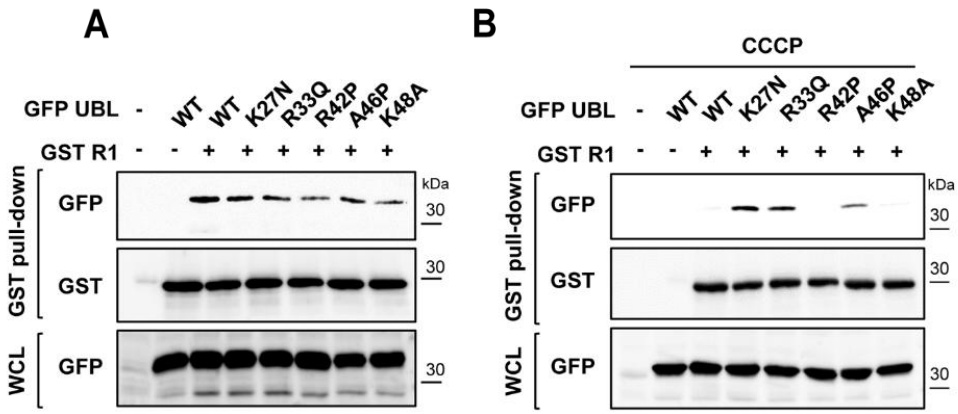

Figure 24. Interaction between the R1 domain and the UBL domain with PD pathogenic mutations of K27N, R33Q or A46P

A-B, The GFP-tagged UBL constructs with K27N, R33Q, R42P, A46P, or K48A mutation and the GST-tagged R1 construct were transfected in HEK293T cells. WCL were subjected to GST pull-down assay followed by immunoblot analyses with anti-GFP antibody (top panel) or anti-GST antibody (middle panel). WCL were immunoblotted with anti-GFP antibody (bottom panel) to detect the expression levels of the GFP-tagged UBL proteins. HEK293T cells were non-treated (*A*) or treated with 20 μM of CCCP for 2 hr (*B*).

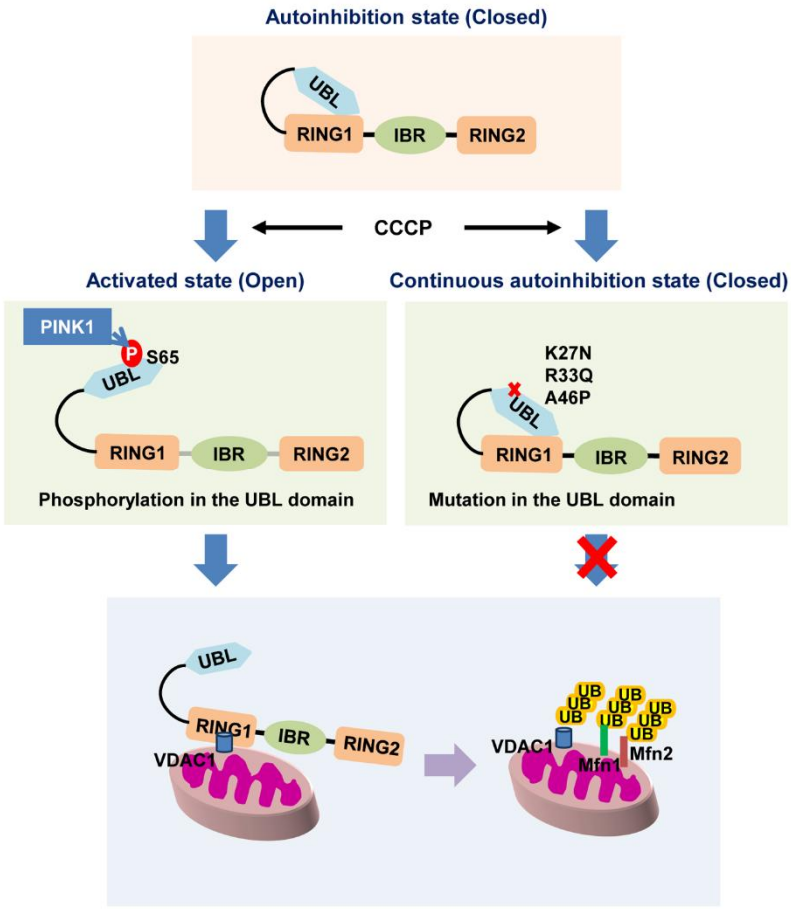
Autoinhibition state (Closed)
UBL
RING1
IBR
RING2
CCCP
Activated state (Open)
Continuous autoinhibition state (Closed)
PINK1
P
S65
UBL
RING1
IBR
RING2
Phosphorylation in the UBL domain
K27N
R33Q
A46P
UBL
RING1
IBR
RING2
Mutation in the UBL domain
UBL
RING1
IBR
RING2
VDAC1
UB
VDAC1
Mfn1
Mfn2

Figure 25. Open and closed conformations of Parkin are regulated by interaction between the R1 and the UBL domain

An intramolecular regulation of Parkin by the UBL domain. Parkin activity is inhibited by interaction of the catalytic R1 domain and the UBL domain. When the UBL domain binds to the R1 domain, Parkin rests in an auto-inhibited, or "closed" state (top panel). Phosphorylation of the UBL domain by PINK1 at S65 leads to decreased binding between the UBL domain and the R1 domain (middle panel, left). The "open" C-terminal catalytic site of Parkin can promote substrate ubiquitination. The R1 domain of Parkin also interacts with VDAC1, and Parkin can translocate to the mitochondria. Parkin localized to mitochondria can ubiquitinate various mitochondrial proteins, including Mfn1, Mfn2, and VDAC1 (bottom panel). Some pathogenic Parkin mutants with missense mutations in the UBL domain (K27N, R33Q and A46P) do not respond to CCCP treatment and maintain the "closed" state (middle panel, right).

Discussion

In this study, I presented evidence that the R1 domain and the UBL domain of Parkin interact, and that this interaction leads to reduced Parkin E3 ligase activity. I also showed that the R1 domain directly binds to VDAC1, and that competitive binding of the UBL domain to the R1 domain prevents Parkin translocation to the mitochondria. Moreover, I demonstrated that PINK1-dependent phosphorylation of Parkin at S65 negatively regulates the interaction between the R1 domain and the UBL domain, suggesting a novel mechanism of how PINK1 regulates Parkin activation (Fig. 25).

Various proteins and functional domains, including ubiquitin-associated proteins (UBAs), ubiquitin-binding proteins (UBPs), ubiquitin-binding domains (UBDs) and ubiquitin-like domain (UBL) share structural similarities with ubiquitin and consist of a L8-I44-V70 hydrophobic patch that interacts with ubiquitin or other target proteins (Beasley et al., 2012; Chaugule et al., 2011; Dieckmann et al., 1998; Lowe et al., 2006; Walters, Kleijnen, Goh, Wagner, & Howley, 2002). The UBL domain of Parkin harbors a hydrophobic patch with a similar structure with conserved I44 and V70 residues. Recently, the determination of the structure of rat FL Parkin by low-resolution X-ray crystallography raised the possibility that the R1 domain may interact with the UBL domain, via the I44 residue of the

hydrophobic patch and the surrounding hydrophobic surface (Trempe et al., 2013). I tested whether the hydrophobic patch in the UBL domain is required for binding between the R1 domain and the UBL domain by generating UBL domain mutants where the I44 or V70 residue was mutated to an alanine. Using co-IP and auto-ubiquitination assays, I showed that there was no effect on interaction between the R1 domain and the UBL domain with I44A or V70A mutation, and that there was no difference in auto-ubiquitination levels of the UBL domain mutants compared to WT. From these data, I deduced that additional amino acids in addition to the hydrophobic patch are required for binding between the R1 domain and the UBL domain.

To further identify amino acid residues that are required for binding between the R1 domain and the UBL domain of Parkin, I generated two Parkin UBL domain derivatives, in which one consisted of amino acid residues 1-35 and the other, of the remaining amino acids, residues 36-76. By co-IP assays, I showed that residues 1-35 of the UBL domain are necessary for binding of the UBL domain to the R1 domain. Three-dimensional structural analysis of the Parkin UBL domain obtained from Research Collaboratory for Structural Bioinformatics (RCSB) Protein Data Bank revealed that four amino acid residues of the UBL domain, F4, R6, P14 and E16, are externally exposed and lie in the same plane (Tashiro et

al., 2003; Tomoo et al., 2008). Furthermore, through sequence analysis, I found that the four amino acid residues are conserved in humans and Drosophila. To investigate whether these residues are required for binding of the UBL domain to the R1 domain, I mutated F4, R6, P14 and E16 into alanines and observed that the interaction between the R1 domain and the UBL domain was abolished. From this, I concluded that the N-terminus of the UBL domain mediates binding to the R1 domain.

As phosphorylation of the Parkin UBL domain at S65 leads to a decreased interaction between the R1 domain and the UBL domain, I investigated whether S65 phosphorylation affects the amino acid residues that participate in binding of the two domains. To do so, I measured the distance between the residues in a 3D configuration. Interestingly, S65 was located not far from the F4 and R6 residues of Parkin, suggesting the possibility that phosphorylation at S65 may affect the interaction between the R1 domain and the UBL domain by interfering these two amino acid residues.

Recently, it has been reported that phosphorylation of Parkin S65 forms a cleft in the 3D structure formed between the UBL domain and C, and that the cleft is filled with an increased number of water molecules (Caulfield et al., 2014). With the conformational change, the distance between the UBL domain and the R1 domain increases from 20 Å to more

than 50 Å, and the binding site of ubiquitin-conjugated E2 within the R1 domain is revealed, leading to docking of the UbcH5a/UBE2D1 E2 enzyme to the R1 domain. This promotes Parkin ubiquitination at C431 and its E3 ligase activity.

In agreement with these structural analyses, I found that phosphorylation of Parkin UBL domain at S65 by PINK1 leads to a decreased interaction between the R1 domain and the UBL domain (Fig. 12). Consistent with this finding, the UBL domain with S65D phophomimetic mutation failed to suppress poly-ubiquitination of Parkin endogenous substrates, in contrast to wild-type or the UBL domain with S65A mutation (Fig. 14). Moreover, I further demonstrated that interaction between Parkin R1 domain and Parkin substrate VDAC1 is regulated by S65 phosphorylation of the UBL domain. Collectively, I provided evidence that PINK1 phosphorylation of Parkin at S65, by preventing binding between the UBL domain and the R1 catalytic region, exposes the R1 domain and, consequently, promotes Parkin E3 ligase activity and translocation to the mitochondria (Fig. 25).

The PINK1 phosphorylation site in the UBL domain is conserved in ubiquitin; ubiquitin is also phosphorylated by PINK1 at S65. Phosphorylation of ubiquitin at S65 leads to increased activation of FL Parkin. Furthermore, Parkin activation is increased in an in vitro ubiquitin

assay when phospho-ubiquitin is co-expressed with WT or S65A mutant of FL Parkin (Koyano et al., 2014; Wauer, Simicek, Schubert, & Komander, 2015a). In order for Parkin to be fully activated, phosphorylation at the S65 residue of both ubiquitin and Parkin UBL domain is required (Kazlauskaite, Kondapalli, et al., 2014). In a recent study, the crystal structure of phospho-ubiquitin and a UBL domain-deleted mutant Parkin (amino acids 140-461) of *Pediculus humanus corporis* was reported. This report suggests the possibility that Parkin activation may be regulated not only by interaction between the R1 domain and the UBL domain, but also by interaction between the R1 domain and phospho-ubiquitin (Wauer, Simicek, Schubert, & Komander, 2015b). In this study, I showed that binding to the R1 domain is decreased when the UBL domain is phosphorylated at S65 (Fig. 12), and that activation of FL Parkin is suppressed when co-expressed with the WT UBL domain or the UBL domain with S65A mutation, but not efficiently (Fig. 13-18). This may be explained by the fact that phospho-ubiquitin also regulates Parkin activation. Further study is needed to address whether phosphorylation of S65 in ubiquitin, in addition to phosphorylation of S65 in the UBL domain, regulates the interaction between the R1 domain and the UBL domain of Parkin.

I found that the interaction between the R1 domain and the UBL domain with K27N, R33Q or A46P mutation was not dissociated by CCCP

treatment (Fig. 23). The tight interaction between the R1 domain and the UBL domain with K27N, R33Q or A46P mutation in the presence of CCCP prevents Parkin translocation to mitochondria and inhibits Parkin auto-ubiquitination (Fig. 22 and Fig. 23). These data suggest that, of the mutations found in PD patients, K27N, R33Q or A46P mutation in the UBL domain leads to a continuous interaction of the UBL domain with the R1 domain, and that the UBL domain interferes with the interaction of the R1 domain with its substrates or E2 enzymes to prevent Parkin activation.

There is also another possibility that K27N, R33Q, and A46P mutations in the UBL domain may inhibit PINK1-dependent Parkin activation by suppressing phosphorylation at S65, which results in continued interaction of the R1 domain and the UBL domain. According to Pao et al. and Shiba-Fukushima et al., Parkin with K27N or A46P mutation decreased the phosphorylation at S65 in the UBL domain compared to WT Parkin (Pao et al., 2016; Shiba-Fukushima et al., 2012).

An additional mechanism of Parkin activation, which involves the phosphorylation of ubiquitin at S65 by PINK1, and the resulting interaction between phosphorylated ubiquitin and the R1 domain of Parkin, has been reported to be required to fully activate Parkin E3 ligase activity (Aguirre, Dunkerley, Mercier, & Shaw, 2017; Koyano & Matsuda, 2015; Koyano et al., 2014). Parkin with K27N or A46P mutation was also resistant to

activation by phosphorylated ubiquitin (Kazlauskaite et al., 2015). This result suggests that K27N and A46P mutations in the UBL domain of Parkin were either not phosphorylated at S65 in the UBL domain or that phosphorylated S65 on ubiquitin did not interact with the R1 domain, leading to inactivated Parkin.

However, Parkin with R33Q mutation showed no difference in ubiquitination at S65 in the UBL domain and in activating with phosphorylated ubiquitin, compared to WT Parkin (Pao et al., 2016). The R33 residue on the UBL domain of Parkin is necessary for interaction with IBR domains, which is crucial for maintaining a folding structure of Parkin. The R33Q patient mutant displayed decreased protein stability as a result of Parkin structural instability (Safadi, Barber, & Shaw, 2011; Trempe et al., 2013). Taken together, these results suggest the possibility that R33Q mutation on Parkin continues to suppress Parkin activity as a result of their abnormal structure that results in continued interaction with the R1 domain of Parkin. However, further study is needed to support this suggestion.

From this, I suggest a new mechanism of PD pathogenesis, in which failure to regulate the interaction between the R1 domain and the UBL domain to regulate Parkin activation, leads to the development of PD.

In summary, my findings indicated that the interaction between the R1 domain and the UBL domain is critical for proper regulation of Parkin function, and that interruption of this regulation may lead to PD pathogenesis. Given the importance of modulating the binding between the two domains in Parkin, development of a new drug that can regulate this interaction may offer exciting possibilities of hindering PD pathogenesis by regulation of Parkin activity and of controlling various cellular processes, such as mitochondrial homeostasis, mitochondrial dynamics, and mitophagy.

PART 2

PINK1-Parkin pathway regulates mitophagy and apoptosis through VDAC1 mono- and poly-ubiquitination

Background

The PINK1-Parkin pathway is important in understanding for the pathological mechanism of Parkinson's disease, which regulates and maintains mitochondrial homeostasis in dopaminergic cells by regulating multiple processes, such as mitophagy and mitochondria-mediated apoptosis.

The PINK1-Parkin pathway regulates apoptosis. Upon mitochondrial depolarization, PINK1 phosphorylates the anti-apoptotic protein Bcl-xL, which prevents apoptotic cell death (Arena et al., 2013). In addition, when cells are treated with mitochondrial uncouplers, such as CCCP that depolarizes mitochondria, PINK1/Parkin-dependent cell death is promoted, and expression of a constitutively active form of PINK1 induces apoptosis (Akabane et al., 2016). Ubiquitination of anti-apoptotic proteins Bcl-xL and Mcl-1 by Parkin results in their degradation, which subsequently induces apoptosis (Carroll et al., 2014; Hollville, Carroll, Cullen, & Martin, 2014). As discussed above, the mechanisms of apoptosis controlled by the PINK1-Parkin pathway is controversial and is not sufficient in explaining that loss of dopaminergic neurons is resulted from the abnormal control of apoptosis in PD patients with mutations in PINK1 or Parkin.

Voltage-dependent anion-selective channel 1 (VDAC1) is one of the

critical Parkin substrates known to be responsible for regulation of mitophagy and apoptosis. VDAC1 localizes at the outer mitochondrial membrane (OMM) and forms a pore consisting of 19 beta-strands with beta barrel structure (Hiller et al., 2008). Also, by forming a complex with cyclophilin D from mitochondrial matrix and adenine nucleotide translocase (ANT) from the inner mitochondrial membrane (IMM), VDAC1 functions as a critical component of mitochondrial permeability transition pore (mPTP), which transports molecules under 1,500 daltons, such as metabolites, calcium and cytochrome C (Baines, 2009; Bernardi & Di Lisa, 2015; Bonora & Pinton, 2014). The released cytochrome C in the cytoplasm activates the mitochondria-dependent caspase cascade to induce apoptosis in the cell.

VDAC1 also regulates mitophagy through interaction with Parkin, which catalyzes K27-linked poly-ubiquitination. This poly-ubiquitination of VDAC1 has been reported to promote the recruitment of Parkin and p62/SQSTM1 to mitochondria (Geisler et al., 2010).

I figure out the PINK1-Parkin pathway can mediate mitophagy and apoptosis process via VDAC1. My research shows that the factor by which the PINK1-Parkin pathway controls mitophagy and apoptosis signaling is VDAC1. Depending on PINK1 and Parkin activation, VDAC1 can be mono- or poly-ubiquitinated at different lysine residues. The poly-

ubiquitination regulates Parkin-mediated mitophagy, while the mono-ubiquitination regulates calcium uptake by mitochondria, which ultimately regulates apoptosis. I also found that K211N Parkin mutant decreases poly-ubiquitination of VDAC1, and T415N Parkin mutant decreases mono-ubiquitination of VDAC1. By showing defective regulation of VDAC1 ubiquitination in Parkin mutants, I try to explain a novel pathological mechanism of PD and propose that VDAC1 can act as a new target for the treatment of PD.

VDAC1 mono- and poly-ubiquitination occur independently and is dependent on PINK1 and Parkin activity

VDAC1 is a critical mitochondrial substrate for Parkin that mediates mitophagy and apoptosis under mitochondrial damage conditions (Geisler et al., 2010; Sun et al., 2012). To investigate the mechanistic steps by which Parkin regulates VDAC1, I examined changes in VDAC1 ubiquitination status in the presence of wild type (WT) Parkin or inactivated form of Parkin C431S (CS), upon CCCP treatment. HEK293T cells were transfected with VDAC1 WT and ubiquitin, and either WT or CS Parkin mutants were treated with CCCP. As expected, VDAC1 was poly-ubiquitinated in the presence of WT Parkin, but no ubiquitination was observed in the cells expressing Parkin CS mutant (Fig. 26). Intriguingly, a characteristic mono-ubiquitination band appeared in VDAC1 protein depending on WT Parkin activity. To confirm the ubiquitination pattern of VDAC1 by Parkin, I employed K0-ubiquitin in which all lysine residues were substituted with arginines, allowing only mono-ubiquitination to occur (Fig. 27). These results confirmed that VDAC1 mono- and poly-ubiquitination occur independently in response to the activity of Parkin.

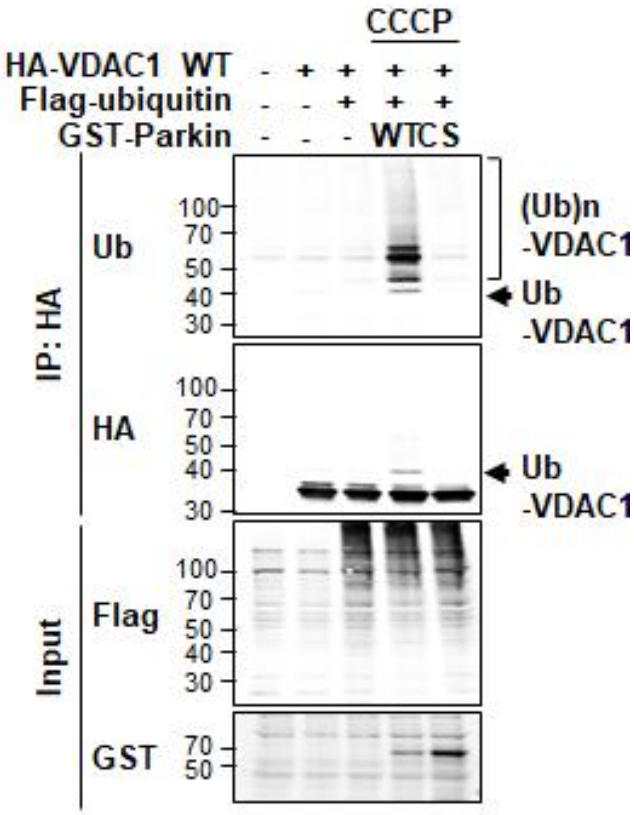

Figure 26. VDAC1 mono- and poly-ubiquitination are induced by Parkin activity

Ubiquitination assays for VDAC1 is depending on Parkin activity. HEK293T cells were transfected with HA-tagged VDAC1 WT and Flag-tagged ubiquitin and GST-tagged Parkin wild type (WT) or activity-dead mutant (CS; C431S) as indicated. HEK293T cells were non-treated or treated with 20 μM CCCP for 4 hr. Samples were analyzed by immunoblot with indicated antibodies.

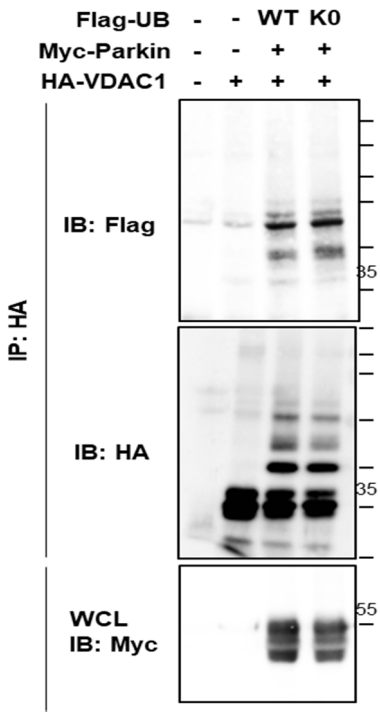

Figure 27. Mono-ubiquitination of VDAC1 is induced by Parkin

HEK293T cells were transfected with HA-tagged VDAC1 WT and Flag-tagged ubiquitin wild type (WT) or ubiquitin mutant with all 7 lysine residues replaced by arginines (K0) as indicated. HEK293T cells were treated with 20 μM CCCP for 4 hr. Samples were analyzed by immunoblot with indicated antibodies.

To identify the residues of VDAC1 where poly- and mono-ubiquitination took place, I aligned and compared VDAC1 sequences over various animal species and found several lysine residues conserved among them (Fig. 28). I generated VDAC1 mutants that replaced conserved lysine residues with arginines and performed an ubiquitination assay in HEK293T cells. As a result, I found lysine residues that corresponded to two different states of ubiquitinated VDAC1: the mono-ubiquitinated lysine residue of VDAC1 was in position of 274, and the poly-ubiquitinated lysine residues were in positions of 12, 20, 53, 109 and 110. To visualize the positions of ubiquitinated lysine residues on VDAC1 protein, I predicted the 3D structure of human VDAC1 protein (Fig. 29). The lysine residues exist at the cytosolic face of the outer mitochondrial membrane, confirming the possibility of the lysine residues acting as ubiquitination sites by Parkin. Also, I observed that the lysine residues in VDAC1 protein are conserved among different species.

To confirm the ubiquitination residues of mono- and poly-ubiquitination on VDAC1, first I transfected HA-tagged VDAC1 WT or K274R (henceforth, Mono KR) and substitutions of lysines at 12, 20, 53, 109 and 110 to arginines of poly-ubiquitination deficient mutant (henceforth, Poly KR) and either WT Parkin or CS Parkin with CCCP treatment in HeLa cells lacking the endogenous Parkin protein. I observed

that Mono KR completely abolished mono-ubiquitination of VDAC1 by Parkin, while Poly KR maintained mono-ubiquitination (Fig. 30).

In my previous study, I established that PINK1 is an upstream regulator of Parkin activity. To test whether ubiquitination of VDAC1 was regulated by PINK1 kinase activity, I performed ubiquitination assay of VDAC1 WT, Mono KR and Poly KR in HEK293T cells expressing PINK1 WT or a kinase-dead form PINK1 mutant (3KD; K219A/D362A/D384A). In VDAC1 Mono KR expressing cells, only mono-ubiquitination of VDAC1 was abolished, while poly-ubiquitination remained (Fig. 31). In contrast, poly-ubiquitination of VDAC1 was decreased in VDAC1 Poly KR expressing cells, and there was no difference in mono-ubiquitination of VDAC1 Poly KR compared to VDAC1 WT. However, both VDAC1 mono- and poly-ubiquitination were not induced by 3KD PINK1-expressing cells. These results indicate that Parkin induces the mono- and poly-ubiquitination of VDAC1 depending on PINK1 activity during mitochondrial damage.

Next, I asked how poly- or mono-ubiquitination of VDAC1 by Parkin occurs differentially. To address this, I sought to list the known E2 enzymes presumed to interact with Parkin and examined their function in determination of VDAC1 ubiquitination types. Upon knockdown of UBE2L3 elicited remarkable decrease of poly-ubiquitination, whereas mono-ubiquitination was intact (Fig. 32). These results suggest that VDAC1

ubiquitination is selectively conferred by different E2 enzymes according to each ubiquitination type.

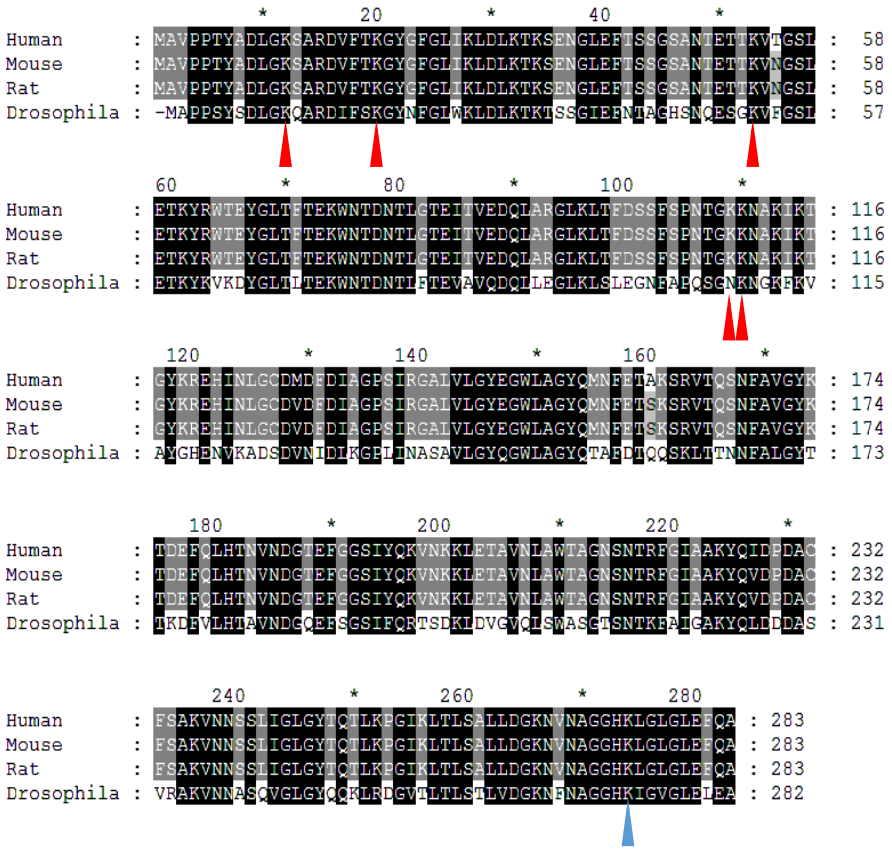

Figure 28. Sequence alignment of VDAC1 proteins from various species

VDAC1 sequences included in the alignment are those of human (P2179.2), mouse (NP_035824.1), rat (NP_112643.1) and *Drosophila* (NP_001260365.1) as indicated. Ubiquitinated lysine residues of VDAC1 are indicated by arrowhead (Red: poly-ubiquitination sites and blue: mono-ubiquitination site). Alignments were generated using the Clustal W server (https://embnet.vital-it.ch/software/ClustalW.html).

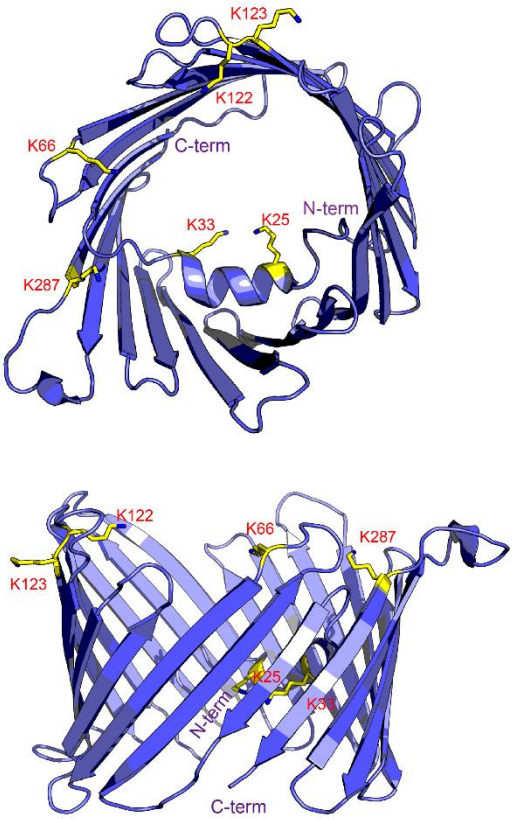

Figure 29. Ubiquitinated amino acid residues on VDAC1 protein

Structural predictions for human VDAC1. Protein structures were predicted using the Phyre_v2.0 server (RCSB PDB file; 5JDP).

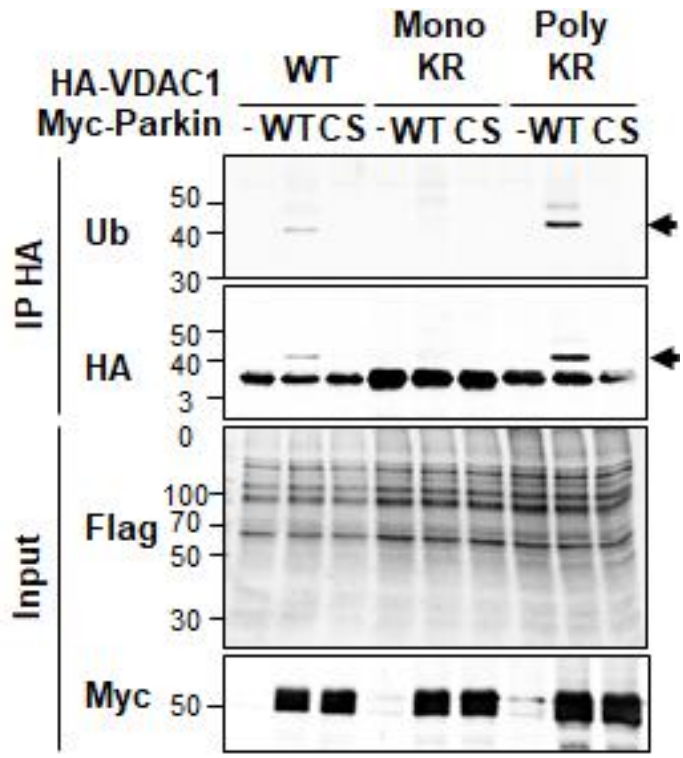

Figure 30. Lysine 274 residue of VDAC1 is mono-ubiquitinated by Parkin activity

HA-tagged WT, Mono KR, or Poly KR VDAC1 was co-expressed with myc-tagged Parkin WT or C431S (CS) in HeLa cells. All cells were also expressed Flag-tagged ubiquitin and treated with 20 μM CCCP for 4 hr. Cell lysates were analyzed for immunoblot with indicated antibody. The mono-ubiquitinated VDAC1 is indicated by arrow.

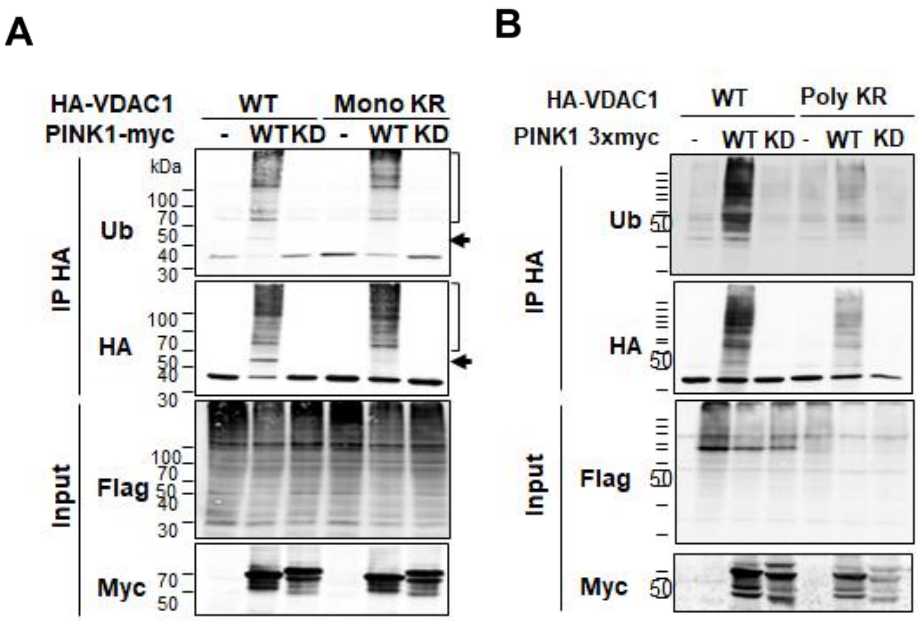

Figure 31. Poly- and mono-ubiquitination on VDAC1 protein depend on PINK1 activity

The C-terminus 3×Myc-tagged PINK1 wild-type (WT) or kinase dead mutant (3KD; K219A, D362A, D384A) was co-expressed with HA-tagged WT or Mono KR or Poly KR mutant VDAC1 in HEK293T as indicated. Samples were immunoblotted with indicated antibodies. The mono-ubiquitinated VDAC1 is indicated by arrow.

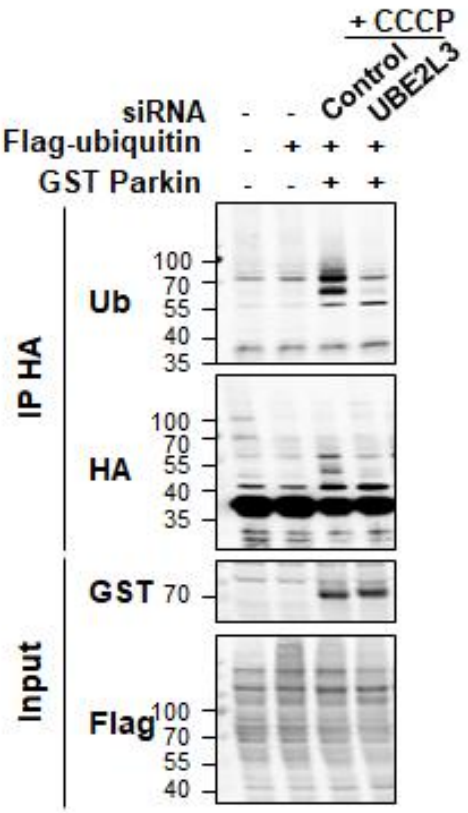

Figure 32. UBE2L3 mediates poly-ubiquitination of VDAC1 by Parkin

HA-tagged WT VDAC1 was expressed with GST-tagged Parkin WT and Flag-tagged ubiquitin in HEK293T. Cells were transfected with control or UBE2L3 siRNA, and treated with 20 μM CCCP for 4 hr as indicated. Samples were analyzed for immunoblot with indicated antibodies.

VDAC1 mono- and poly-ubiquitination determine apoptosis and mitophagy, respectively

Having shown that VDAC1 can be either poly- or mono-ubiquitinated by Parkin, I sought to examine the functional role of both types of ubiquitination in mitochondria-related physiologies such as mitophagy and apoptosis. Parkin-mediated mitophagy occurs when various mitochondrial proteins, including VDAC1, are ubiquitinated and recruit p62/SQSTM1 proteins that have an ubiquitin binding motif. LC3B binds with p62 to induce mitophagy. To detect mitophagy, I expressed either the VDAC1 WT or VDAC1 mutants of Mono KR or Poly KR in mouse embryonic fibroblast (MEF) VDAC1 knockout (KO) cell lines co-expressing YFP-Parkin and monitored the recruitment of p62/SQSTM1 and LC3B to mitochondria upon CCCP treatment. Interestingly, expression of VDAC1 Poly KR in VDAC1 KO cells strongly impaired the recruitment of p62/SQSTM1 to mitochondria when treated with CCCP for 6 hr (Fig. 33*A*). In addition, the proportion of mitochondrial LC3B recruitment was defective in VDAC1 KO cells expressing VDAC1 Poly KR compared to expressing VDAC1 WT and Mono KR, which showed increased LC3B recruitment to mitochondria (Fig. 33*B*). These data indicate that poly-ubiquitination of VDAC1 by Parkin is critical for Parkin-mediated mitophagy upon mitochondrial damage.

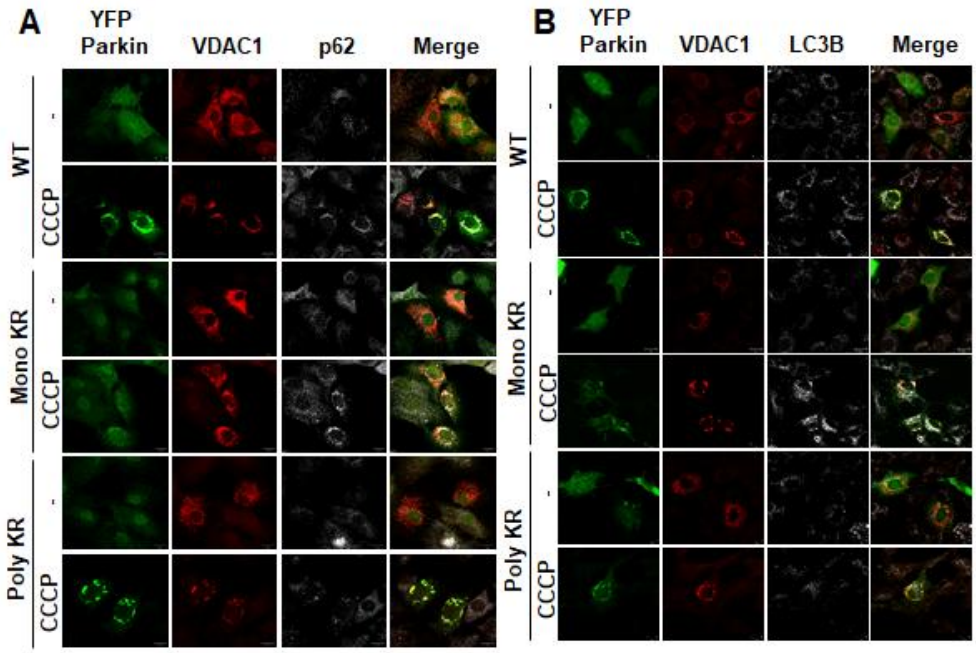

Figure 33. Poly-ubiquitination of VDAC1 regulates recruitment of p62/SQSTM1 and LC3B to mitochondria in Parkin-mediated mitophagy

Confocal images for the recruitment of p62/SQSPM1 and LC3B. VDAC1 knockout MEF cells were transfected with YFP-tagged Parkin and HA-tagged VDAC1 WT, Mono KR or poly KR. Samples were treated with 30 uM CCCP for 8 hr and stained with anti-HA (red), -p62/SQSTM1, or -LC3B antibody (grey).

In contrast to tolerable mitochondrial damage, which leads to mitophagy to reform cellular fidelity via mitochondrial clearance, overwhelming mitochondrial damage often leads to apoptosis (Wang & Youle, 2009). Bax, a pro-apoptotic protein that is a member of the Bcl-2 family, exists in an inactive form in the cytosol of healthy cells. In response to apoptotic stimuli, Bax undergoes conformational change and is inserted into the outer mitochondrial membrane and oligomerized. As a result, cytochrome C is released from mitochondria into the cytosol, which activates Apaf-1 and caspase 9 and subsequently caspases 3 and 7. This ultimately causes mitochondria-mediated cell death (Sarkar, Rahman, & Li, 2003; Smaili, Hsu, Sanders, Russell, & Youle, 2001).

To visualize the apoptotic status affected by expression of VDAC1 WT, Mono KR and Poly KR, I monitored Bax localized in mitochondria and cytochrome C (Cyto C) released to the cytosol in HeLa cells stably expressing GFP-Parkin. I observed that HeLa cells expressing Mono KR had increased levels of Bax in mitochondria and elevated Cyto C release to the cytosol, compared to HeLa cells expressing VDAC1 WT and Poly KR (Fig. 34*A* and Fig. 35). Quantitative analyses revealed that about 30% of cells showed translocation of Bax to mitochondria when VDAC1 Mono KR was expressed. However, in cells expressing VDAC1 WT and Poly KR mutant, Bax localized in mitochondrial was rare, if not detected (Fig. 34*B*).

In addition, I performed western blot analysis of an apoptosis marker, cleaved PARP, to determine whether apoptosis is regulated by VDAC1 Mono KR mutant. Dose-dependent expression of VDAC1 WT, mono KR, and poly KR mutants in GFP-Parkin stably expressing HeLa cells revealed that increase in VDAC1 Mono KR expression was correlated with increased expression of the apoptosis marker cleaved PARP. VDAC1 WT and Poly KR overexpression displayed no such changes in apoptosis marker levels (Fig. 36).

These data suggest that mono-ubiquitination of VDAC1 normally inhibits apoptosis. Taken together with aforementioned data, I conclude that the ubiquitination of VDAC1 by Parkin serves as a signaling converter for either mitophagy or apoptosis depending on the level of mitochondrial damage in the given cellular context.

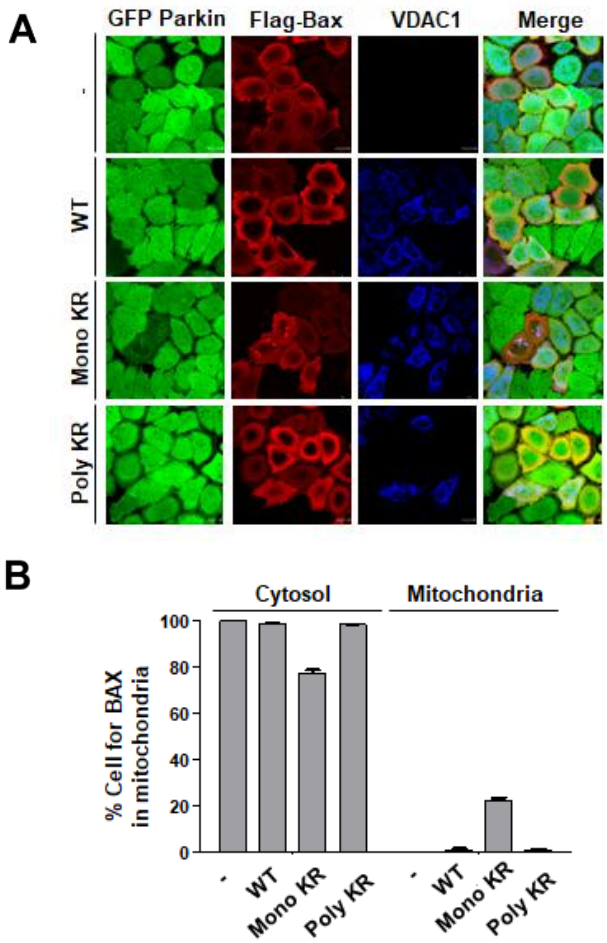

Figure 34. Translocation of Bax to mitochondria was increased by VDAC1 mutant defective in mono-ubiquitination

A, Flag-tagged Bax and HA-tagged VDAC1 were co-transfected in HeLa cells stably expressing GFP-Parkin. Confocal data indicates that Bax (red) and VDAC1 (Grant et al.). *B,* Percentages of cells with Bax localized in mitochondria. n=200 from three independent experiments.

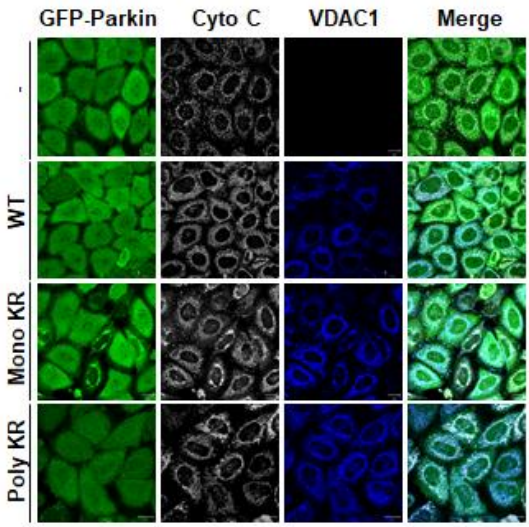

Figure 35. Increased cytochrome C release from mitochondria by VDAC1 mutant defective in mono-ubiquitination

HA-tagged VDAC1 WT, Mono KR or Poly KR was transfected in HeLa cells stably expressing GFP-Parkin. Samples were immunostained for cytochrome C (grey) and HA-tagged VDAC1 (Grant et al.).

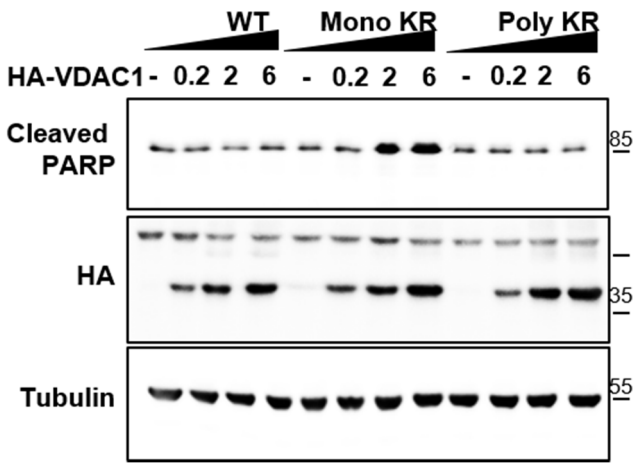

Figure 36. Dose-dependent induction of apoptosis by VDAC1 mutant defective in mono-ubiquitination

Indicated plasmid DNA amounts for expression of HA-tagged VDAC1 WT, Mono KR, or Poly KR were transfected in HeLa cells stably expressing GFP-Parkin. Samples were analyzed with indicated antibodies.

Mono-ubiquitination-deficient VDAC1 mutant induces apoptosis by augmenting mitochondrial calcium uptake

In my previous data, I found that mono- and poly-ubiquitination of VDAC1 by Parkin regulates apoptosis and mitophagy, respectively. To determine whether mono- and poly-ubiquitination of VDAC1 changes mitochondrial morphology by unregulated mitophagy and apoptosis in cells, I analyzed images of mitochondria with OMX delta vision and electron microscopy. I expressed HA-tagged VDAC1 WT or Mono KR in HeLa cells stably expressing GFP-Parkin, and observed mitochondrial morphology by staining the mitochondrial marker TOM20. Interestingly, expression of VDAC1 Mono KR in cells significantly increased mitochondrial size in OMX images, compared to VDAC1 WT (Fig. 37*A*). Consistent with the OMX imaging results, electron microscopic analysis of mitochondria revealed that bigger mitochondria with abnormal cristae dominated in the cell expressing VDAC1 Mono KR, while long and thin mitochondria with intact cristae was abundant in control cells (Fig. 37*B*). Mitochondrial morphology I observed in VDAC1 Mono KR expressed cells was very similar to swollen mitochondria shown in previous reports (von Ahsen et al., 2000; N. Yu et al., 2012).

Mitochondrial swelling has been related to increased mitochondrial calcium uptake following the opening of mitochondrial membrane

permeability transition pores (mPTP), of which VDAC1 is a critical component. Increased mitochondrial calcium uptake induced by mPTP opening can induce cell death by apoptosis (Shoshan-Barmatz, De, et al., 2017; Shoshan-Barmatz, Krelin, & Chen, 2017; Shoshan-Barmatz, Krelin, & Shteinfer-Kuzmine, 2017). Therefore, I hypothesized that the mono-ubiquitination of VDAC1 could be a regulatory process for apoptosis in cells by changing mitochondrial calcium uptake. To test this hypothesis, I measured the mitochondrial calcium level by using 4mitD3 as a mitochondrial calcium indicator (Poburko, Liao, van Breemen, & Demaurex, 2009). This calcium indicator has absorbance wavelength of 433 nm and 536 nm. The intensity of red signal is increased when mitochondrial calcium concentration rises, which indicates that the ratio between green and red signals can be used to visualize an increase in mitochondrial calcium. As expected, mitochondrial calcium levels were significantly increased in cells expressing VDAC1 Mono KR in VDAC1 KO MEF cell lines. There was no difference in mitochondrial calcium levels in cells expressing VDAC1 WT in VDAC1 KO MEF cells or VDAC1 KO MEF cells with empty vector (Fig. 38).

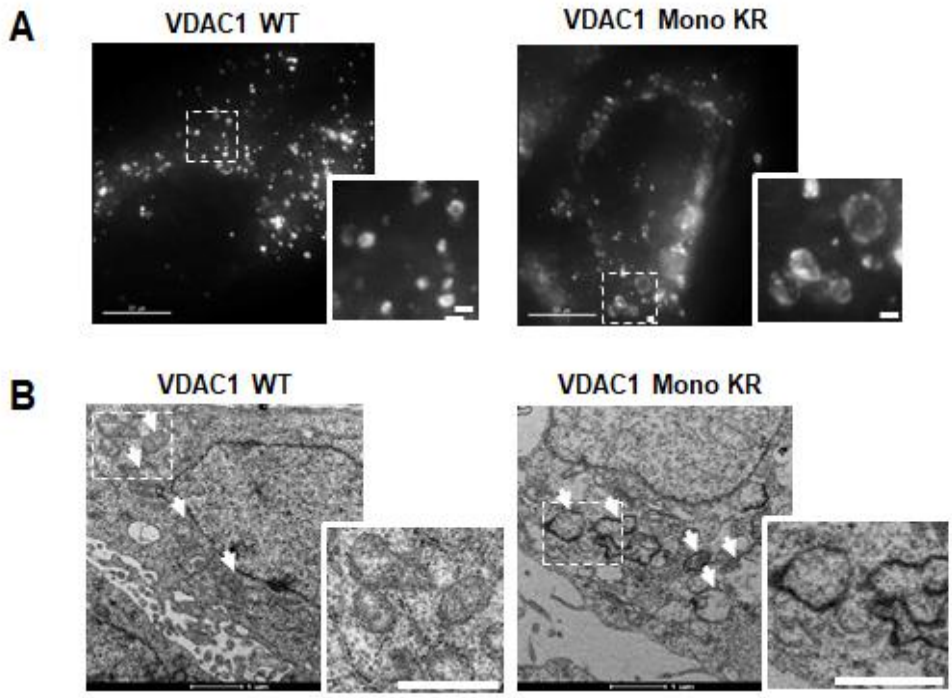

Figure 37. Mono-ubiquitination of VDAC1 is important to maintain normal mitochondrial morphology

A-B, HA-tagged VDAC1 WT or Mono KR was expressed in HeLa cells stably expressing GFP-Parkin. *A,* OMX microscopy images for mitochondrial staining using anti-TOM20 antibody. Bars were 20 um for original images (left). Bars of zoomed images were 1 um (Z. Li et al.).

B, Mitochondrial morphology imaged by electron microscopy. Bars were 1 um.

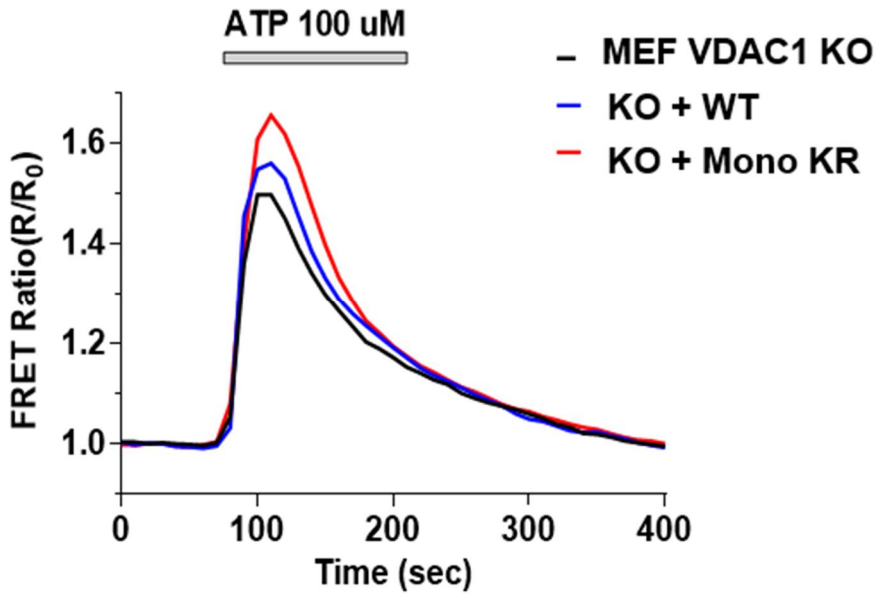

Figure 38. Mono-ubiquitination of VDAC1 regulated mitochondrial calcium uptake

Measurement of mitochondrial calcium in VDAC1 wild type (WT) or knockout (KO) MEF cells. VDAC1 KO MEF cells were transfected with HA-tagged VDAC1 WT or Mono KR mutant. I used the calcium indicator 4mit3D to measure mitochondrial calcium levels. Graph indicates the ratio between green and red signals.

Based on the observation that VDAC1 Mono KR expression increased apoptosis, I hypothesized that Mono KR likely elevated the level of mitochondrial calcium, possibly by opening mPTP. To test this, I first treated the cells expressing Mono KR with the potent mPTP blocker cyclosporin A (CsA) (Sharov, Todor, Khanal, Imai, & Sabbah, 2007). Remarkably, CsA treatment strongly suppressed generation of the apoptotic responses marker cleaved PARP that was induced by Mono KR expression (Fig. 39*A*). Supporting this observation, treatment of mPTP blockers also inhibited mitochondrial localization of Bax mediated by Mono KR expression. These results indicate that increased mPTP opening is the causative factor for VDAC1 Mono KR-mediated apoptosis (Fig. 40).

To further support my hypothesis that blocking mitochondrial calcium uptake suppresses mitochondrial apoptosis induced by VDAC1 Mono KR expression, I used the mitochondrial channel uniporter (MCU) inhibitor Ru360 (Moore, 1971; Ying, Emerson, Clarke, & Sanadi, 1991). MCU was recently reported to be a necessary component for calcium influx to mitochondria, and is located on the inner mitochondrial membrane. I transfected HA-tagged VDAC1 WT or Mono KR in HeLa cells stably expressing GFP-Parkin and analyzed cleaved PARP with or without treatment of Ru360 for 6 hr. As expected, induced apoptosis response of cleaved PARP by Mono KR VDAC1 was significantly decreased when

treated with Ru360 (Fig. 39*B*).

To determine whether Bax localization to mitochondria is suppressed when mitochondrial calcium uptake was blocked in VDAC1 Mono KR-expressing cells, I observed Bax localization in control and Ru360 treated cells. To do this, I transfected GFP-Parkin stably expressing cells with HA-tagged VDAC1 WT, Mono KR, or Poly KR, and then co-transfected with Flag-tagged Bax. Confocal images showed that Bax moved from the cytosol to mitochondria only in Mono KR-expressing cells, but the mitochondrial translocation of Bax was abolished in cells treated with 0.5 mM Ru360 for 6 hr (Fig. 40*A*). In a quantitative analysis, 28% of VDAC1 Mono KR mutant expressing cells showed mitochondrial translocation of Bax, while it was observed in only 1-2% in Ru360 treated control cells. Mitochondrial localization of Bax was rarely or not observed in control VDAC1 WT-expressing cells (Fig. 40*B*). Therefore, I was able to conclude that increased translocation of Bax to mitochondria caused by VDAC1 Mono KR was completely suppressed by blocking mitochondrial calcium uptake. These data showed that VDAC1 Mono KR expression-induced apoptotic responses were mediated by increased mitochondrial calcium uptake, and that this uptake likely occurs by mPTP and MCU, located on the outer and inner mitochondrial membranes.

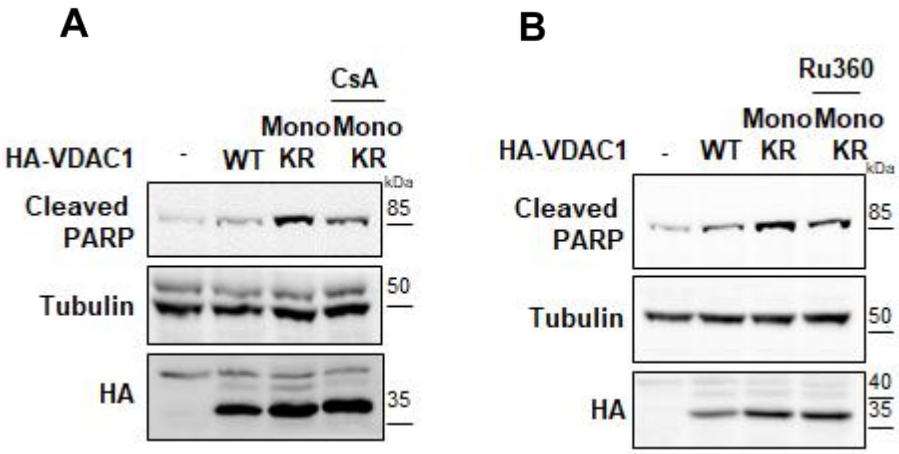

Figure 39. Blocking of mPTP or MCU activity inhibits the apoptosis induced by VDAC1 mutant defective in mono-ubiquitination

A-B, HA-tagged VDAC1 WT or Mono KR was transfected in HeLa cells stably expressing GFP-Parkin. Samples were treated with 1 uM cyclosporine A (CsA) for 6 hr (*A*) or 0.5 mM Ru360 for 8 hr (*B*). All samples were analyzed with indicated antibodies.

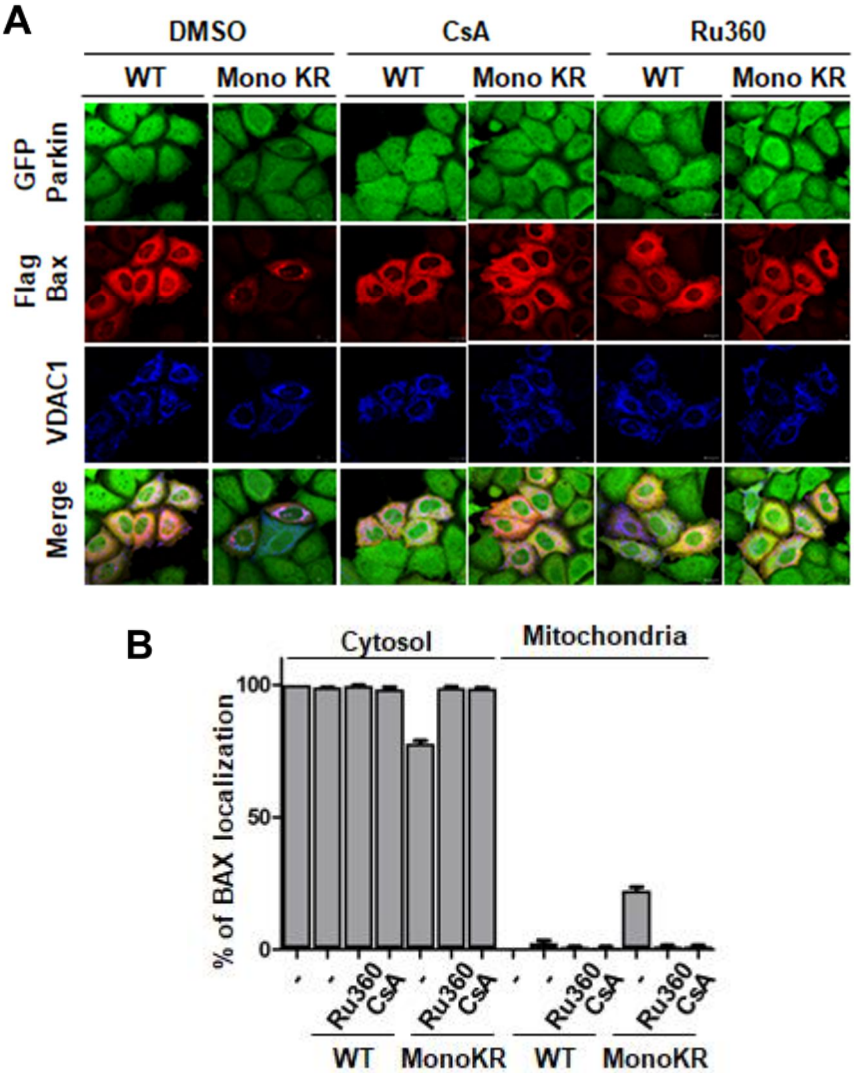
A
DMSO
CsA
Ru360
WT
Mono KR
WT
Mono KR
WT
Mono KR
GFP Parkin
Flag Bax
VDAC1
Merge
B
Cytosol
Mitochondria
% of BAX localization
100
50
0
-
-
Ru360
CsA
-
Ru360
CsA
-
-
Ru360
CsA
-
Ru360
CsA
WT
MonoKR
WT
MonoKR

Figure 40. Inhibition of mPTP or MCU activity blocks mitochondrial translocation of Bax

A, Confocal images for the mitochondrial translocation of Bax. Flag-tagged Bax and HA-tagged VDAC1 were transfected and immunostained using anti-Flag antibody for Bax staining (red) and anti-HA antibody for VDAC1 (Grant et al.) in HeLa cells stably expressing GFP-Parkin. *B,* Quantification analysis for the percentage of cells for the mitochondrial translocation of Bax (n=200, independent three experiments).

VDAC1 mutant flies defective in mono-ubiquitination show enhanced parkinsonian phenotypes

To confirm the results in *Drosophila*, I generated porin (a gene homologous to human VDAC1) WT, Mono KR (K273R), or Poly KR (K12, 20, 53 and 110) expression transgenic flies. Among the poly-ubiquitinated lysine residues in human VDAC1, lysine 109 site was not conserved in *Drosophila*. First, I analyzed expression of porin WT, Mono KR, or Poly KR in the transgenic flies by western blot and concluded that they had equal amounts, and used these *Drosophila* lines to observe PD phenotypes (Park et al., 2006). To observe levels of dopaminergic neuronal loss in porin WT, mono KR, and poly KR expressing flies, I counted the number of dopaminergic neurons in the dorsolateral region 1 (DL1) of the *Drosophila* adult brain. I stained 30-day-old fly brains with tyrosine hydroxylase antibody to visualize individual dopaminergic (DA) neurons, and compared the number of DA neurons of *w1118* (Fig. 41*A*). Porin Mono KR flies showed decreased number of dopaminergic neurons, while porin WT or porin poly KR flies showed similar numbers of dopaminergic neurons compared to the controls (Fig. 41*A* and *B*).

In addition to the number of dopaminergic neurons, I also analyzed wing posture, and mitochondrial morphology and TUNEL assay in thorax muscle of 3-day-old flies. Over 40% of porin Mono KR flies had abnormal

wing posture, while this phenotype was observed in less than 10% in porin WT and poly KR flies (Fig. 42*A*). When I observed mitochondrial morphology in the thoraces of flies, porin Mono KR and Poly KR transgenic flies displayed swollen and clustered mitochondria in thorax muscle. Porin WT flies showed smaller and dispersed mitochondria morphology than the control (Fig. 42*B*). To see if apoptotic processes that were observed in VDAC1 Mono KR-expressing mammalian cells could be replicated in vivo, I performed TUNEL assay in the thorax of *Drosophila*. I observed increased TUNEL signaling only in porin Mono KR transgenic flies, while control, porin WT and porin Poly KR transgenic flies all had no TUNEL signals (Fig. 42*C*). Finally, to examine if VDAC1 ubiquitination affects motor ability in the transgenic flies, I performed climbing ability assay of porin WT, Mono KR and Poly KR flies. While *w1118* control flies or porin WT-expressing flies took 10 seconds or less, porin Mono KR flies took 8 times as long and porin poly KR flies took 3 times as long to complete the task and complete the climbing assay (Fig. 43). Collectively, the results gained from *Drosophila* validated those gained from mammalian cells, and showed that apoptosis occurs in porin Mono KR flies, which ultimately leads to severe PD phenotypes in *Drosophila* models. Porin Poly KR flies also showed mild PD phenotypes, suggesting that poly-ubiquitination also plays a role in PD-related phenotypes, such as mitochondrial homeostasis and

dopaminergic neurons.

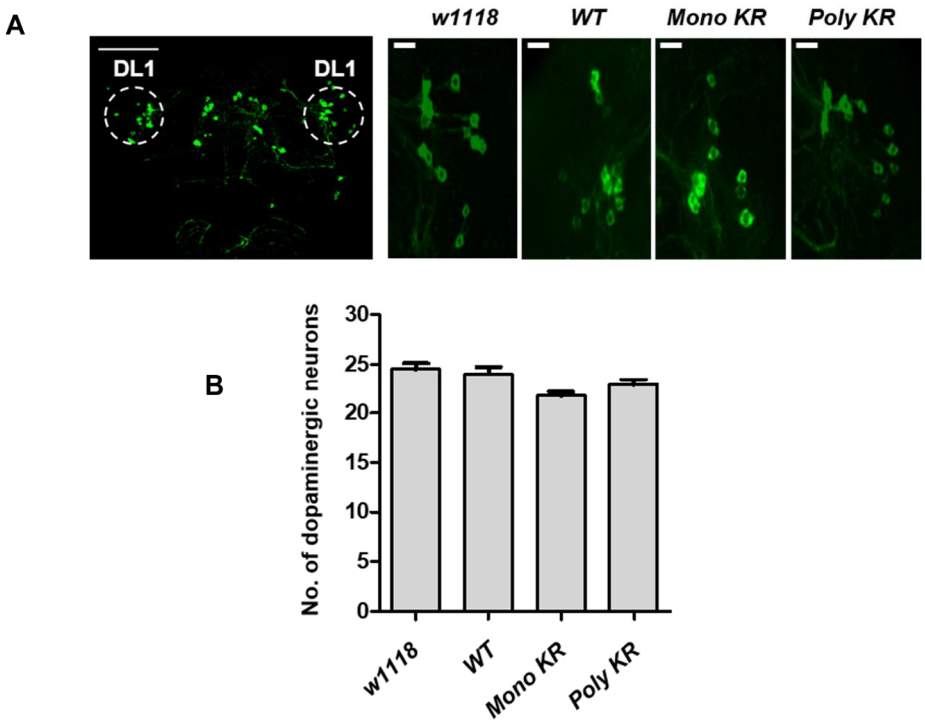

Figure 41. Dopaminergic neuronal degeneration in *Drosophila* expressing porin mutants

A-B, Drosophila porin is homologous with human VDAC1. Dopaminergic neuron clusters called DL1 region marked by TH antibody (green) in adult female brains (30-day-old). Scale bars, 20 uM. *C*, Graphs indicate the number of dopaminergic neurons in DL1 clusters (n=10).

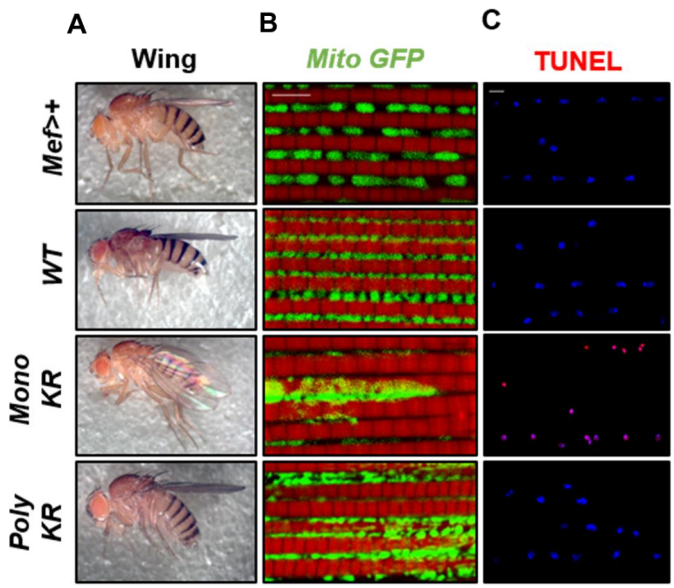

Figure 42. Characterization of *Drosophila* expressing porin mutants

A, Down-postured wing phenotype of the transgenic flies expressing porin WT and mutants including Mono KR (K273R) and poly KR (K12, 20, 53, 110R). *B,* Images of mitochondrial morphology stained by streptavidin HRP (green) in the thoraces of porin mutants. Red color staining for muscle fibers by phalloidin. *C,* Merged images of TUNEL (red) and nuclei staining (Hoeschst 33258, blue) in the thoraces of porin mutants.

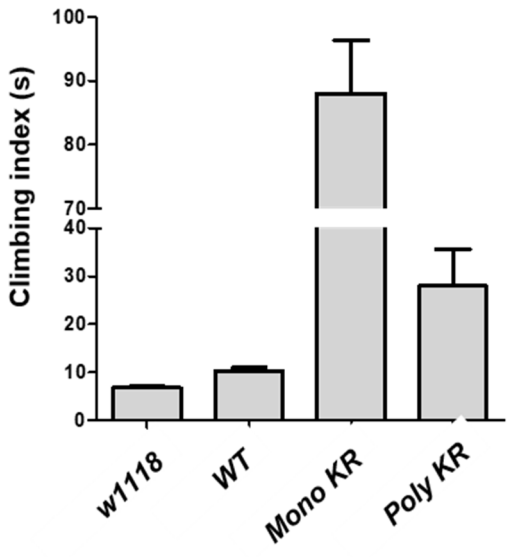

Figure 43. Climbing phenotypes of *Drosophila* expressing porin mutants

Graphs showing different climbing indices in 3-day-old female flies expressing porin mutants as indicated (n=10, four independent experiments).

Parkin patient mutations with impaired mono- and poly-ubiquitination of VDAC1 show defects in mitophagy and apoptosis

To observe whether the pathogenesis of PD can be induced by impairing regulation of VDAC1 ubiquitination in PD patients, I performed VDAC1 ubiquitination assays on Parkin with patient mutations. Ubiquitin-like (UBL) in the N-term region, and RING0, RING1, in-between-ring (IBR), and RING2 domains in the C-term region are important for activation of Parkin E3 ligase, so mutations in these domains are expected to critical for the pathogenesis of PD (Fig. 44) (Corti, Lesage, & Brice, 2011). A total of 58 patient mutations were generated in Parkin, and I measured their activity to induce mono- and poly-ubiquitination of VDAC1 and compared with that of WT Parkin in HEK293T cells. The results were displayed in Table 2. Both mono- and poly-ubiquitination was abolished in VDAC1 with mutations in cysteine residues in the R1 domain, which are essential in maintaining RING finger structure in Parkin. Parkin with mutations in the R0 domain, including K161N, C166Y, R234Q, induced mono-ubiquitination but not poly-ubiquitination in VDAC1. Meanwhile, mutations in the R2 domain, such as T415N, abolished mono-ubiquitnation but retain poly-ubiquitination. From these results, I conclude that mono- and poly-ubiquitination of VDAC1 are impaired in several Parkin patient mutations and, interestingly, some of them affect only one of the

ubiquitination types of VDAC1.

To further study, I selected two Parkin mutations with differential ubiquitination activities, T415N and K211N, which did not affect the structure of RING finger motifs in Parkin, and investigated their impact on mitophagy and apoptosis. Analysis of the 3D structure suggested that positions of the two mutations were especially prone to mutated. T415N, circled in red, showed defective in mono-ubiquitination on VDAC1 with intact poly-ubiquitination. Parkin with K211N mutation circled in blue showed no defects in mono-ubiquitination compared to WT Parkin but showed defective poly-ubiquitination on VDAC1 (Fig. 45). To observe the effects of the two Parkin mutations on mitophagy, I performed immunostaining using anti-TOM20 antibody after treating cells with CCCP. As expected, I detected TOM20 signals only in HeLa cells expressing Parkin WT and K211N whereas those expressing Parkin T415N failed to show any detectable TOM20 signals (Fig. 46).

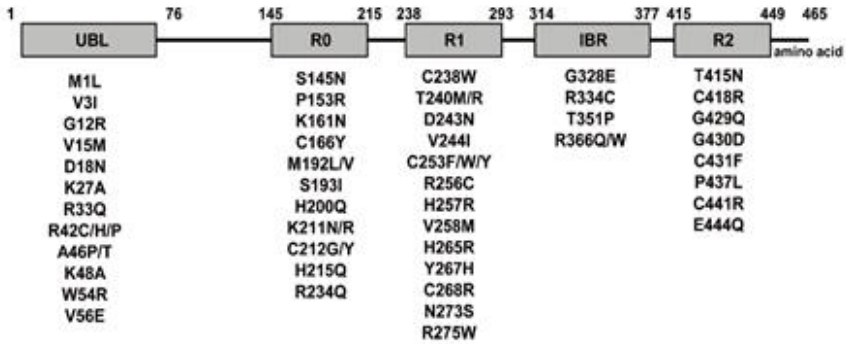

Figure 44. Parkin patient mutations in the domains of Parkin protein

Parkin consists of ubiquitin-like domain (UBL) in the N-terminal, and Really interesting new gene (RING) 0, RING1, in between RING (IBR) and RING2 domains in the C-terminal region. I tested mono- and poly-ubiquitination of VDAC1 by Parkin with various PD patient mutations in different domains.

Table 2. Screening results for mono- and poly-ubiquitination of VDAC1 by Parkin patient mutants

Domain	Mutant	Mono ubiquitination	Poly ubiquitination
WT		+++	+++
R0	K161N	+++	-
	C166Y	+++	-
	K211N	+++	-
	C212G	+++	-
	C212Y	+++	-
	R234Q	+++	++
R1	C238W	-	-
	T240R	-	-
	C253F	-	-
	C253W	-	-
	C253Y	-	-
	H257R	+++	-
	G284R	-	-
	C289G	-	-
R2	T415N	-	++
	C418R	-	-
	G430D	-	-
	C431F	-	-
	P437L	+++	-
	C441R	-	-

++, modest difference and +++, significant difference and -, no difference, compared with the ubiquitination of VDAC1 by wild type Parkin

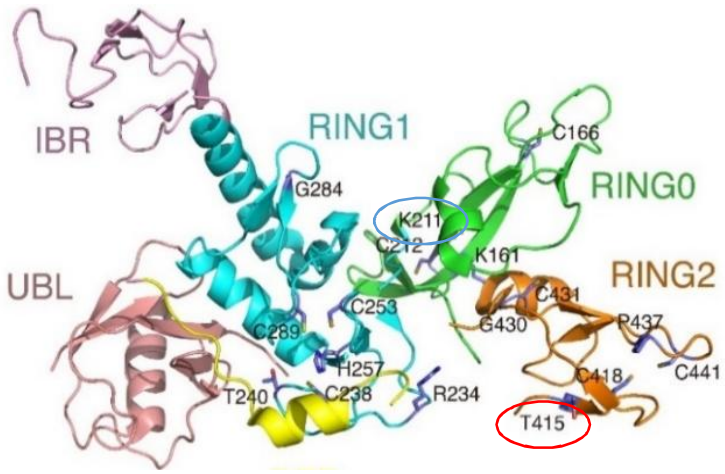

Figure 45. Ribbon diagram of the 3D structure of Parkin

The K211 residue on RING0 domain marked by a blue circle. The T415 residue on the RING2 domain indicated by a red circle.

In these data, Parkin-mediated mitophagy did not occur normally in Parkin K211N patient mutant which is defective in VDAC1 poly-ubiquitination. These results were consistent with the results of expressing poly-ubiquitination defective VDAC1 mutant in mammalian cells, indicating that Parkin induces mitophagy through inducing poly-ubiquitination of VDAC1.

To confirm changes in mitochondrial calcium uptake in Parkin patient mutants, I next measured mitochondrial calcium concentrations. I expressed Parkin WT, K211N in Parkin KO MEF cell line, then measured mitochondrial calcium concentrations and compared with Parkin KO cells with empty vector as control. Interestingly, significant increase in mitochondrial calcium concentrations was observed in Parkin KO MEF cells. This increased mitochondrial calcium was noticeably reduced when WT Parkin or K211N Parkin was expressed. However, in case of T415N Parkin mutant, there still was an increase in mitochondrial calcium concentration (Fig. 47). These data were consistent with the previous VDAC1 results in mammals that VDAC1 mono-ubiquitination plays an important role in mitochondrial calcium uptake.

In addition, I looked to see if apoptosis was induced in cells in response to mitochondrial calcium uptake by observing amounts of cleaved caspase 3, an apoptosis marker. In Parkin WT and Parkin KO MEF cells, an

increased cleaved caspase 3 was observed only in Parkin KO cells. Hence, I overexpressed Parkin WT, K211N and T415N in Parkin KO MEF cells, and measured their cleaved caspase 3 level. In Parkin KO cells, the increase in cleaved PARP was effectively reduced by expression of Parkin WT and K211N while cells expressing T415N still showed increased cleaved PARP levels compared to the control (Fig. 48). This result was consistent with the previous data of mitochondrial calcium measurement (Fig. 38), and indicates that apoptosis was induced by mitochondrial calcium increase in Parkin T415N mutant. My results indicate that the mono- and poly-ubiquitination of VDAC1 induced by the PINK1 and Parkin pathway are two critical regulatory mechanisms to determine mitophagy and apoptosis that are integral to the pathogenesis of PD.

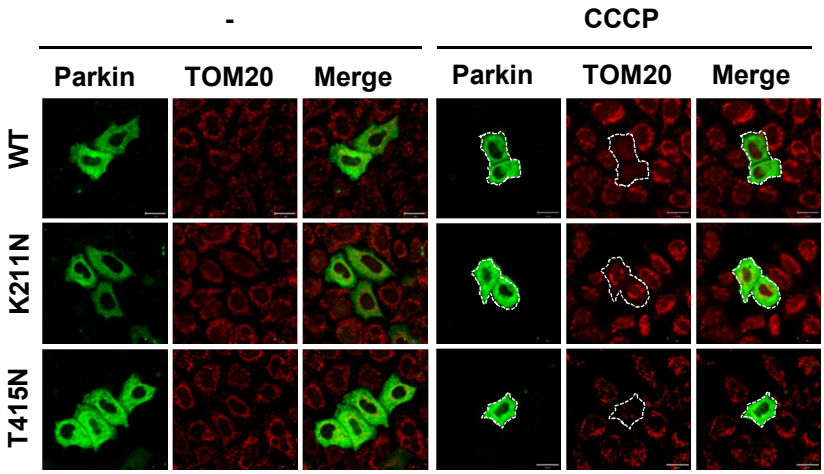

Figure 46. Induction of mitophagy is defective by Parkin with patient mutation at K211N

Confocal images of TOM20 staining in the cells expressing Parkin WT, K211N, or T415N mutant. Myc-tagged Parkin was expressed in HeLa cells and treated with 20 uM CCCP for 24 hr or with DMSO. Samples were stained for Parkin using anti-Myc antibody (green) and for mitochondria by anti-TOM20 antibody (red).

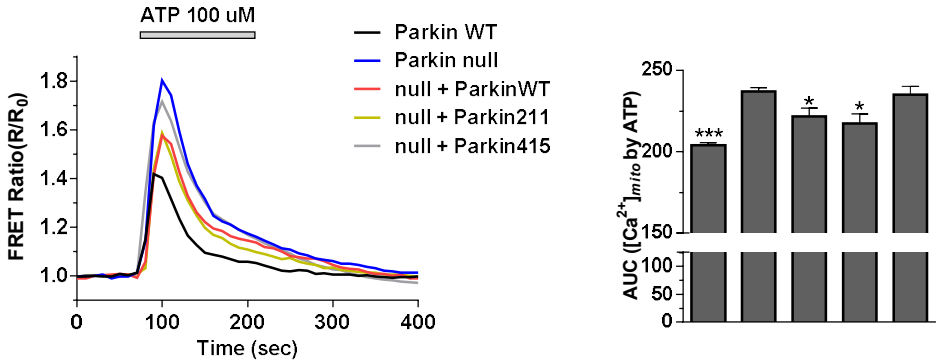

Figure 47. Mitochondrial calcium uptake is highly induced by T415N mutation in Parkin

A, Graph showing mitochondrial calcium uptake in Parkin mutations. I measured mitochondrial calcium concentration in Parkin WT, KO MEF cell lines with empty vector or in MEF KO cell lines with Parkin WT, K211N and T415N. *B,* Bar graph for AUC of mitochondrial calcium uptake.

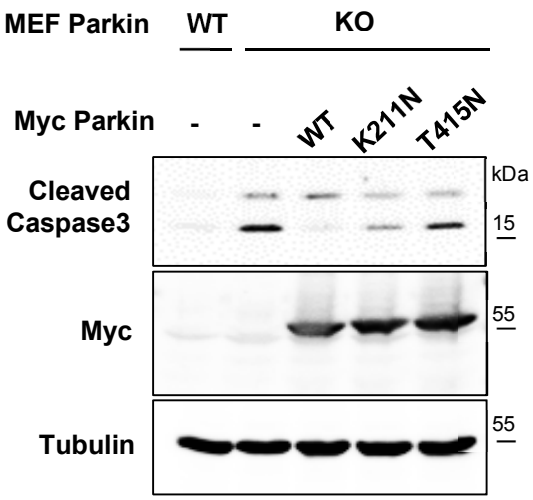

Figure 48. Apoptosis is induced by Parkin T415N mutant

Parkin KO MEF cells were transfected with empty vector or expression vector coding Myc-tagged Parkin WT, K211N and T415N mutants as indicated. Samples were analyzed for western blot by indicated antibodies.

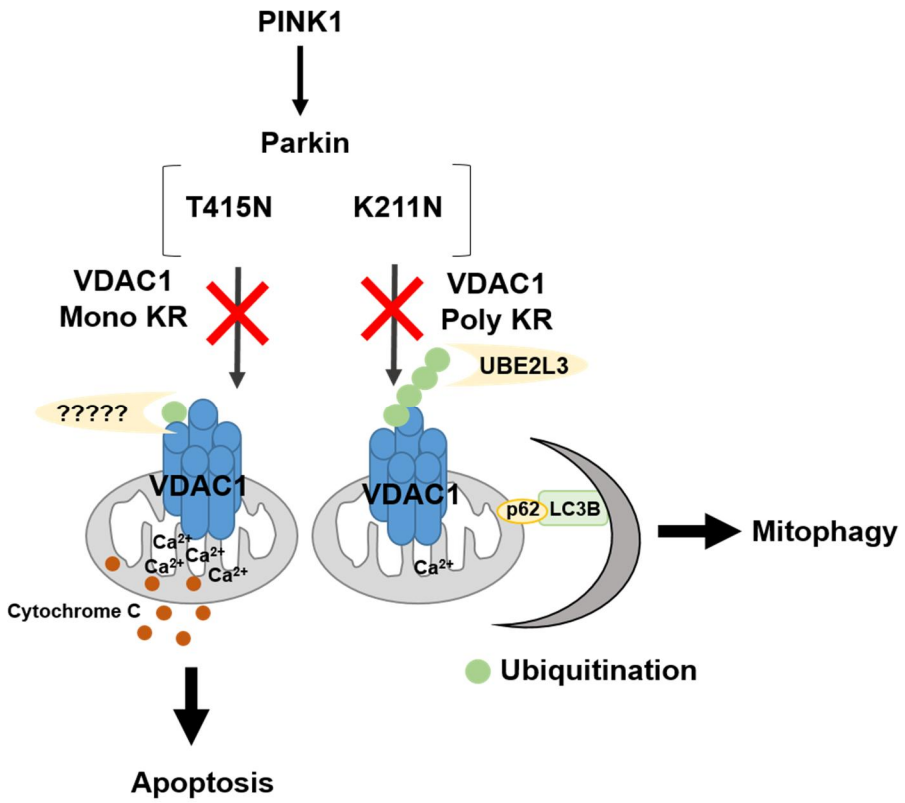

Figure 49. The PINK1-Parkin pathway determines apoptosis and mitophagy by regulating mono- and poly-ubiquitination of VDAC1

Discussion

In this study, I demonstrated VDAC1 ubiquitination by the PINK1-Parkin pathway, and showed that Parkin selectively requires different types of E2 enzymes depending on the type of ubiquitination. Parkin either mono- or poly-ubiquitinated VDAC1 to regulate mitophagy or apoptosis, respectively. Two patient mutations of Parkin were studied; Parkin K211N mutation was defective in poly-ubiquitinating VDAC1, which inhibited mitophagy, while Parkin T415N mutation increased mitochondrial calcium concentration, which induced apoptosis (Fig. 49).

Ubiquitin ligation process involves ubiquitin-activating enzyme (E1), ubiquitin-conjugating enzyme (E2) and ubiquitin-protein ligase (E3). Of these, E2 is involved specifically in ubiquitin chain elongation before the ubiquitin chain is attached to lysine of the substrate. In the course of chain elongation, E2 utilizes its unique structure to selectively bind to an ubiquitin chain linked to a certain lysine (W. Li & Ye, 2008). For example, K63 linkage is preferred by Mms2 E3 ligase and Ubc13 complex (Eddins, Carlile, Gomez, Pickart, & Wolberger, 2006; McKenna et al., 2003; VanDemark, Hofmann, Tsui, Pickart, & Wolberger, 2001), while K48 linkage is preferred by Cdc34 (Petroski & Deshaies, 2005). In addition, UbcH5 E2 enzyme is known to selectively bind to K11, K48 and K63 linkages (Jin, Williamson, Banerjee, Philipp, & Rape, 2008) while UBE2K preferred K48

linkage (Rajsbaum et al., 2014). In my study, I demonstrated that VDAC1 mono- and poly-ubiquitination require different E2 enzymes. My results revealed the involvement of UBE2L3 in VDAC1 poly-ubiquitination (Fig. 32). VDAC1 is normally ubiquitinated using K11, K27 and K63 linkages, and the majority of ubiquitin chains are currently known to utilize K27 linkage. Interestingly, UBE2L3 is reported to prefer K63 linkage, and UBE2L3 knockdown is known to inhibit p62 and LC3B recruitment and subsequent Parkin-mediated mitophagy (Fiesel et al., 2014). My result is consistent with those from previous studies, and strongly suggests that poly-ubiquitination of VDAC1 by UBE2L3 regulates mitophagy. Furthermore, because knockdown of the E2 enzyme that inhibits VDAC1 poly-ubiquitination has no effect on VDAC1 mono-ubiquitination, it is likely that there is a specific E2 that mediates mono-ubiquitination of VDAC1. It has been reported that the E2 enzymes of the UbcH5 (Y. Li et al., 2014) or the UbcH4 family mono-ubiquitinates its substrates (Rodrigo-Brenni & Morgan, 2007), and that the UbE2E1 E2 is essential for histone 2A mono-ubiquitination (Wheaton et al., 2017). Likewise, specific E2 enzymes determine the type of VDAC1 ubiquitination, and one protein can become either mono- or poly-ubiquitinated.

In fact, post-translational modification by ubiquitin is known to regulate various signal transduction pathways. In case of poly-ubiquitination,

use of specific linkage type is reported to determine which signal is to be produced. While it is known that K27-linkage poly-ubiquitination controls mitochondrial transport (Birsa et al., 2014), I have shown that it can also induce mitophagy in VDAC1. K63-linkage poly-ubiquitination is involved in regulation of autophagy by serving as a lysosomal targeting signaling (J. M. Tan et al., 2008). On the contrary, signals induced by mono-ubiquitination are relatively unknown. Only few studies have reported the possibility that mono-ubiquitination controls apoptosis, as I have discovered in my research. When signal transducers and activator of transcription 3 (STAT3) is mono-ubiquitinated, TNF-α induced apoptotic cell death is suppressed (Ray et al., 2014). Meanwhile, mono-ubiquitination of death effector domain (DED) containing DNA binding protein (DEDD) was reported to induce apoptosis (Lee, Wang, Schickling, & Peter, 2005). These studies suggest that mono-ubiquitination of certain proteins can regulate apoptotic signal transduction.

In addition, previous studies have reported that mitophagy and apoptosis occur differentially, depending on the degree of mitochondrial damage. Mitophagy is promoted when ROS levels or mtDNA damage is modest, while apoptosis is facilitated when ROS or mtDNA damage is irreparable by antioxidant or DNA repair systems. Furthermore, an increase in cellular apoptosis has been reported to suppress autophagy induction

(Kubli & Gustafsson, 2012). For instance, caspases that are activated during apoptosis cleave Beclin1, creating Beclin1 fragments that block Vps34 formation, which suppresses autophagy (Kang, Zeh, Lotze, & Tang, 2011). Atg5 is also cleaved by calpain as a result of apoptotic stimuli (Yousefi et al., 2006). Finally, knockdown of AMBRA1, an autophagy regulator, has been shown to increase apoptosis, but when AMBRA1 is cleaved by caspases and calpain, autophagy is inactivated (W. Gu et al., 2014; Pagliarini et al., 2012). Taken together, these results indicate that mitochondria undergo either mitophagy or apoptosis depending on the degree of mitochondrial damage, and that mitophagy and apoptosis act as an antagonist to each other to determine cellular fate. There has evidence that 4 hours of CCCP treatment induces modest mitochondrial damage, and results in simultaneous mono- and poly-ubiquitination of VDAC1 by Parkin. In this case, mitophagy is promoted while apoptosis is suppressed. This result suggests that under conditions of mitochondrial damage in which mitophagy is promoted, poly- and mono-ubiquitination of VDAC1 is increased, while when apoptosis is activated, poly- and mono-ubiquitination should be suppressed. Further investigation was required to support these claims.

According to my results, mono-ubiquitination of VDAC1 regulates mitochondrial calcium influx and subsequent induction of apoptosis. Possible candidates involved in this process include hexokinase 1, 2, BCL-

xL, BID and BAX, which regulate the opening and closure of the VDAC1 pore (Abu-Hamad et al., 2009; Arzoine et al., 2009; Rostovtseva et al., 2004; Shi et al., 2003; Shimizu et al., 2001; Shoshan-Barmatz et al., 2010; Shoshan-Barmatz et al., 2009; Tsujimoto & Shimizu, 2000). Interaction between these proteins and VDAC1 can be altered by mono-ubiquitination of VDAC1, and I have shown that overexpressed VDAC1 WT is extensively mono-ubiquitinated under pro-apoptotic situations such as CCCP treatment, and mono-ubiqutination resulted in an inhibition of apoptosis. This inhibitory effect was indeed rescued by BCL-xL knockdown. Also, overexpression of mono-ubiquitination-deficient VDAC1 mutant resulted in increased apoptosis, and this effect was reduced by BID knockdown, suggesting that non-mono-ubiquitinated VDAC1 interacts with BID to induce apoptosis while mono-ubiquitinated VDAC1 interacts with anti-apoptotic proteins such as BCL-xL to inhibit apoptosis.

I also propose that VDAC1 oligomerization leads to increased mitochondrial calcium influx and results in inducing apoptosis. Reported cryo-EM images indicate that VDAC1 self-oligomerizes up to hexamer structure, which intensifies when apoptosis is induced (Goncalves et al., 2007; Shoshan-Barmatz et al., 2013; Ujwal et al., 2009). Interestingly, VDAC1 oligomerization was significantly increased in HEK293T cells overexpressed with VDAC1 Mono KR mutants, whose mono-ubiquitination

site is mutated into arginine, compared to those of cells overexpressed with VDAC1 WT. These results indicate that VDAC1 oligomerization or regulators of its pore opening are regulated by its mono-ubiquitination status, which results in regulation of mitochondrial calcium influx and apoptosis.

Parkin functions as both HECT and RING type E3 ligases. It utilizes its active site cysteine 431 to form Ub~HECT thioester intermediates before ligating ubiquitin to its substrate (HECT type). It also functions as a scaffold for Ub~E2 and its substrate to catalyze ubiquitin transfer (RING type) (Riley et al., 2013). The Parkin patient mutation K211N is located within the R0 domain, and was defective in poly-ubiquitinating VDAC1. T415N mutation, however, is located in the R2 domain, and was defective in mono-ubiquitinating VDAC1. There is a possibility that two types of ubiquitination are each regulated by different types of Parkin E3 function. According to previous reports, Parkin K211 forms the putative binding site for phosphorylated ubiquitin (pUb) with K161 and R163. pUb binding to Parkin causes structural changes, which exposes the active site C431 of Parkin. The E2 enzyme involved in this process is UBCH7 (UBE2L3), which catalyzes thioester conjugate formation upon exposure of C431 (Kazlauskaite et al., 2015; Koyano et al., 2014; Sauve et al., 2015). These results suggest that Parkin functions as a HECT type E3 ligase to poly-ubiquitinate its substrates, including VDAC1. Thus, the patient mutation

K211N may prevent pUb binding, which in turn inhibits the thioester bond formation of UBCH7~Ub leading to a defect in poly-ubiquitination of VDAC1. On the contrary, UBCH8 (UBE2L6), which participates in mono-ubiquitination of VDAC1, binds to IBR-R2 domain of Parkin. T415N mutation is reported to eliminate this protein-protein interaction and prevent UBCH8 from binding to Parkin, resulting in a defect in mono-ubiquitination of VDAC1. These results indicate that E2 enzymes determine whether HECT or RING type E3 ligation is used for Parkin, and this serves as a key mechanism for driving mono- or poly-ubiquitination of VDAC1.

Using the in vivo Drosophila model, I have concluded that dysfunctions in both VDAC/porin mono- and poly-ubiquitination lead to PD phenotypes including defects in climbing, abnormal mitochondrial morphology, and loss of dopaminergic neurons, confirming the importance of VDAC/porin ubiquitination in PD pathogenesis in vivo. In cases in which these mechanisms are disturbed, PD pathogenesis is induced, which implies that a novel method that mimics VDAC ubiquitination is a promising candidate for future PD treatment.

Conclusion

PD is a neurodegenerative disease and is often accompanied with accumulation of dysfunctional mitochondria, which causes a decrease in ATP level and an increase in apoptosis ultimately leading to cell death. In the substantial nigra, dopaminergic neurons of PD patients show a decreased ATP level and an increase in ROS production caused by reduction in mitochondrial electron chain complex I activity (M. Gu, Cooper, Taanman, & Schapira, 1998). These changes have been reported to induce intracellular apoptosis, and similar phenotype has been observed in PINK1 or Parkin null fly, which indicates a close relationship between regulation of mitochondria and PD pathogenesis.

Furthermore, Aging is the strongest risk factor for the development of PD. The prevalence of PD is 0.3% in the general population, and this number increases to 1% of individuals over 60 and 5% of those over 85 years of age (de Lau & Breteler, 2006; Wood-Kaczmar, Gandhi, & Wood, 2006). Thus, in the inherited forms of PD, patients are symptom free for many decades despite the fact that the disease-causing mutation is present from birth. Aging is associated with mitochondrial dysfunction, such as increase of free radical production and oxidative stress, which lead to general DNA mutation and also mitochondrial DNA mutation. And also substantia nigra region in the brain showed decline of proteasome activity,

defect of chaperone degradation and imbalanced autophagic recycling during aging (Reeve, Simcox, & Turnbull, 2014). Those defects result in aggregation of proteins in the brain and lead to loss of dopaminergic neurons, causing PD pathogenesis. Jason F Cooper et al. demonstrated that the relation between aging and PD pathogenesis. Worm models of PD expressing mutant alpha-synuclein (A53T) or LRRK2 (G2019S) was rescued the degeneration of dopaminergic neurons and deficits in dopaminergic neuron-dependent behaviors by crossed with the long-lived insulin-IGF1 receptor mutant, daf-2 (Cooper et al., 2015). These results suggest that slowing down aging processes delays PD phenotypes, demonstrating the strong relationship between aging and PD pathogenesis.

Aging is also associated with regulation of mitochondrial function. Especially, substantia nigra in the brain of PD patient shows increased mutations in mtDNA and decreased complex I activity compare to normal brain, which leads to increased ROS and oxidative stress (Haddad & Nakamura, 2015; Surmeier, Guzman, Sanchez-Padilla, & Schumacker, 2011). Why these dopamine neurons have selective vulnerability in SN regions during aging? The reason why dopamine neurons in substantia nigra region have enormous exonal field with hundreds of thousands of transmitter release site than other regions in the brain. Substantia nigra

dopaminergic neurons form 100,000 to 245,000 synapses in the striatum. However, ventral tegmental area (VTA) DA neurons appear to have less extensive branching and only form 12,000–30,000 synapses (Arbuthnott & Wickens, 2007; W. Matsuda et al., 2009; Nicholls, 2008). Substantia nigra dopaminergic neurons need higher energy demands than dopaminergic neurons in any other regions in the brain, so that frequent energy crisis caused by mitochondrial dysfunction during aging may lead to specific degeneration of dopaminergic neurons in substantia nigra. Thus, mitochondrial function is important for developing PD in substantia nigra region and substantia nigra dopaminergic neurons are more sensitive to mitochondrial stress.

The selective sensitivity of the dopaminergic neurons in substantia nigra is supported by previous reports. Those reports observed that PD symptom can be induced in animal models following treatment of mitochondrial stressors or neurotoxins, such as 6-hydrodopamine (6-OHDA) in rats, 1-methyl-4-phenyl-1, 2, 3, 6-tetrahydropyridine (MPTP) in mice and rotenone in human (Betarbet et al., 2000; Przedborski, Tieu, Perier, & Vila, 2004; Simola, Morelli, & Carta, 2007).

Cells normally maintain their mitochondrial quality control via mitophagy. Mitophagy is in turn regulated by the PINK1-Parkin pathway to

selectively eliminate dysfunctional mitochondria. This is mediated by aforementioned regulation of the UBL domain-mediated autoinhibition by the pathway which activates the E3 ligase activity of Parkin. Poly-ubiquitination of VDAC1 induces mitophagy. This emphasizes the point that removal of dysfunctional mitochondria is a key mechanism in suppressing PD pathogenesis by the PINK1-Parkin pathway.

In cases where defective mitochondria are not efficiently removed, intracellular ROS level increases or calcium homeostasis is disrupted, resulting in apoptotic cell death, which can cause the onset of PD. VDAC1 plays an important role in regulation of apoptosis by the PINK1-Parkin pathway. My research in Part2 suggests a mechanism in which mono-ubiquitination of VDAC1 regulates apoptosis. Furthermore, VDAC1 interacts with MCU to control mitochondrial calcium influx, which can also regulate apoptosis. These results indicate that inhibition of mitochondrial calcium influx is possible to suppress apoptosis and potentially rescue PD phenotypes. According to a recent study, in which dopaminergic neuronal blastoma SH-SY5Y cell line was used, PINK1 knockdown increased the level of mitochondrial depolarization and subsequent mitochondrial calcium efflux (Gandhi et al., 2009). Similarly, overexpressing the active form of Na^{+}/Ca^{2+} exchanger (NCLX) decreases mitochondrial calcium overload

(Kostic et al., 2015). Also, an IMM calcium channel called leucine zipper-EF-hand containing transmembrane protein 1 (LETM1) is reported to be phosphorylated by PINK1, inhibiting mitochondrial calcium influx through suppressing mPTP opening, and preventing primary neuronal cell death (E. Huang et al., 2017). Overall, these results suggest that inhibiting mitochondrial calcium influx effectively reduces apoptotic cell death, and may serve as a potential treatment to PD.

The core mechanism through which the PINK1-Parkin pathway regulates mitochondrial homeostasis is ubiquitination on mitochondrial proteins. Parkin functions as an E3 ligase, and induces mitophagy by ubiquitinating various mitochondria proteins. Also, VDAC1 is ubiquitinated in two different ways, namely mono- and poly-ubiquitination, and they regulate mitophagy and apoptosis through different regulatory mechanisms. Through these results, my research demonstrated that PD is tightly associated with a series of ubiquitin-dependent protein regulation.

The critical relationship between mitochondrial homeostasis and PD pathogenesis has been thoroughly examined in this thesis study. A novel regulatory mechanism involving VDAC1 has been proposed. Also, PINK1-

Parkin pathway has been extensively studied, and a detailed mechanism of its regulation has been suggested. Altogether, my research extended my current understanding of PD pathogenesis, and has proposed novel pathologic mechanisms to be used for development of future PD treatment.

Reference

Abu-Hamad, S., Arbel, N., Calo, D., Arzoine, L., Israelson, A., Keinan, N., Shoshan-Barmatz, V. (2009). The VDAC1 N-terminus is essential both for apoptosis and the protective effect of anti-apoptotic proteins. *J Cell Sci, 122*(Pt 11), 1906-1916. doi:10.1242/jcs.040188

Abu-Hamad, S., Zaid, H., Israelson, A., Nahon, E., & Shoshan-Barmatz, V. (2008). Hexokinase-I protection against apoptotic cell death is mediated via interaction with the voltage-dependent anion channel-1: mapping the site of binding. *J Biol Chem, 283*(19), 13482-13490. doi:10.1074/jbc.M708216200

Aguileta, M. A., Korac, J., Durcan, T. M., Trempe, J. F., Haber, M., Gehring, K., Husnjak, K. (2015). The E3 ubiquitin ligase parkin is recruited to the 26 S proteasome via the proteasomal ubiquitin receptor Rpn13. *J Biol Chem, 290*(12), 7492-7505. doi:10.1074/jbc.M114.614925

Aguirre, J. D., Dunkerley, K. M., Mercier, P., & Shaw, G. S. (2017). Structure of phosphorylated UBL domain and insights into PINK1-orchestrated parkin activation. *Proc Natl Acad Sci U S A, 114*(2), 298-303. doi:10.1073/pnas.1613040114

Akabane, S., Matsuzaki, K., Yamashita, S., Arai, K., Okatsu, K., Kanki, T., Oka, T. (2016). Constitutive Activation of PINK1 Protein Leads to Proteasome-mediated and Non-apoptotic Cell Death Independently of Mitochondrial Autophagy. *J Biol Chem, 291*(31), 16162-16174. doi:10.1074/jbc.M116.714923

Arbuthnott, G. W., & Wickens, J. (2007). Space, time and dopamine. *Trends Neurosci, 30*(2), 62-69. doi:10.1016/j.tins.2006.12.003

Arena, G., Gelmetti, V., Torosantucci, L., Vignone, D., Lamorte, G., De Rosa, P., Valente, E. M. (2013). PINK1 protects against cell death induced by mitochondrial depolarization, by phosphorylating Bcl-xL and impairing its pro-apoptotic cleavage. *Cell Death Differ, 20*(7), 920-930. doi:10.1038/cdd.2013.19

Arzoine, L., Zilberberg, N., Ben-Romano, R., & Shoshan-Barmatz, V. (2009). Voltage-dependent anion channel 1-based peptides interact with hexokinase to prevent its anti-apoptotic activity. *J Biol Chem, 284*(6), 3946-3955. doi:10.1074/jbc.M803614200

Azoulay-Zohar, H., Israelson, A., Abu-Hamad, S., & Shoshan-Barmatz, V. (2004). In self-defence: hexokinase promotes voltage-dependent anion channel closure and prevents mitochondria-mediated apoptotic cell death. *Biochem J, 377*(Pt 2), 347-355. doi:10.1042/BJ20031465

Baba, Y., Markopoulou, K., Putzke, J. D., Whaley, N. R., Farrer, M. J., Wszolek, Z. K., & Uitti, R. J. (2006). Phenotypic commonalities in familial and sporadic Parkinson disease. *Arch Neurol, 63*(4), 579-

583. doi:10.1001/archneur.63.4.579
Baines, C. P. (2009). The molecular composition of the mitochondrial permeability transition pore. *J Mol Cell Cardiol, 46*(6), 850-857. doi:10.1016/j.yjmcc.2009.02.007
Beasley, S. A., Hristova, V. A., & Shaw, G. S. (2007). Structure of the Parkin in-between-ring domain provides insights for E3-ligase dysfunction in autosomal recessive Parkinson's disease. *Proc Natl Acad Sci U S A, 104*(9), 3095-3100. doi:10.1073/pnas.0610548104
Beasley, S. A., Safadi, S. S., Barber, K. R., & Shaw, G. S. (2012). Solution structure of the E3 ligase HOIL-1 Ubl domain. *Protein Sci, 21*(7), 1085-1092. doi:10.1002/pro.2080
Bernardi, P., & Di Lisa, F. (2015). The mitochondrial permeability transition pore: molecular nature and role as a target in cardioprotection. *J Mol Cell Cardiol, 78*, 100-106. doi:10.1016/j.yjmcc.2014.09.023
Berndsen, C. E., & Wolberger, C. (2014). New insights into ubiquitin E3 ligase mechanism. *Nat Struct Mol Biol, 21*(4), 301-307. doi:10.1038/nsmb.2780
Betarbet, R., Sherer, T. B., MacKenzie, G., Garcia-Osuna, M., Panov, A. V., & Greenamyre, J. T. (2000). Chronic systemic pesticide exposure reproduces features of Parkinson's disease. *Nat Neurosci, 3*(12), 1301-1306. doi:10.1038/81834
Bingol, B., Tea, J. S., Phu, L., Reichelt, M., Bakalarski, C. E., Song, Q., Sheng, M. (2014). The mitochondrial deubiquitinase USP30 opposes parkin-mediated mitophagy. *Nature, 510*(7505), 370-37 doi:10.1038/nature13418
Birsa, N., Norkett, R., Wauer, T., Mevissen, T. E., Wu, H. C., Foltynie, T., Kittler, J. T. (2014). Lysine 27 ubiquitination of the mitochondrial transport protein Miro is dependent on serine 65 of the Parkin ubiquitin ligase. *J Biol Chem, 289*(21), 14569-14582. doi:10.1074/jbc.M114.563031
Bonifati, V. (2001). Monogenic Parkinsonisms and the genetics of Parkinson's disease. *Funct Neurol, 16*(1), 35-44.
Bonora, M., & Pinton, P. (2014). The mitochondrial permeability transition pore and cancer: molecular mechanisms involved in cell death. *Front Oncol, 4*, 302. doi:10.3389/fonc.2014.00302
Carroll, R. G., Hollville, E., & Martin, S. J. (2014). Parkin sensitizes toward apoptosis induced by mitochondrial depolarization through promoting degradation of Mcl-1. *Cell Rep, 9*(4), 1538-1553. doi:10.1016/j.celrep.2014.10.046
Caulfield, T. R., Fiesel, F. C., Moussaud-Lamodiere, E. L., Dourado, D. F., Flores, S. C., & Springer, W. (2014). Phosphorylation by PINK1 releases the UBL domain and initializes the conformational opening

of the E3 ubiquitin ligase Parkin. *PLoS Comput Biol, 10*(11), e1003935. doi:10.1371/journal.pcbi.1003935

Chan, N. C., Salazar, A. M., Pham, A. H., Sweredoski, M. J., Kolawa, N. J., Graham, R. L., Chan, D. C. (2011). Broad activation of the ubiquitin-proteasome system by Parkin is critical for mitophagy. *Hum Mol Genet, 20*(9), 1726-1737. doi:10.1093/hmg/ddr048

Chaugule, V. K., Burchell, L., Barber, K. R., Sidhu, A., Leslie, S. J., Shaw, G. S., & Walden, H. (2011). Autoregulation of Parkin activity through its ubiquitin-like domain. *EMBO J, 30*(14), 2853-2867. doi:10.1038/emboj.2011.204

Chen, Y., & Dorn, G. W., 2nd. (2013). PINK1-phosphorylated mitofusin 2 is a Parkin receptor for culling damaged mitochondria. *Science, 340*(6131), 471-475. doi:10.1126/science.1231031

Clerici, M., Luna-Vargas, M. P., Faesen, A. C., & Sixma, T. K. (2014). The DUSP-Ubl domain of USP4 enhances its catalytic efficiency by promoting ubiquitin exchange. *Nat Commun, 5*, 5399. doi:10.1038/ncomms6399

Cooper, J. F., Dues, D. J., Spielbauer, K. K., Machiela, E., Senchuk, M. M., & Van Raamsdonk, J. M. (2015). Delaying aging is neuroprotective in Parkinson's disease: a genetic analysis in C. elegans models. *NPJ Parkinsons Dis, 1*, 15022. doi:10.1038/npjparkd.2015.22

Corti, O., Lesage, S., & Brice, A. (2011). What genetics tells us about the causes and mechanisms of Parkinson's disease. *Physiol Rev, 91*(4), 1161-1218. doi:10.1152/physrev.00022.2010

de Lau, L. M., & Breteler, M. M. (2006). Epidemiology of Parkinson's disease. *Lancet Neurol, 5*(6), 525-535. doi:10.1016/S1474-4422(06)70471-9

Dev, K. K., van der Putten, H., Sommer, B., & Rovelli, G. (2003). Part I: parkin-associated proteins and Parkinson's disease. *Neuropharmacology, 45*(1), 1-13.

Dieckmann, T., Withers-Ward, E. S., Jarosinski, M. A., Liu, C. F., Chen, I. S., & Feigon, J. (1998). Structure of a human DNA repair protein UBA domain that interacts with HIV-1 Vpr. *Nat Struct Biol, 5*(12), 1042-1047. doi:10.1038/4220

Eddins, M. J., Carlile, C. M., Gomez, K. M., Pickart, C. M., & Wolberger, C. (2006). Mms2-Ubc13 covalently bound to ubiquitin reveals the structural basis of linkage-specific polyubiquitin chain formation. *Nat Struct Mol Biol, 13*(10), 915-920. doi:10.1038/nsmb1148

Elliott, P. R., Liu, H., Pastok, M. W., Grossmann, G. J., Rigden, D. J., Clague, M. J., Barsukov, I. L. (2011). Structural variability of the ubiquitin specific protease DUSP-UBL double domains. *FEBS Lett, 585*(21), 3385-3390. doi:10.1016/j.febslet.2011.09.040

Faesen, A. C., Luna-Vargas, M. P., & Sixma, T. K. (2012). The role of UBL domains in ubiquitin-specific proteases. *Biochem Soc Trans, 40*(3), 539-545. doi:10.1042/BST20120004

Fiesel, F. C., Moussaud-Lamodiere, E. L., Ando, M., & Springer, W. (2014). A specific subset of E2 ubiquitin-conjugating enzymes regulate Parkin activation and mitophagy differently. *J Cell Sci, 127*(Pt 16), 3488-3504. doi:10.1242/jcs.147520

Gandhi, S., Wood-Kaczmar, A., Yao, Z., Plun-Favreau, H., Deas, E., Klupsch, K., Abramov, A. Y. (2009). PINK1-associated Parkinson's disease is caused by neuronal vulnerability to calcium-induced cell death. *Mol Cell, 33*(5), 627-638. doi:10.1016/j.molcel.2009.02.013

Geisler, S., Holmstrom, K. M., Skujat, D., Fiesel, F. C., Rothfuss, O. C., Kahle, P. J., & Springer, W. (2010). PINK1/Parkin-mediated mitophagy is dependent on VDAC1 and p62/SQSTM1. *Nat Cell Biol, 12*(2), 119-131. doi:10.1038/ncb2012

Geisler, S., Vollmer, S., Golombek, S., & Kahle, P. J. (2014). The ubiquitin-conjugating enzymes UBE2N, UBE2L3 and UBE2D2/3 are essential for Parkin-dependent mitophagy. *J Cell Sci, 127*(Pt 15), 3280-3293. doi:10.1242/jcs.146035

Glauser, L., Sonnay, S., Stafa, K., & Moore, D. J. (2011). Parkin promotes the ubiquitination and degradation of the mitochondrial fusion factor mitofusin 1. *J Neurochem, 118*(4), 636-645. doi:10.1111/j.1471-4159.2011.07318.x

Goncalves, R. P., Buzhynskyy, N., Prima, V., Sturgis, J. N., & Scheuring, S. (2007). Supramolecular assembly of VDAC in native mitochondrial outer membranes. *J Mol Biol, 369*(2), 413-418. doi:10.1016/j.jmb.2007.03.063

Grant, L. M., Kelm-Nelson, C. A., Hilby, B. L., Blue, K. V., Paul Rajamanickam, E. S., Pultorak, J. D., Ciucci, M. R. (2015). Evidence for early and progressive ultrasonic vocalization and oromotor deficits in a PINK1 gene knockout rat model of Parkinson's disease. *J Neurosci Res, 93*(11), 1713-1727. doi:10.1002/jnr.23625

Gu, M., Cooper, J. M., Taanman, J. W., & Schapira, A. H. (1998). Mitochondrial DNA transmission of the mitochondrial defect in Parkinson's disease. *Ann Neurol, 44*(2), 177-186. doi:10.1002/ana.410440207

Gu, W., Wan, D., Qian, Q., Yi, B., He, Z., Gu, Y., He, S. (2014). Ambra1 is an essential regulator of autophagy and apoptosis in SW620 cells: pro-survival role of Ambra1. *PLoS One, 9*(2), e90151. doi:10.1371/journal.pone.0090151

Haddad, D., & Nakamura, K. (2015). Understanding the susceptibility of

dopamine neurons to mitochondrial stressors in Parkinson's disease. *FEBS Lett, 589*(24 Pt A), 3702-3713. doi:10.1016/j.febslet.2015.10.021

Hampe, C., Ardila-Osorio, H., Fournier, M., Brice, A., & Corti, O. (2006). Biochemical analysis of Parkinson's disease-causing variants of Parkin, an E3 ubiquitin-protein ligase with monoubiquitylation capacity. *Hum Mol Genet, 15*(13), 2059-2075. doi:10.1093/hmg/ddl131

Harper, S., Besong, T. M., Emsley, J., Scott, D. J., & Dreveny, I. (2011). Structure of the USP15 N-terminal domains: a beta-hairpin mediates close association between the DUSP and UBL domains. *Biochemistry, 50*(37), 7995-8004. doi:10.1021/bi200726e

Hatano, Y., Li, Y., Sato, K., Asakawa, S., Yamamura, Y., Tomiyama, H., Hattori, N. (2004). Novel PINK1 mutations in early-onset parkinsonism. *Ann Neurol, 56*(3), 424-427. doi:10.1002/ana.20251

Henn, I. H., Gostner, J. M., Lackner, P., Tatzelt, J., & Winklhofer, K. F. (2005). Pathogenic mutations inactivate parkin by distinct mechanisms. *J Neurochem, 92*(1), 114-122. doi:10.1111/j.1471-4159.2004.02854.x

Heo, J. M., Ordureau, A., Paulo, J. A., Rinehart, J., & Harper, J. W. (2015). The PINK1-PARKIN Mitochondrial Ubiquitylation Pathway Drives a Program of OPTN/NDP52 Recruitment and TBK1 Activation to Promote Mitophagy. *Mol Cell, 60*(1), 7-20. doi:10.1016/j.molcel.2015.08.016

Hiller, S., Garces, R. G., Malia, T. J., Orekhov, V. Y., Colombini, M., & Wagner, G. (2008). Solution structure of the integral human membrane protein VDAC-1 in detergent micelles. *Science, 321*(5893), 1206-1210. doi:10.1126/science.1161302

Hollville, E., Carroll, R. G., Cullen, S. P., & Martin, S. J. (2014). Bcl-2 family proteins participate in mitochondrial quality control by regulating Parkin/PINK1-dependent mitophagy. *Mol Cell, 55*(3), 451-466. doi:10.1016/j.molcel.2014.06.001

Hu, M., Li, P., Song, L., Jeffrey, P. D., Chenova, T. A., Wilkinson, K. D., Shi, Y. (2005). Structure and mechanisms of the proteasome-associated deubiquitinating enzyme USP14. *EMBO J, 24*(21), 3747-3756. doi:10.1038/sj.emboj.7600832

Huang, C., Andres, A. M., Ratliff, E. P., Hernandez, G., Lee, P., & Gottlieb, R. A. (2011). Preconditioning involves selective mitophagy mediated by Parkin and p62/SQSTM1. *PLoS One, 6*(6), e20975. doi:10.1371/journal.pone.0020975

Huang, E., Qu, D., Huang, T., Rizzi, N., Boonying, W., Krolak, D., Park, D. S. (2017). PINK1-mediated phosphorylation of LETM1 regulates

mitochondrial calcium transport and protects neurons against mitochondrial stress. *Nat Commun, 8*(1), 1399. doi:10.1038/s41467-017-01435-1

Jin, L., Williamson, A., Banerjee, S., Philipp, I., & Rape, M. (2008). Mechanism of ubiquitin-chain formation by the human anaphase-promoting complex. *Cell, 133*(4), 653-665. doi:10.1016/j.cell.2008.04.012

Kang, R., Zeh, H. J., Lotze, M. T., & Tang, D. (2011). The Beclin 1 network regulates autophagy and apoptosis. *Cell Death Differ, 18*(4), 571-580. doi:10.1038/cdd.2010.191

Kazlauskaite, A., Kelly, V., Johnson, C., Baillie, C., Hastie, C. J., Peggie, M., Muqit, M. M. (2014). Phosphorylation of Parkin at Serine65 is essential for activation: elaboration of a Miro1 substrate-based assay of Parkin E3 ligase activity. *Open Biol, 4*, 130213. doi:10.1098/rsob.130213

Kazlauskaite, A., Kondapalli, C., Gourlay, R., Campbell, D. G., Ritorto, M. S., Hofmann, K., Muqit, M. M. (2014). Parkin is activated by PINK1-dependent phosphorylation of ubiquitin at Ser65. *Biochem J, 460*(1), 127-139. doi:10.1042/BJ20140334

Kazlauskaite, A., Martinez-Torres, R. J., Wilkie, S., Kumar, A., Peltier, J., Gonzalez, A., Muqit, M. M. (2015). Binding to serine 65-phosphorylated ubiquitin primes Parkin for optimal PINK1-dependent phosphorylation and activation. *EMBO Rep, 16*(8), 939-954. doi:10.15252/embr.201540352

Keinan, N., Pahima, H., Ben-Hail, D., & Shoshan-Barmatz, V. (2013). The role of calcium in VDAC1 oligomerization and mitochondria-mediated apoptosis. *Biochim Biophys Acta, 1833*(7), 1745-1754. doi:10.1016/j.bbamcr.2013.03.017

Khandelwal, P. J., Dumanis, S. B., Feng, L. R., Maguire-Zeiss, K., Rebeck, G., Lashuel, H. A., & Moussa, C. E. (2010). Parkinson-related parkin reduces alpha-Synuclein phosphorylation in a gene transfer model. *Mol Neurodegener, 5*, 47. doi:10.1186/1750-1326-5-47

Kitada, T., Asakawa, S., Hattori, N., Matsumine, H., Yamamura, Y., Minoshima, S., Shimizu, N. (1998). Mutations in the parkin gene cause autosomal recessive juvenile parkinsonism. *Nature, 392*(6676), 605-608. doi:10.1038/33416

Kondapalli, C., Kazlauskaite, A., Zhang, N., Woodroof, H. I., Campbell, D. G., Gourlay, R., Muqit, M. M. (2012). PINK1 is activated by mitochondrial membrane potential depolarization and stimulates Parkin E3 ligase activity by phosphorylating Serine 65. *Open Biol, 2*(5), 120080. doi:10.1098/rsob.120080

Kostic, M., Ludtmann, M. H., Bading, H., Hershfinkel, M., Steer, E., Chu,

C. T., Sekler, I. (2015). PKA Phosphorylation of NCLX Reverses Mitochondrial Calcium Overload and Depolarization, Promoting Survival of PINK1-Deficient Dopaminergic Neurons. *Cell Rep, 13*(2), 376-386. doi:10.1016/j.celrep.2015.08.079

Koyano, F., & Matsuda, N. (2015). Molecular mechanisms underlying PINK1 and Parkin catalyzed ubiquitylation of substrates on damaged mitochondria. *Biochim Biophys Acta, 1853*(10 Pt B), 2791-2796. doi:10.1016/j.bbamcr.2015.02.009

Koyano, F., Okatsu, K., Kosako, H., Tamura, Y., Go, E., Kimura, M., Matsuda, N. (2014). Ubiquitin is phosphorylated by PINK1 to activate parkin. *Nature, 510*(7503), 162-166. doi:10.1038/nature13392

Kubli, D. A., & Gustafsson, A. B. (2012). Mitochondria and mitophagy: the yin and yang of cell death control. *Circ Res, 111*(9), 1208-1221. doi:10.1161/CIRCRESAHA.112.265819

Lan, C. H., Sheng, J. Q., Fang, D. C., Meng, Q. Z., Fan, L. L., & Huang, Z. R. (2010). Involvement of VDAC1 and Bcl-2 family of proteins in VacA-induced cytochrome c release and apoptosis of gastric epithelial carcinoma cells. *J Dig Dis, 11*(1), 43-49. doi:10.1111/j.1751-2980.2009.00412.x

Lazarou, M., Jin, S. M., Kane, L. A., & Youle, R. J. (2012). Role of PINK1 binding to the TOM complex and alternate intracellular membranes in recruitment and activation of the E3 ligase Parkin. *Dev Cell, 22*(2), 320-333. doi:10.1016/j.devcel.2011.12.014

Lazarou, M., Narendra, D. P., Jin, S. M., Tekle, E., Banerjee, S., & Youle, R. J. (2013). PINK1 drives Parkin self-association and HECT-like E3 activity upstream of mitochondrial binding. *J Cell Biol, 200*(2), 163-172. doi:10.1083/jcb.201210111

Lazarou, M., Sliter, D. A., Kane, L. A., Sarraf, S. A., Wang, C., Burman, J. L., Youle, R. J. (2015). The ubiquitin kinase PINK1 recruits autophagy receptors to induce mitophagy. *Nature, 524*(7565), 309-314. doi:10.1038/nature14893

Lee, J. C., Wang, G. X., Schickling, O., & Peter, M. E. (2005). Fusing DEDD with ubiquitin changes its intracellular localization and apoptotic potential. *Apoptosis, 10*(6), 1483-1495. doi:10.1007/s10495-005-1833-z

Lesage, S., & Brice, A. (2009). Parkinson's disease: from monogenic forms to genetic susceptibility factors. *Hum Mol Genet, 18*(R1), R48-59. doi:10.1093/hmg/ddp012

Li, W., & Ye, Y. (2008). Polyubiquitin chains: functions, structures, and mechanisms. *Cell Mol Life Sci, 65*(15), 2397-2406. doi:10.1007/s00018-008-8090-6

Li, Y., Sun, X. X., Elferich, J., Shinde, U., David, L. L., & Dai, M. S. (2014). Monoubiquitination is critical for ovarian tumor domain-containing ubiquitin aldehyde binding protein 1 (Otub1) to suppress UbcH5 enzyme and stabilize p53 protein. *J Biol Chem, 289*(8), 5097-5108. doi:10.1074/jbc.M113.533109

Li, Z., Melandri, F., Berdo, I., Jansen, M., Hunter, L., Wright, S., Figueiredo-Pereira, M. E. (2004). Delta12-Prostaglandin J2 inhibits the ubiquitin hydrolase UCH-L1 and elicits ubiquitin-protein aggregation without proteasome inhibition. *Biochem Biophys Res Commun, 319*(4), 1171-1180. doi:10.1016/j.bbrc.2004.05.098

Liao, Y., Hao, Y., Chen, H., He, Q., Yuan, Z., & Cheng, J. (2015). Mitochondrial calcium uniporter protein MCU is involved in oxidative stress-induced cell death. *Protein Cell, 6*(6), 434-442. doi:10.1007/s13238-015-0144-6

Lowe, E. D., Hasan, N., Trempe, J. F., Fonso, L., Noble, M. E., Endicott, J. A., Brown, N. R. (2006). Structures of the Dsk2 UBL and UBA domains and their complex. *Acta Crystallogr D Biol Crystallogr, 62*(Pt 2), 177-188. doi:10.1107/S0907444905037777

Matsuda, N., Kitami, T., Suzuki, T., Mizuno, Y., Hattori, N., & Tanaka, K. (2006). Diverse effects of pathogenic mutations of Parkin that catalyze multiple monoubiquitylation in vitro. *J Biol Chem, 281*(6), 3204-3209. doi:10.1074/jbc.M510393200

Matsuda, N., Sato, S., Shiba, K., Okatsu, K., Saisho, K., Gautier, C. A., Tanaka, K. (2010). PINK1 stabilized by mitochondrial depolarization recruits Parkin to damaged mitochondria and activates latent Parkin for mitophagy. *J Cell Biol, 189*(2), 211-221. doi:10.1083/jcb.200910140

Matsuda, W., Furuta, T., Nakamura, K. C., Hioki, H., Fujiyama, F., Arai, R., & Kaneko, T. (2009). Single nigrostriatal dopaminergic neurons form widely spread and highly dense axonal arborizations in the neostriatum. *J Neurosci, 29*(2), 444-453. doi:10.1523/JNEUROSCI.4029-08.2009

McKenna, S., Moraes, T., Pastushok, L., Ptak, C., Xiao, W., Spyracopoulos, L., & Ellison, M. J. (2003). An NMR-based model of the ubiquitin-bound human ubiquitin conjugation complex Mms2.Ubc13. The structural basis for lysine 63 chain catalysis. *J Biol Chem, 278*(15), 13151-13158. doi:10.1074/jbc.M212353200

Moore, C. L. (1971). Specific inhibition of mitochondrial Ca++ transport by ruthenium red. *Biochem Biophys Res Commun, 42*(2), 298-305.

Narendra, D. P., Jin, S. M., Tanaka, A., Suen, D. F., Gautier, C. A., Shen, J., Youle, R. J. (2010). PINK1 is selectively stabilized on impaired mitochondria to activate Parkin. *PLoS Biol, 8*(1), e1000298.

doi:10.1371/journal.pbio.1000298
Nicholls, D. G. (2008). Oxidative stress and energy crises in neuronal dysfunction. *Ann N Y Acad Sci, 1147*, 53-60. doi:10.1196/annals.1427.002
Nurit Keinan, D. T. a. V. S.-B. (2010). Oligomerization of the mitochondrial protein voltage-dependent anion channel is coupled to the induction of apoptosis. *Molecular and Cellular Biology, 30*(24), 5698-5709.
Okatsu, K., Saisho, K., Shimanuki, M., Nakada, K., Shitara, H., Sou, Y. S., Matsuda, N. (2010). p62/SQSTM1 cooperates with Parkin for perinuclear clustering of depolarized mitochondria. *Genes Cells, 15*(8), 887-900. doi:10.1111/j.1365-2443.2010.01426.x
Oliveira, S. A., Scott, W. K., Martin, E. R., Nance, M. A., Watts, R. L., Hubble, J. P., Vance, J. M. (2003). Parkin mutations and susceptibility alleles in late-onset Parkinson's disease. *Ann Neurol, 53*(5), 624-629. doi:10.1002/ana.10524
Ozawa, K., Komatsubara, A. T., Nishimura, Y., Sawada, T., Kawafune, H., Tsumoto, H., Yoshizumi, M. (2013). S-nitrosylation regulates mitochondrial quality control via activation of parkin. *Sci Rep, 3*, 2202. doi:10.1038/srep02202
Pagliarini, V., Wirawan, E., Romagnoli, A., Ciccosanti, F., Lisi, G., Lippens, S., Piacentini, M. (2012). Proteolysis of Ambra1 during apoptosis has a role in the inhibition of the autophagic pro-survival response. *Cell Death Differ, 19*(9), 1495-1504. doi:10.1038/cdd.2012.27
Pao, K. C., Stanley, M., Han, C., Lai, Y. C., Murphy, P., Balk, K., Virdee, S. (2016). Probes of ubiquitin E3 ligases enable systematic dissection of parkin activation. *Nat Chem Biol, 12*(5), 324-331. doi:10.1038/nchembio.2045
Park, J., Lee, S. B., Lee, S., Kim, Y., Song, S., Kim, S., Chung, J. (2006). Mitochondrial dysfunction in Drosophila PINK1 mutants is complemented by parkin. *Nature, 441*(7097), 1157-1161. doi:10.1038/nature04788
Patergnani, S., Suski, J. M., Agnoletto, C., Bononi, A., Bonora, M., De Marchi, E., Pinton, P. (2011). Calcium signaling around Mitochondria Associated Membranes (MAMs). *Cell Commun Signal, 9*, 19. doi:10.1186/1478-811X-9-19
Petroski, M. D., & Deshaies, R. J. (2005). Mechanism of lysine 48-linked ubiquitin-chain synthesis by the cullin-RING ubiquitin-ligase complex SCF-Cdc34. *Cell, 123*(6), 1107-1120. doi:10.1016/j.cell.2005.09.033
Poburko, D., Liao, C. H., van Breemen, C., & Demaurex, N. (2009). Mitochondrial regulation of sarcoplasmic reticulum Ca2+ content in vascular smooth muscle cells. *Circ Res, 104*(1), 104-112.

doi:10.1161/CIRCRESAHA.108.180612
Przedborski, S., Tieu, K., Perier, C., & Vila, M. (2004). MPTP as a mitochondrial neurotoxic model of Parkinson's disease. *J Bioenerg Biomembr, 36*(4), 375-379. doi:10.1023/B:JOBB.0000041771.66775.d5
Rajsbaum, R., Versteeg, G. A., Schmid, S., Maestre, A. M., Belicha-Villanueva, A., Martinez-Romero, C., Garcia-Sastre, A. (2014). Unanchored K48-linked polyubiquitin synthesized by the E3-ubiquitin ligase TRIM6 stimulates the interferon-IKKepsilon kinase-mediated antiviral response. *Immunity, 40*(6), 880-895. doi:10.1016/j.immuni.2014.04.018
Ray, S., Zhao, Y., Jamaluddin, M., Edeh, C. B., Lee, C., & Brasier, A. R. (2014). Inducible STAT3 NH2 terminal mono-ubiquitination promotes BRD4 complex formation to regulate apoptosis. *Cell Signal, 26*(7), 1445-1455. doi:10.1016/j.cellsig.2014.03.007
Reeve, A., Simcox, E., & Turnbull, D. (2014). Ageing and Parkinson's disease: why is advancing age the biggest risk factor? *Ageing Res Rev, 14*, 19-30. doi:10.1016/j.arr.2014.01.004
Riley, B. E., Lougheed, J. C., Callaway, K., Velasquez, M., Brecht, E., Nguyen, L., Johnston, J. A. (2013). Structure and function of Parkin E3 ubiquitin ligase reveals aspects of RING and HECT ligases. *Nat Commun, 4*, 1982. doi:10.1038/ncomms2982
Rodrigo-Brenni, M. C., & Morgan, D. O. (2007). Sequential E2s drive polyubiquitin chain assembly on APC targets. *Cell, 130*(1), 127-139. doi:10.1016/j.cell.2007.05.027
Rostovtseva, T. K., Antonsson, B., Suzuki, M., Youle, R. J., Colombini, M., & Bezrukov, S. M. (2004). Bid, but not Bax, regulates VDAC channels. *J Biol Chem, 279*(14), 13575-13583. doi:10.1074/jbc.M310593200
Safadi, S. S., Barber, K. R., & Shaw, G. S. (2011). Impact of autosomal recessive juvenile Parkinson's disease mutations on the structure and interactions of the parkin ubiquitin-like domain. *Biochemistry, 50*(13), 2603-2610. doi:10.1021/bi200065g
Sarkar, F. H., Rahman, K. M., & Li, Y. (2003). Bax translocation to mitochondria is an important event in inducing apoptotic cell death by indole-3-carbinol (I3C) treatment of breast cancer cells. *J Nutr; 133*(7 Suppl), 2434S-2439S.
Sauve, V., Lilov, A., Seirafi, M., Vranas, M., Rasool, S., Kozlov, G., Gehring, K. (2015). A Ubl/ubiquitin switch in the activation of Parkin. *EMBO J, 34*(20), 2492-2505. doi:10.15252/embj.201592237
Sharov, V. G., Todor, A., Khanal, S., Imai, M., & Sabbah, H. N. (2007). Cyclosporine A attenuates mitochondrial permeability transition and

improves mitochondrial respiratory function in cardiomyocytes isolated from dogs with heart failure. *J Mol Cell Cardiol, 42*(1), 150-158. doi:10.1016/j.yjmcc.2006.09.013

Shi, Y., Chen, J., Weng, C., Chen, R., Zheng, Y., Chen, Q., & Tang, H. (2003). Identification of the protein-protein contact site and interaction mode of human VDAC1 with Bcl-2 family proteins. *Biochem Biophys Res Commun, 305*(4), 989-996.

Shiba-Fukushima, K., Imai, Y., Yoshida, S., Ishihama, Y., Kanao, T., Sato, S., & Hattori, N. (2012). PINK1-mediated phosphorylation of the Parkin ubiquitin-like domain primes mitochondrial translocation of Parkin and regulates mitophagy. *Sci Rep, 2*, 1002. doi:10.1038/srep01002

Shimizu, S., Matsuoka, Y., Shinohara, Y., Yoneda, Y., & Tsujimoto, Y. (2001). Essential role of voltage-dependent anion channel in various forms of apoptosis in mammalian cells. *J Cell Biol, 152*(2), 237-250.

Shimura, H., Hattori, N., Kubo, S., Mizuno, Y., Asakawa, S., Minoshima, S., Suzuki, T. (2000). Familial Parkinson disease gene product, parkin, is a ubiquitin-protein ligase. *Nat Genet, 25*(3), 302-305. doi:10.1038/77060

Shoshan-Barmatz, V., De Pinto, V., Zweckstetter, M., Raviv, Z., Keinan, N., & Arbel, N. (2010). VDAC, a multi-functional mitochondrial protein regulating cell life and death. *Mol Aspects Med, 31*(3), 227-285. doi:10.1016/j.mam.2010.03.002

Shoshan-Barmatz, V., De, S., & Meir, A. (2017). The Mitochondrial Voltage-Dependent Anion Channel 1, Ca(2+) Transport, Apoptosis, and Their Regulation. *Front Oncol, 7*, 60. doi:10.3389/fonc.2017.00060

Shoshan-Barmatz, V., Krelin, Y., & Chen, Q. (2017). VDAC1 as a player in mitochondria-mediated apoptosis and target for modulating apoptosis. *Curr Med Chem*. doi:10.2174/0929867324666170616105200

Shoshan-Barmatz, V., Krelin, Y., & Shteinfer-Kuzmine, A. (2017). VDAC1 functions in Ca(2+) homeostasis and cell life and death in health and disease. *Cell Calcium*. doi:10.1016/j.ceca.2017.06.007

Shoshan-Barmatz, V., Mizrachi, D., & Keinan, N. (2013). Oligomerization of the mitochondrial protein VDAC1: from structure to function and cancer therapy. *Prog Mol Biol Transl Sci, 117*, 303-334. doi:10.1016/B978-0-12-386931-9.00011-8

Shoshan-Barmatz, V., Zakar, M., Rosenthal, K., & Abu-Hamad, S. (2009). Key regions of VDAC1 functioning in apoptosis induction and regulation by hexokinase. *Biochim Biophys Acta, 1787*(5), 421-430. doi:10.1016/j.bbabio.2008.11.009

Simola, N., Morelli, M., & Carta, A. R. (2007). The 6-hydroxydopamine model of Parkinson's disease. *Neurotox Res, 11*(3-4), 151-167.

Smaili, S. S., Hsu, Y. T., Sanders, K. M., Russell, J. T., & Youle, R. J. (2001). Bax translocation to mitochondria subsequent to a rapid loss of mitochondrial membrane potential. *Cell Death Differ, 8*(9), 909-920. doi:10.1038/sj.cdd.4400889

Sun, Y., Vashisht, A. A., Tchieu, J., Wohlschlegel, J. A., & Dreier, L. (2012). Voltage-dependent anion channels (VDACs) recruit Parkin to defective mitochondria to promote mitochondrial autophagy. *J Biol Chem, 287*(48), 40652-40660. doi:10.1074/jbc.M112.419721

Surmeier, D. J., Guzman, J. N., Sanchez-Padilla, J., & Schumacker, P. T. (2011). The role of calcium and mitochondrial oxidant stress in the loss of substantia nigra pars compacta dopaminergic neurons in Parkinson's disease. *Neuroscience, 198*, 221-231. doi:10.1016/j.neuroscience.2011.08.045

Szabadkai, G., Bianchi, K., Varnai, P., De Stefani, D., Wieckowski, M. R., Cavagna, D., Rizzuto, R. (2006). Chaperone-mediated coupling of endoplasmic reticulum and mitochondrial Ca2+ channels. *J Cell Biol, 175*(6), 901-911. doi:10.1083/jcb.200608073

Tajeddine, N., Galluzzi, L., Kepp, O., Hangen, E., Morselli, E., Senovilla, L., Kroemer, G. (2008). Hierarchical involvement of Bak, VDAC1 and Bax in cisplatin-induced cell death. *Oncogene, 27*(30), 4221-4232. doi:10.1038/onc.2008.63

Tan, E. K., & Skipper, L. M. (2007). Pathogenic mutations in Parkinson disease. *Hum Mutat, 28*(7), 641-653. doi:10.1002/humu.20507

Tan, J. M., Wong, E. S., Kirkpatrick, D. S., Pletnikova, O., Ko, H. S., Tay, S. P., Lim, K. L. (2008). Lysine 63-linked ubiquitination promotes the formation and autophagic clearance of protein inclusions associated with neurodegenerative diseases. *Hum Mol Genet, 17*(3), 431-439. doi:10.1093/hmg/ddm320

Tanaka, A., Cleland, M. M., Xu, S., Narendra, D. P., Suen, D. F., Karbowski, M., & Youle, R. J. (2010). Proteasome and p97 mediate mitophagy and degradation of mitofusins induced by Parkin. *J Cell Biol, 191*(7), 1367-1380. doi:10.1083/jcb.201007013

Tashiro, M., Okubo, S., Shimotakahara, S., Hatanaka, H., Yasuda, H., Kainosho, M., Shindo, H. (2003). NMR structure of ubiquitin-like domain in PARKIN: gene product of familial Parkinson's disease. *J Biomol NMR, 25*(2), 153-156.

Terreni, L., Calabrese, E., Calella, A. M., Forloni, G., & Mariani, C. (2001). New mutation (R42P) of the parkin gene in the ubiquitinlike domain associated with parkinsonism. *Neurology, 56*(4), 463-466.

Tomoo, K., Mukai, Y., In, Y., Miyagawa, H., Kitamura, K., Yamano, A.,

Ishida, T. (2008). Crystal structure and molecular dynamics simulation of ubiquitin-like domain of murine parkin. *Biochim Biophys Acta, 1784*(7-8), 1059-1067. doi:10.1016/j.bbapap.2008.04.009

Trempe, J. F., Sauve, V., Grenier, K., Seirafi, M., Tang, M. Y., Menade, M., Gehring, K. (2013). Structure of parkin reveals mechanisms for ubiquitin ligase activation. *Science, 340*(6139), 1451-1455. doi:10.1126/science.1237908

Tsujimoto, Y., & Shimizu, S. (2000). VDAC regulation by the Bcl-2 family of proteins. *Cell Death Differ, 7*(12), 1174-1181. doi:10.1038/sj.cdd.4400780

Ujwal, R., Cascio, D., Chaptal, V., Ping, P., & Abramson, J. (2009). Crystal packing analysis of murine VDAC1 crystals in a lipidic environment reveals novel insights on oligomerization and orientation. *Channels (Austin), 3*(3), 167-170.

VanDemark, A. P., Hofmann, R. M., Tsui, C., Pickart, C. M., & Wolberger, C. (2001). Molecular insights into polyubiquitin chain assembly: crystal structure of the Mms2/Ubc13 heterodimer. *Cell, 105*(6), 711-720.

von Ahsen, O., Renken, C., Perkins, G., Kluck, R. M., Bossy-Wetzel, E., & Newmeyer, D. D. (2000). Preservation of mitochondrial structure and function after Bid- or Bax-mediated cytochrome c release. *J Cell Biol, 150*(5), 1027-1036.

Walters, K. J., Kleijnen, M. F., Goh, A. M., Wagner, G., & Howley, P. M. (2002). Structural studies of the interaction between ubiquitin family proteins and proteasome subunit S5a. *Biochemistry, 41*(6), 1767-1777.

Wang, C., & Youle, R. J. (2009). The role of mitochondria in apoptosis*. *Annu Rev Genet, 43*, 95-118. doi:10.1146/annurev-genet-102108-134850

Wang, H., Song, P., Du, L., Tian, W., Yue, W., Liu, M., Chen, Q. (2011). Parkin ubiquitinates Drp1 for proteasome-dependent degradation: implication of dysregulated mitochondrial dynamics in Parkinson disease. *J Biol Chem, 286*(13), 11649-11658. doi:10.1074/jbc.M110.144238

Wang, X., Winter, D., Ashrafi, G., Schlehe, J., Wong, Y. L., Selkoe, D., Schwarz, T. L. (2011). PINK1 and Parkin target Miro for phosphorylation and degradation to arrest mitochondrial motility. *Cell, 147*(4), 893-906. doi:10.1016/j.cell.2011.10.018

Wauer, T., & Komander, D. (2013). Structure of the human Parkin ligase domain in an autoinhibited state. *EMBO J, 32*(15), 2099-2112. doi:10.1038/emboj.2013.125

Wauer, T., Simicek, M., Schubert, A., & Komander, D. (2015a). Erratum: Mechanism of phospho-ubiquitin-induced PARKIN activation. *Nature, 526*(7575), 728. doi:10.1038/nature15531

Wauer, T., Simicek, M., Schubert, A., & Komander, D. (2015b). Mechanism of phospho-ubiquitin-induced PARKIN activation. *Nature, 524*(7565), 370-374. doi:10.1038/nature14879

Wenzel, D. M., Lissounov, A., Brzovic, P. S., & Klevit, R. E. (2011). UBCH7 reactivity profile reveals parkin and HHARI to be RING/HECT hybrids. *Nature, 474*(7349), 105-108. doi:10.1038/nature09966

Wheaton, K., Sarkari, F., Stanly Johns, B., Davarinejad, H., Egorova, O., Kaustov, L., Sheng, Y. (2017). UbE2E1/UBCH6 Is a Critical in Vivo E2 for the PRC1-catalyzed Ubiquitination of H2A at Lys-119. *J Biol Chem, 292*(7), 2893-2902. doi:10.1074/jbc.M116.749564

Wood-Kaczmar, A., Gandhi, S., & Wood, N. W. (2006). Understanding the molecular causes of Parkinson's disease. *Trends Mol Med, 12*(11), 521-528. doi:10.1016/j.molmed.2006.09.007

Ying, W. L., Emerson, J., Clarke, M. J., & Sanadi, D. R. (1991). Inhibition of mitochondrial calcium ion transport by an oxo-bridged dinuclear ruthenium ammine complex. *Biochemistry, 30*(20), 4949-4952.

Yousefi, S., Perozzo, R., Schmid, I., Ziemiecki, A., Schaffner, T., Scapozza, L., Simon, H. U. (2006). Calpain-mediated cleavage of Atg5 switches autophagy to apoptosis. *Nat Cell Biol, 8*(10), 1124-1132. doi:10.1038/ncb1482

Yu, N., Wang, S., Wang, P., Li, Y., Li, S., Wang, L., Wang, Y. (2012). The calcium uniporter regulates the permeability transition pore in isolated cortical mitochondria. *Neural Regen Res, 7*(2), 109-113. doi:10.3969/j.issn.1673-5374.2012.02.005

Yu, W., Sun, Y., Guo, S., & Lu, B. (2011). The PINK1/Parkin pathway regulates mitochondrial dynamics and function in mammalian hippocampal and dopaminergic neurons. *Hum Mol Genet, 20*(16), 3227-3240. doi:10.1093/hmg/ddr235

Zhang, C., Lee, S., Peng, Y., Bunker, E., Giaime, E., Shen, J., Liu, X. (2014). PINK1 triggers autocatalytic activation of Parkin to specify cell fate decisions. *Curr Biol, 24*(16), 1854-1865. doi:10.1016/j.cub.2014.07.014

Zhang, Y., Gao, J., Chung, K. K., Huang, H., Dawson, V. L., & Dawson, T. M. (2000). Parkin functions as an E2-dependent ubiquitin- protein ligase and promotes the degradation of the synaptic vesicle-associated protein, CDCrel-1. *Proc Natl Acad Sci U S A, 97*(24), 13354-13359. doi:10.1073/pnas.240347797

파킨슨병의 발병기전을 이해하기 위해 PINK1, Parkin, VDAC1에 의한 파킨슨병 관련 기능조절기전 연구를 진행하였다. 세포 내 미토콘드리아가 정상일 때 Parkin 의 UBL 도메인과 RING1 도메인 간의 결합으로 스스로의 활성을 억제하고 있음을 보았다. 이런 Parkin 의 활성 억제기전은 미토콘드리아 손상상황에서 상위조절자인 PINK1에 의해 Parkin 의 UBL 도메인 내 위치한 serine 65번 잔기 인산화가 되어 Parkin 의 UBL 도메인과 RING1 도메인과의 결합이 감소됨에 따라 조절된다. PINK1에 의한 Parkin 의 UBL 도메인 내 serine 65번 잔기의 인산화는 Parkin 의 기질인 Mfn1, Mfn2, VDAC1의 유비퀴틴화와 Parkin 에 의해 유도되는 미토콘드리아 선택적 제거 과정을 촉진시킴을 확인하였다. 이 결과로 PINK1에 의해 Parkin 의 UBL 도메인 내 serine 65잔기가 인산화되면 Parkin 의 E3 ligase 기능이 활성화됨을 보았다. 또한 Parkin 의 UBL 도메인 내 존재하는 파킨슨병 환자돌연변이들 중 K27N, R33Q, A46P 돌연변이를 가진 Parkin 의 경우 PINK1에 의한 RING1 도메인과 UBL 도메인 간의 결합이 감소되지 않고 지속적으로 유지되고 있음을

보았고 이로인해 Parkin 의 활성이 억제되어 있음을 밝혔다. 이는 Parkin 과 관련된 파킨슨병 발병기전에 Parkin 의 UBL 도메인과 RING1 도메인간의 결합이 중요한 역할을 하고 있음을 의미한다. PINK1에 의해 활성화된 Parkin 은 미토콘드리아 외막에 위치한 VDAC1 단백질을 두 가지 형태로 유비퀴틴화시키며, 이로 인해 미토콘드리아 선택적 제거과정과 세포사멸 기작이 결정됨을 보았다. PINK1-Parkin 기전에 의해 VDAC1의 lysine 274번 잔기에 mono-ubiquitination 되면 세포사멸과정을 억제하며, VDAC1의 lysine 12, 20, 53, 109, 110 번 잔기에 poly-ubiquitination 되면 미토콘드리아의 선택적 제거과정이 촉진됨을 밝혔다. 또한 VDAC1의 mono-ubiquitination 에 의해 조절되는 세포사멸과정은 미토콘드리아 내의 칼슘유입에 필수적인 역할을 하는 MCU 라는 미토콘드리아 내막에 위치한 칼슘채널과 미토콘드리아 통로인 mPTP 에 의해 미토콘드리아 칼슘유입이 조절되어 발생함을 확인하였다. 이 결과로 PINK1-Parkin 신호전달 기전에 의해 VDAC1의 mono-와 poly-ubiquitination 이 독립적으로 발생함을 확인하였다. 더 나아가 Parkin 의 환자돌연변이들 중 K211N 은 VDAC1의 poly-ubiquitination 이 억제되어 있음을 관찰하였고, T415N 는

VDAC1의 mono-ubiquitination 이 망가져 있음을 확인하였다. Parkin 의 K211N 환자돌연변이는 Parkin 에 의해 유도되는 미토콘드리아 선택적 제거과정이 억제되어있음을 보았다. 또한 Parkin 의 T415N 환자돌연변이에 의해 미토콘드리아 칼슘유입이 증가되어 있음을 관찰하였으며, 이로 인해 세포 내 세포사멸과정이 유도됨을 보았다. 저자의 연구로 파킨슨병의 병리학적 기전에 PINK1에 의한 Parkin 의 활성조절기작과 PINK1-Parkin pathway 에 의해 조절되는 VDAC1의 mono-와 poly-ubiquitination 을 통한 미토콘드리아 항상성 조절기작이 중요함을 보았다. 또한 파킨슨병의 발병기전을 조절하는 새로운 조절자인 VDAC1의 분자적 기전연구로 인해 파킨슨병 발병기전의 이해도를 높였으며, 파킨슨병의 치료제의 새로운 타깃 단백질을 제시하였다.

주요어: 파킨슨병, PINK1, Parkin, VDAC1, 세포사멸, 미토콘드리아 선택적 제거

학번: 2011-20236